Supporting Information

Synthesis and antiproliferative activity of 6-naphthylpterocarpans

Ádám Szappanos,[a,b] Attila Mándi,*[a] Katalin Gulácsi,[a†] Erika Lisztes,[c] Balázs István Tóth,[c] Tamás Bíró,[d] Sándor Antus,[a] Tibor Kurtán*[a]

[a]Department of Organic Chemistry, University of Debrecen, P. O. Box 400, 4002 Debrecen, Hungary Fax: +36-52-512-744

[b]Doctoral School of Chemistry, University of Debrecen, Egyetem tér 1, 4032 Debrecen, Hungary

[c]Department of Physiology, Faculty of Medicine, University of Debrecen, Debrecen, Hungary

[d]Department of Immunology, Faculty of Medicine, University of Debrecen, Debrecen, Hungary

[†]deceased

Dedicated in honor and to the memory of Prof. Koji Nakanishi

E-mail: kurtan.tibor@science.unideb.hu.

Table of Contents

1 Experimental Section forPreviously Reported Derivatives 5

1.1 General Procedure for the Preparation of Chalcone Analogues (**12a-d**) 5

1.2 General Procedure for the Synthesis of 4-Chromanone Derivatives (**13a-d**) 6

1.3 General Procedure for the Preparation of 2*H*-chromenes (**7a-d**) 7

1.4 General Procedure for the Synthesis of Chroman-4-ol derivatives (**14a-d**) 8

1.5 References of known compounds 9

2 NMR and IR Spectra 10

Figure S1. ^{1}H NMR (400 MHz) spectrum of **9a** in $CDCl_3$ 10

Figure S2. ^{13}C NMR (100 MHz) spectrum of **9a** in $CDCl_3$ 11

Figure S3. COSY spectrum of **9a** in $CDCl_3$ 12

Figure S4. HSQC spectrum of **9a** in $CDCl_3$ 13

Figure S5. NOESY spectrum of **9a** in $CDCl_3$ 14

Figure S6. IR spectrum of **9a** recorded as KBr disc 15

Figure S7. ^{1}H NMR (360 MHz) spectrum of **9b** in $CDCl_3$ 16

Figure S8. ^{13}C NMR (90 MHz) spectrum of **9b** in $CDCl_3$ 17

Figure S9. IR spectrum of **9b** recorded as KBr disc 18

Figure S10. ^{1}H NMR (400 MHz) spectrum of **9c** in $CDCl_3$ 19

Figure S11. ^{13}C NMR (100 MHz) spectrum of **9c** in $CDCl_3$ 20
Figure S12. IR spectrum of **9c** recorded as KBr disc 21
Figure S13. ^{1}H NMR (360 MHz) spectrum of **9d** in $CDCl_3$ 22
Figure S14. ^{13}C NMR (90 MHz) spectrum of **9d** in $CDCl_3$ 23
Figure S15. IR spectrum of **9d** recorded as KBr disc 24
Figure S13. ^{1}H NMR (400 MHz) spectrum of **17** in $CDCl_3$ 25
Figure S14. ^{13}C NMR (100 MHz) spectrum of **17** in $CDCl_3$ 26
Figure S16. ^{1}H NMR (360 MHz) spectrum of **10a** in $CDCl_3$ 27
Figure S17. ^{13}C NMR (90 MHz) spectrum of **10a** in $CDCl_3$ 28
Figure S18. IR spectrum of **10a** recorded as KBr disc 29
Figure S19. ^{1}H NMR (400 MHz) spectrum of **10b** in $CDCl_3$ 30
Figure S20. ^{13}C NMR (100 MHz) spectrum of **10b** in $CDCl_3$ 31
Figure S21. IR spectrum of **10b** recorded as KBr disc 32
Figure S22. ^{1}H NMR (360 MHz) spectrum of **10c** in $CDCl_3$ 33
Figure S23. ^{13}C NMR (90 MHz) spectrum of **10c** in $CDCl_3$ 34
Figure S24. IR spectrum of **10c** recorded as KBr disc 35
Figure S25. ^{1}H NMR (400 MHz) spectrum of **10d** in $CDCl_3$ 36
Figure S26. ^{13}C NMR (100 MHz) spectrum of **10d** in $CDCl_3$ 37
Figure S27. IR spectrum of **10d** recorded as KBr disc 38
Figure S28. ^{1}H NMR (360 MHz) spectrum of **7a** in $CDCl_3$ 39
Figure S29. ^{13}C NMR (90 MHz) spectrum of **7a** in $CDCl_3$ 40
Figure S30. IR spectrum of **7a** recorded as KBr disc 41
Figure S31. ^{1}H NMR (360 MHz) spectrum of **7b** in $CDCl_3$ 42
Figure S32. ^{13}C NMR (90 MHz) spectrum of **7b** in $CDCl_3$ 43
Figure S33. IR spectrum of **7b** recorded as KBr disc 44
Figure S34. ^{1}H NMR (360 MHz) spectrum of **7c** in $CDCl_3$ 45
Figure S35. ^{13}C NMR (90 MHz) spectrum of **7c** in $CDCl_3$ 46
Figure S36. ^{1}H NMR (360 MHz) spectrum of **7d** in $CDCl_3$ 47
Figure S37. ^{13}C NMR (90 MHz) spectrum of **7d** in $CDCl_3$ 48
Figure S38. ^{1}H NMR (360 MHz) spectrum of **14a** in $CDCl_3$ 49
Figure S39. ^{13}C NMR (90 MHz) spectrum of **14a** in $CDCl_3$ 50
Figure S40. ^{1}H NMR (360 MHz) spectrum of **14b** in $CDCl_3$ 51
Figure S41. ^{13}C NMR (90 MHz) spectrum of **14b** in $CDCl_3$ 52
Figure S42. ^{1}H NMR (400 MHz) spectrum of **14c** in $CDCl_3$ 53
Figure S43. ^{13}C NMR (100 MHz) spectrum of **14c** in $CDCl_3$ 54

Figure S44. COSY spectrum of **14c** in $CDCl_3$ 55
Figure S45. HSQC spectrum of **14c** in $CDCl_3$ 56
Figure S46. ^1H NMR (360 MHz) spectrum of **14d** in $CDCl_3$ 57
Figure S47. ^{13}C NMR (90 MHz) spectrum of **14d** in $CDCl_3$ 58
Figure S48. ^1H NMR (360 MHz) spectrum of **13a** in $CDCl_3$ 59
Figure S49. ^{13}C NMR (90 MHz) spectrum of **13a** in $CDCl_3$ 60
Figure S50. ^1H NMR (360 MHz) spectrum of **13b** in $CDCl_3$ 61
Figure S51. ^{13}C NMR (90 MHz) spectrum of **13b** in $CDCl_3$ 62
Figure S52. ^1H NMR (360 MHz) spectrum of **13c** in $CDCl_3$ 63
Figure S53. ^{13}C NMR (90 MHz) spectrum of **13c** in $CDCl_3$ 64
Figure S54. ^1H NMR (360 MHz) spectrum of **13d** in $CDCl_3$ 65
Figure S55. ^{13}C NMR (90 MHz) spectrum of **13d** in $CDCl_3$ 66
Figure S56. ^1H NMR (360 MHz) spectrum of **12a** in $CDCl_3$ 67
Figure S57. ^{13}C NMR (90 MHz) spectrum of **12a** in $CDCl_3$ 68
Figure S58. ^1H NMR (360 MHz) spectrum of **12b** in $CDCl_3$ 69
Figure S59. ^{13}C NMR (90 MHz) spectrum of **12b** in $CDCl_3$ 70
Figure S60. ^1H NMR (400 MHz) spectrum of **12c** in $CDCl_3$ 71
Figure S61. ^{13}C NMR (100 MHz) spectrum of **12c** in $CDCl_3$ 72
Figure S62. ^1H NMR (400 MHz) spectrum of **12d** in $CDCl_3$ 73
Figure S63. ^{13}C NMR (100 MHz) spectrum of **12d** in $CDCl_3$ 74
3 Antiproliferative activity experiments 75
Figure S64. Concentration-dependent effect of **9a** on the viability of A2780 cells. 75
Figure S65. Concentration-dependent effect of **9a** on the viability of WM35 cells.. 76
Figure S66. Concentration-dependent effect of **9b** on the viability of A2780 cells. 77
Figure S67. Concentration-dependent effect of **9b** on the viability of WM35 cells. 78
4 Chiral HPLC-ECD Spectra 79
Figure S69. HPLC-ECD spectra of the first- [(6*S*,6a*R*,11a*R*), black] and second-eluting [(6*R*,6a*S*,11a*S*), red] enantiomers of **9c**. 79
Figure S70. HPLC-UV and –ECD traces of **9d** on Chiralpak IA column with hexane/2-propanol 80:20 eluent monitored at 310 nm. 80
Figure S71. HPLC-ECD spectra of the first- [(6*S*,6a*R*,11a*R*), black] and second-eluting [(6*R*,6a*S*,11a*S*), red] enantiomers of **9d**. 80
Figure S72. HPLC-UV and –ECD traces of **10a** on Chiralpak IA column with hexane/2-propanol 95:5 eluent monitored at 270 nm. 81
Figure S73. HPLC-ECD spectra of the first- [(6*S*,12*S*), black] and second-eluting [(6*R*,12*R*), red] enantiomers of **10a**. 81

Figure S74. HPLC-UV and –ECD traces of **10b** on Chiralpak IA column with hexane/2-propanol 80:20 eluent monitored at 270 nm..... 82

Figure S75. HPLC-ECD spectra of the first- [(6*S*,12*S*), black] and second-eluting [(6*R*,12*R*), red] enantiomers of **10b**.... 82

Figure S76. HPLC-UV and –ECD traces of **10c** on Chiralpak IA column with hexane/2-propanol 80:20 eluent monitored at 310 nm..... 83

Figure S77. HPLC-ECD spectra of the first- [(6*R*,12*R*), black] and second-eluting [(6*S*,12*S*), red] enantiomers of **10c**. ... 83

Figure S78. HPLC-UV and –ECD traces of **10d** on Chiralpak IA column with hexane/2-propanol 80:20 eluent monitored at 250 nm..... 84

Figure S79. HPLC-ECD spectra of the first- [(6*R*,12*R*), black] and second-eluting [(6*S*,12*S*), red] enantiomers of **10d**.... 84

Figure S80. HPLC-UV trace of **13a** on Chiralpak IC column with hexane/2-propanol 75:25 eluent. 85

Figure S81. HPLC-ECD spectra of the first- [(2*S*), black] and second-eluting [(2*R*), red] enantiomers of **13a**. 85

Figure S82. HPLC-UV trace of **13b** on Chiralpak IC column with hexane/2-propanol 75:25 eluent. 86

Figure S83. HPLC-ECD spectra of the first- [(2*S*), black] and second-eluting [(2*R*), red] enantiomers of **13b**. 86

Figure S84. HPLC-UV trace of **13c** on Chiralpak IC column with hexane/2-propanol 75:25 eluent. 87

Figure S85. HPLC-ECD spectra of the first- [(2*S*), black] and second-eluting [(2*R*), red] enantiomers of **13c**..... 87

Figure S86. HPLC-UV trace of **13d** on Chiralpak IC column with hexane/2-propanol 75:25 eluent. 88

Figure S87. HPLC-ECD spectra of the first- [(2*S*), black] and second-eluting [(2*R*), red] enantiomers of **13d**. 88

Figure S88. HPLC-UV trace of **7a** on Chiralcel OD column with hexane/2-propanol 95:5 eluent monitored at 260 nm. .. 89

Figure S89. HPLC-ECD spectra of the first- [(2*R*), black] and second-eluting [(2*S*), red] enantiomers of **7a**. 89

Figure S90. HPLC-UV trace of **7b** on Chiralpak IA column with hexane/2-propanol 95:5 eluent monitored at 280 nm. .. 90

Figure S91. HPLC-ECD spectra of the first- [(2*S*), black] and second-eluting [(2*R*), red] enantiomers of **7b**. 90

Figure S92. HPLC-UV trace of **7c** on Chirlpak IA column with hexane/2-propanol 95:5 eluent monitored at 270 nm..... 91

Figure S93. HPLC-ECD spectra of the first- [(2*S*), black] and second-eluting [(2*R*), red] enantiomers of **7c**..... 91

Figure S94. HPLC-UV trace of **7d** on Chiralcel OD column with hexane/2-propanol 95:5 eluent monitored at 225 nm.. 92

Figure S95. HPLC-ECD spectra of the first- [(2*S*), black] and second-eluting [(2*R*), red] enantiomers of **7d**. 92

Figure S96. Effect of pterocarpan derivatives on the viability and proliferation of tumorigenic cell lines…….....93

Figure S97. B3LYP/TZVP PCM/$CHCl_3$ torsional angle scans of **9a** and **9b**…….....94

1 Experimental Section for Previously Reported Derivatives

1.1 General Procedure for the Preparation of Chalcone Analogues (12a-d)

2-Hydroxyacetophenone **11a** (1 g, 7.34 mmol) or 4-benzyloxyacetophenone **11b**[1] was dissolved in ethanol (50 mL) under stirring. Then NaOH (0.88 g; 22.02 mmol, with a minimum amount of water) was added and the solution was stirred for 5 min. To this solution, the aromatic aldehyde (8.81 mmol) was added and stirring was continued at room temperature for 24 h. The reaction was monitored by TLC. After completion of the reaction, the mixture was poured over crushed ice and acidified with 10 % HCl solution. The separated solid was filtered off and washed with water. The crude product was dried and recrystallized from ethanol to obtain the product in pure form.

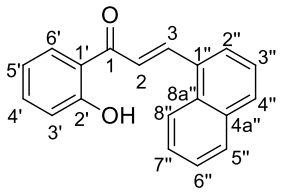

***(E)*-1-(2-Hydroxyphenyl)-3-(1-naphthyl)prop-2-en-1-one (12a)**:[1] yellow crystals, 1.68 g (84 %), mp 107-109 °C, ^{1}H NMR (360 MHz, $CDCl_3$) δ: 6.95 (t, *J* = 7.9 Hz, 1 H, 5'-H), 7.04 (d, *J* = 8.3 Hz, 1 H, 3'-H), 7.55 (m, 4 H, 4'-H, 3"-H, 6"-H, 7"-H), 7.72 (d, *J* = 15.5 Hz, 1 H, 2-H), 7.93 (m, 4 H, 2"-H, 4"-H, 5"-H, 8"-H), 8.26 (d, *J* = 8.3 Hz, 1 H, 6'-H), 8.76 (d, *J* = 15.1 Hz, 1 H, 3-H), 12.87 (s, 1 H, OH). ^{13}C NMR (90 MHz, $CDCl_3$) δ: 118.8 (C-3'), 119.0 (C-5'), 120.1 (C-1'), 122.8 (C-2), 123.5 (C-8"), 125.4 (C-2"), 125.5 (C-3"), 126.5 (C-6"), 127,2 (C-7"), 128.9 (C-6'), 129,8 (C-4"), 131.3 (C-5"), 131.9 (C-8a"), 132.1 (C-4a"), 133.8 (C-1"), 136.6 (C-4'), 142.4 (C-3), 163.8 (C-2'), 193.6 (C-1). HRMS (ESI) calculated for $C_{19}H_{14}NaO_2$ $[M + Na]^+$: 297.0886, found 297.0887.

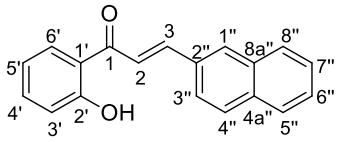

(*E*)-1-(2-Hydroxyphenyl)-3-(2-naphthyl)prop-2-en-1-one (12b):[1] yellow crystals, 1.86 g (93 %), mp 150-152 °C, ^{1}H NMR (360 MHz, $CDCl_3$) δ: 6.95 (t, J = 7.2 Hz, 1 H, 5'-H), 7.02 (d, *J* = 8.3 Hz, 1 H, 3'-H), 7.52 (m, 3 H, H-3", 6"-H, 7"-H), 7.75 (m, 2 H, 3-H, 4'-H), 7.84 (m, 3 H, 4"-H, 5"-H, 8"-H), 7.93 (d, *J* = 8,3 Hz, 1 H, 6'-H), 8.03 (m, 2 H, 2-H, 1"-H), 12.88 (s, 1 H, OH). ^{13}C NMR (90 MHz, $CDCl_3$) δ: 118.1 (C-3'), 118.4 (C-2), 119.6 (C-1'), 119.6 (C-5'), 123.1 (C-3"), 126.4 (C-6"), 127.1 (C-7"), 127.3 (C-5"), 128.2 (C-1"), 128.3 (C-8"), 129.2 (C-4"), 130.6 (C-6'), 131.6 (C-2"), 132.8 (C-4a"), 134.0 (C-8a"), 135.9 (C-4'), 145.0 (C-3), 163.1 (C-2'), 193.1 (C-1). HRMS (ESI) calculated for $C_{19}H_{14}NaO_2$ $[M + Na]^+$: 297.0886, found 297.0886.

1.2 General Procedure for the Synthesis of 4-Chromanone Derivatives (13a-d)

To the stirred solution of chalcone derivatives **12a-d** (1 g, 3.62 mmol) in ethanol (50 mL), sodium acetate solution (4 g in 10 mL water) was added and the reaction mixture was refluxed for 5 h. After cooling to room temperature, the reaction mixture was concentrated under reduced pressure, and extracted with ethyl acetate. The combined organic layers were washed with water, dried over $MgSO_4$, filtered and solvent was evaporated under reduced pressure. The residue was triturated with cold diethyl ether. The precipitate was filtered and dried on air.

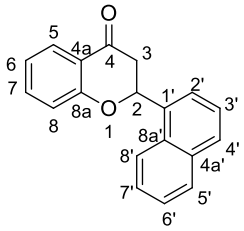

(±)-2-(1-Naphthyl)chromanone (13a):[1] white crystals, 506 mg (51 %), mp 99-101 °C, ^{1}H NMR (360 MHz, $CDCl_3$) δ: 3.05 (dd, *J* = 16.9, 2.8 Hz, 1 H, 3-H_a), 3.24 (m, 1 H, 3-H_b), 6.19 (dd, *J* = 13.3, 2.8 Hz, 1 H, 2-H), 7.08 (m, 2 H, 6-H, 8-H), 7.53 (m, 4 H, 7-H, 2'-H, 3'-H, 7'-H), 7.75 (d, *J* = 6.8 Hz, 1 H, 4'-H), 7.89 (m, 2 H, 5'-H, 6'-H), 8.00 (m, 2 H, 5-H, 8'-H). ^{13}C NMR (90 MHz, $CDCl_3$) δ: 43.9 (C-3), 76.8 (C-2), 118.2 (C-8), 121.1 (C-4a), 121.7 (C-6), 122.7 (C-8'), 123.8 (C-3'), 125.9 (C-7'), 126.6 (C-2), 127.1 (C-5), 129.0 (C-4'), 129.3 (C-5'), 130.1 (C-8a'), 133.8 (C-4a'), 134.1 (C-1), 136.2 (C-7), 161.7 (C-8a), 192.2 (C-4). HRMS (ESI) calculated for $C_{19}H_{14}NaO_2$ $[M + Na]^+$: 297.0886, found 297.0886.
(*S*)-**13a**: t_R = 5.93 min on Chiralpak IC column (hexane/2-propanol 75:25), HPLC-ECD λ [nm] (ϕ): 336 (–6.27), 267sh (–5.09), 247sh (6.67), 228 (84.87), 223 (–35.63), 218sh (–22.55).
(*R*)-**13a**: t_R = 8.67 min on Chiralpak IC column (hexane/2-propanol 75:25), HPLC-ECD λ [nm] (ϕ): 336 (6.16), 267sh (4.48), 247sh (–6.74), 228 (–85.15), 223 (37.94), 218sh (26.31).

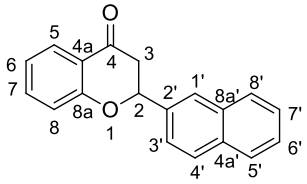

(±)-2-(2-Naphthyl)chromanone (13b):[2] white crystals, 675 mg (68 %) mp 108-110 °C, ^{1}H NMR (360 MHz, $CDCl_3$) δ: 2.90 (dd, *J* = 16.5, 2.5 Hz, 1H, 3-H_a), 3.09 (m, 1H, 3-H_b), 5.56 (dd, *J* = 13.3, 2.2 Hz, 1H, 2-H), 7.05 (m, 2H, 6-H, 8-H), 7.50 (m, 4H, 7-H, 6'-H, 7'-H, 8'-H), 7.88 (m, 5H, 5-H, 1'-H, 3'-H, 4'-H, 5'-H). ^{13}C NMR (90 MHz, $CDCl_3$) δ: 44.5 (C-3), 79.6 (C-2), 118.1 (C-8), 120.9 (C-4a), 121.6 (C-6), 123.6 (C-3'), 125.3 (C-1'), 126.5 (C-4', C-6'), 127.0 (C-7'), 127.7 (C-5), 128.1 (C-5'), 128.7 (C-8a'), 133.0 (C-4a'), 136.0 (C-2'), 136.1 (C-7), 161.4 (C-8a), 191.8 (C-4). HRMS (ESI) calculated for $C_{19}H_{14}NaO_2$ $[M + Na]^+$: 297.0886, found 297.0885.
(*S*)-**13b**: t_R = 7.57 min on Chiralpak IC column (hexane/2-propanol 75:25), HPLC-ECD λ [nm] (ϕ): 340 (1.86), 313 (–3.81), 249 (–3.16), 231 (2.88), 210 (17.62).
(*R*)-**13b**: t_R = 8.92 min on Chiralpak IC column (hexane/2-propanol 75:25),, HPLC-ECD λ [nm] (ϕ): 340 (–1.50), 313 (2.74), 249 (2.66), 231 (–2.63), 210 (–14.60).

1.3 General Procedure for the Preparation of 2*H*-chromenes (7a-d)

Method A

To the stirred solution of chroman-4-ol analogues **14a-d** (100 mg, 0.36 mmol) in acetone (10 mL), 1% HCl solution (20 µL) was added dropwise at room temperature. The reaction was refluxed for 1 h and the conversion was checked by TLC. After completion, the reaction mixture was diluted with water (10 mL) and ethyl-acetate (10 mL) was added. The organic layer was separated and dried over magnesium sulfate. Removal of the solvent under reduced pressure afforded the crude material as orange oil. The residue was purified by column chromatography on silica gel using hexane/ethyl acetate 6:1 as eluent.

Method B

A three necked flask was charged with cerium chloride heptahydrate (4.35 g, 11.68 mmol) and ethanol (15 mL). The mixture was stirred at room temperature under nitrogen to obtain a clear solution. THF (15 mL) was added followed by the addition of the chalcone analogues **12a-d** (1 g, 3.65 mmol). The reaction was cooled to approximately 2 °C (internal temperature), after which sodium borohydride (2.49 g, 65.8 mmol) was added in portions. The reaction was monitored by TLC. When the starting material disappeared, the mixture was quenched by the slow addition of 5 wt % citric acid solution. When the vigorous gas release had subsided, the mixture was refluxed for an additional 20 min, and then extracted with ethyl acetate. The solid material in the aqueous layer was dissolved by adding 1 M HCl (5 mL) and the aqueous phase was extracted with ethyl acetate. The combined organic layers were washed with saturated sodium bicarbonate and brine. The pH value of the final aqueous wash was ca 4–5. The organic layer was dried over $MgSO_4$. Removal of solvent afforded the crude product as orange oil, which was purified by column chromatography on silica using hexane/ethyl acetate 6:1 as eluent.

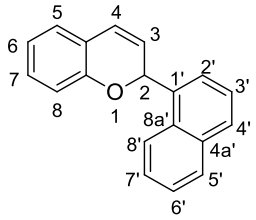

(±)-2-(1-Naphthyl)-2*H*-chromene (7a):[3] colorless oil, 547 mg (58 %), ^{1}H NMR (360 MHz, $CDCl_3$) δ: 5.88 (dd, *J* = 9.7, 3.2 Hz, 1 H, 3-H), 6.61 (m, 2 H, 2-H, 4-H), 6.77 (d, *J* = 7.9 Hz, 1 H, 8-H), 6.88 (m, 1 H, 6-H), 7.07 (m, 2 H, 5-H, 7-H), 7,41 (t, *J* = 7.2 Hz, 1 H, 3'-H), 7.52 (m, 2 H, 6'-H, 7'-H), 7.63 (d, *J* = 6.9 Hz, 1 H, 2'-H), 7.81 (d, *J* = 7.9 Hz, 1 H, 5'-H), 7.86 (d, *J* = 9 Hz, 1 H, 4'-H), 8.29 (d, *J* = 8.3 Hz, 1 H, 8'-H). ^{13}C NMR (90 MHz, $CDCl_3$) δ: 74.7 (C-2), 116.0 (C-8), 121.2 (C-6), 121.5 (C-4a), 123.9 (C-4), 124.7 (C-3), 124.8 (C-6'), 125.2 (C-8'), 125.6 (C-5'), 125.7 (C-3'), 126.2 (C-2'), 126.6 (C-7'), 128.7 (C-4'), 129.0 (C-5'), 129.3 (C-7), 130.8 (C-8a'), 134.0 (C-4a'), 135.3 (C-1'), 153.4 (C-8a).

(*R*)-**7a**: t_R = 10.67 min on Chiralcel OD column (hexane/2-propanol 95:5), HPLC-ECD λ [nm] (ϕ): 314sh (3.11), 283 (5.14), 258sh (–6.69), 227 (32.55), 214 (39.27).

(*S*)-**7a**: t_R = 11.33 min on Chiralcel OD column (hexane/2-propanol 95:5), HPLC-ECD λ [nm] (ϕ): 314sh (–3.67), 283 (–5.49), 258sh (6.43), 227 (32.40), 214 (–44.47).

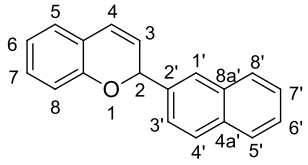

(±)-2-(2-Naphthyl)-2*H*-chromene (7b):[3] colorless oil, 424 mg (45 %), ^{1}H NMR (360 MHz, $CDCl_3$) δ: 5.82 (dd, *J* = 9.7, 3.2 Hz, 1 H, 3-H), 6.06 (s, 1 H, 2-H), 6.54 (dd, *J* = 9.7, 1.1 Hz, 1 H, 4-H) 6.79 (d, *J* = 7.9 Hz, 1 H, 8-H), 6.86 (t, *J* = 7.2 Hz, 1 H, 6-H), 7.00 (dd, *J* = 7.2, 1.1 Hz, 1 H, 3'-H), 7.10 (m, 1 H, 7-H), 7.46 (m, 2 H, 6'-H, 7'-H), 7.57 (dd, *J* = 8.6, 1.4 Hz, 1 H, 4'-H), 7.82 (m, 4 H, 5-H, 1'-H, 5'-H, 8'-H). ^{13}C NMR (90 MHz, $CDCl_3$) δ: 77.2 (C-2), 116.0 (C-8), 121.2 (C-6), 121.3 (C-4a), 124.2 (C-4), 124.9 (C-1'), 126.0 (C-5), 126.2 (C-6', C-7'), 126.6 (C-3'), 127.7 (C-8'), 128.2 (C-5'), 128.6 (C-4'), 129.5 (C-7), 133.2 (C-4a'), 133.3 (C-8a'), 138.0 (C-2'), 153.2 (C-8a).

(*S*)-**7b**: t_R = 3.31 min on Chiralpak IA column (hexane/2-propanol 95:5), HPLC-ECD λ [nm] (ϕ): 315 (–11.60), 259 (–26.40), 235 (10.60), 220 (–21.50), 209 (64.35).

(*R*)-**7b**: t_R = 3.57 min on Chiralpak IA column (hexane/2-propanol 95:5), HPLC-ECD λ [nm] (ϕ): 315 (8.95), 259 (21.64), 235 (–9.41), 220 (20.21), 209 (–65.49).

1.4 General Procedure for the Synthesis of Chroman-4-ol derivatives (14a-d)

To the stirred solution of flavanone analogues **13a-d** (500 mg, 1.81 mmol) in ethanol (30 mL), $NaBH_4$ (103 mg, 2.72 mmol) was added at room temperature. The reaction was monitored by TLC and after completion, the reaction mixture was diluted with water (20 mL), acidified with 10 % HCl solution (pH 6) and extracted with ethyl acetate. The combined organic layers were dried over anhydrous $MgSO_4$, filtered and concentrated. The residue was purified by column chromatography on silica gel using hexane/ethyl acetate 2:1 as eluent.

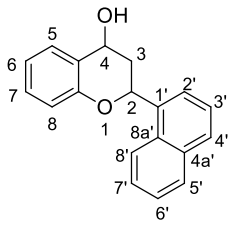

(±)-2-(1-Naphthyl)chroman-4-ol (14a):[4] white crystals, 345 mg (69 %), mp 117-119 °C, ^{1}H NMR (360 MHz, $CDCl_3$) δ: 2.21 (m, 2 H, 3-H_a, OH), 2.57 (dd, *J* = 12.9, 6.1 Hz, 1 H, 3-H_b), 5.10 (dd, *J* =9.7, 6.1 Hz, 1 H, 4-H), 5.80 (d, *J* = 11.5 Hz, 1 H, 2-H), 6.90 (d, *J* = 7.9 Hz, 1 H, 8-H), 6.97 (t, *J* = 7.2 Hz, 1 H, 6-H), 7.19 (t, *J* = 6.8 Hz, 1 H, 7-H), 7.49 (m, 4 H, 2'-H, 3'-H, 6'-H, 7'-H), 7.66 (d, *J* = 7.2 Hz, 1 H, 5-H), 7.82 (m, 2 H, 5-H, 4'-H), 7.98 (m, 1 H, 8'-H). ^{13}C NMR (90 MHz, $CDCl_3$) δ: 38.9 (C-3), 66.0 (C-4), 73.9 (C-2), 116.8 (C-8), 121.1 (C-6), 122.8

(C-6'), 123.5 (C-7'), 125.5 (C-8'), 125.7 (C-3'), 126.0 (C-4a), 126.4 (C-4'), 127.1 (C-2'), 128.7 (C-5), 129.0 (C-5'), 129.2 (C-7), 130.3 (C-8a'), 133.8 (C-4a'), 135.7 (C-1'), 154.6 (C-8a). HRMS (ESI) calculated for $C_{19}H_{16}NaO_2$ $[M + Na]^+$: 299.1043, found 299.1043.

1.5 References of known compounds

1. B. M. Muller, T. J. Litberg, R. A. Yocum, C. A. Pniewski and M. J. Adler, *J. Org. Chem.*, 2016, **81**, 5775-5781.
2. V. Kavala, C. C. Lin, C. W. Kuo, H. L. Fang and C. F. Yao, *Tetrahedron*, 2012, **68**, 1321-1329.
3. T. J. A. Graham and A. G. Doyle, *Org. Lett.*, 2012, **14**, 1616-1619.
4. D. Zhao, B. Beiring and F. Glorius, *Angew. Chem. Int. Ed.*, 2013, **52**, 8454-8458.

2 NMR and IR Spectra

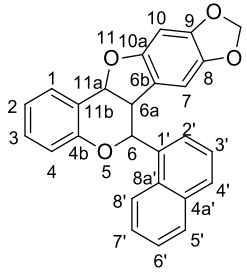

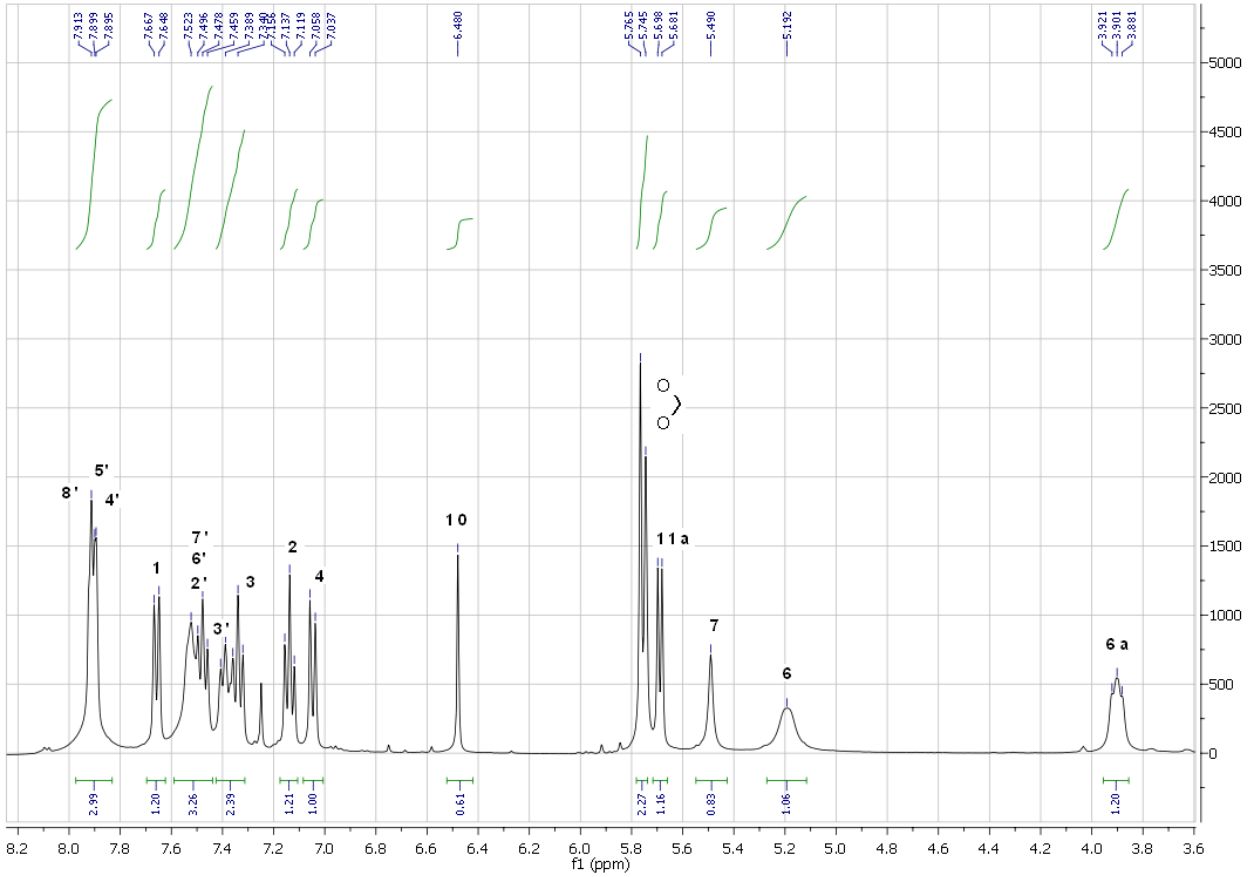

Figure S1. ^{1}H NMR (400 MHz) spectrum of **9a** in $CDCl_3$

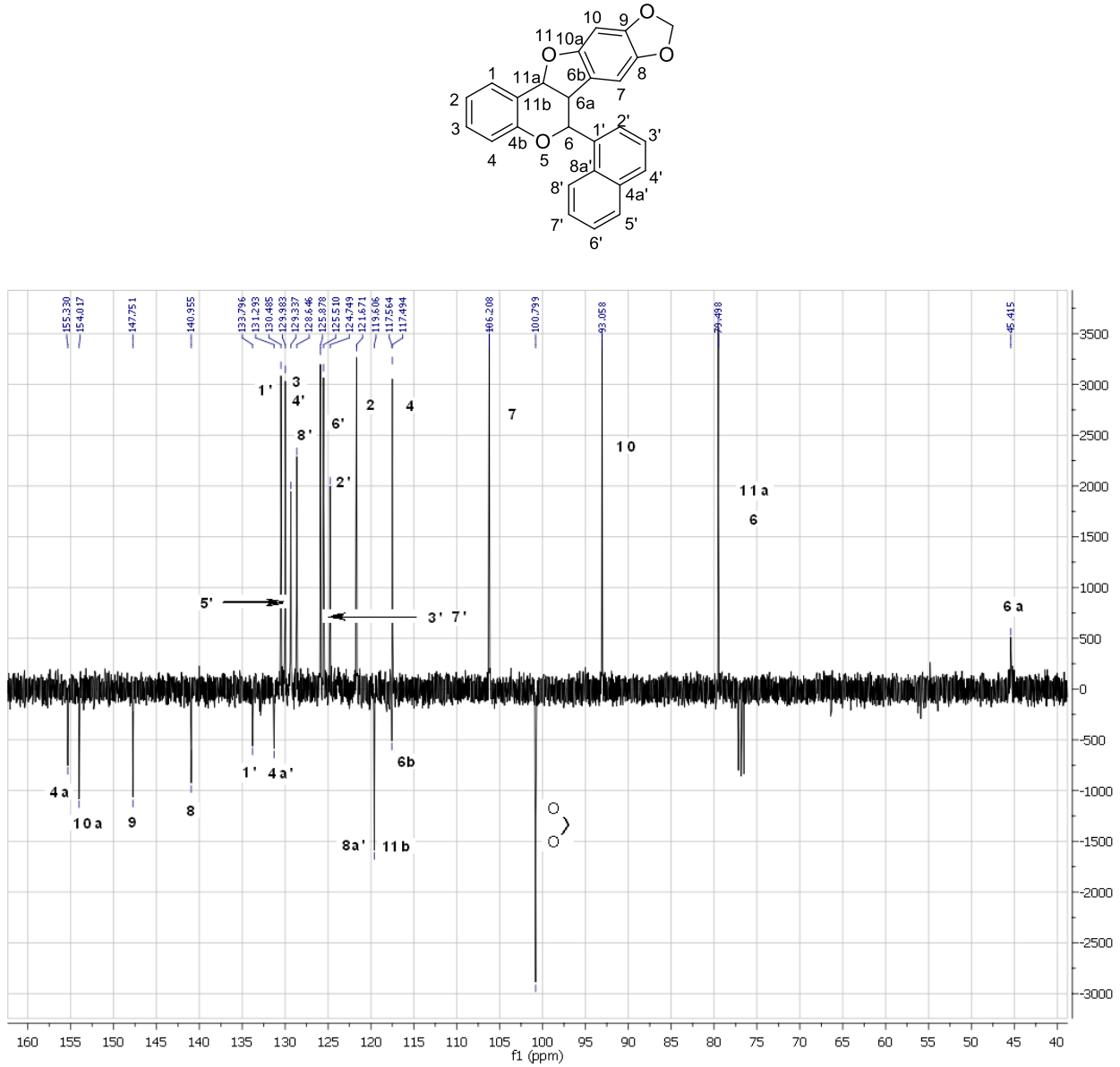

Figure S2. ^{13}C NMR (100 MHz) spectrum of **9a** in $CDCl_3$

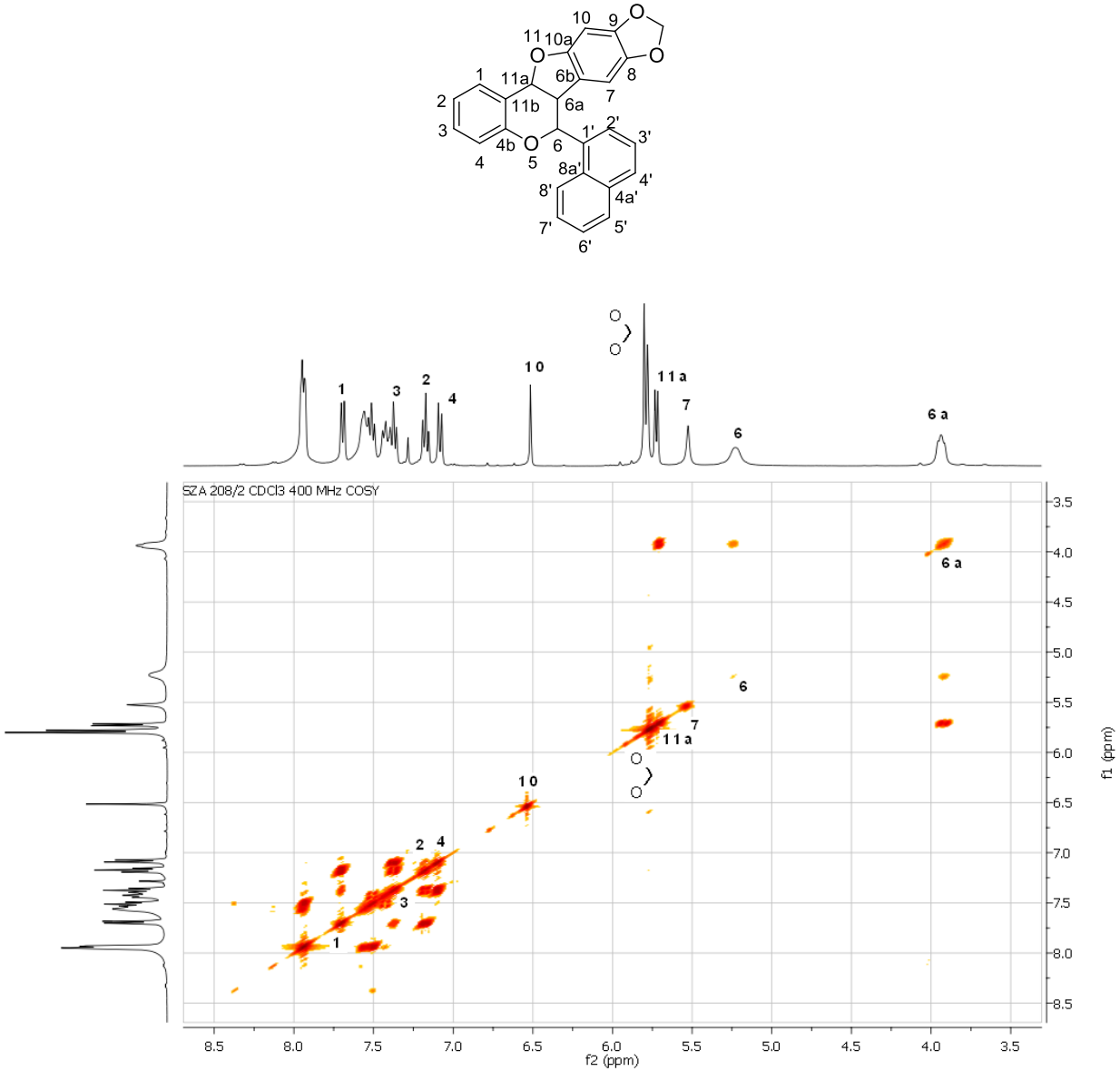

Figure S3. COSY spectrum of **9a** in $CDCl_3$

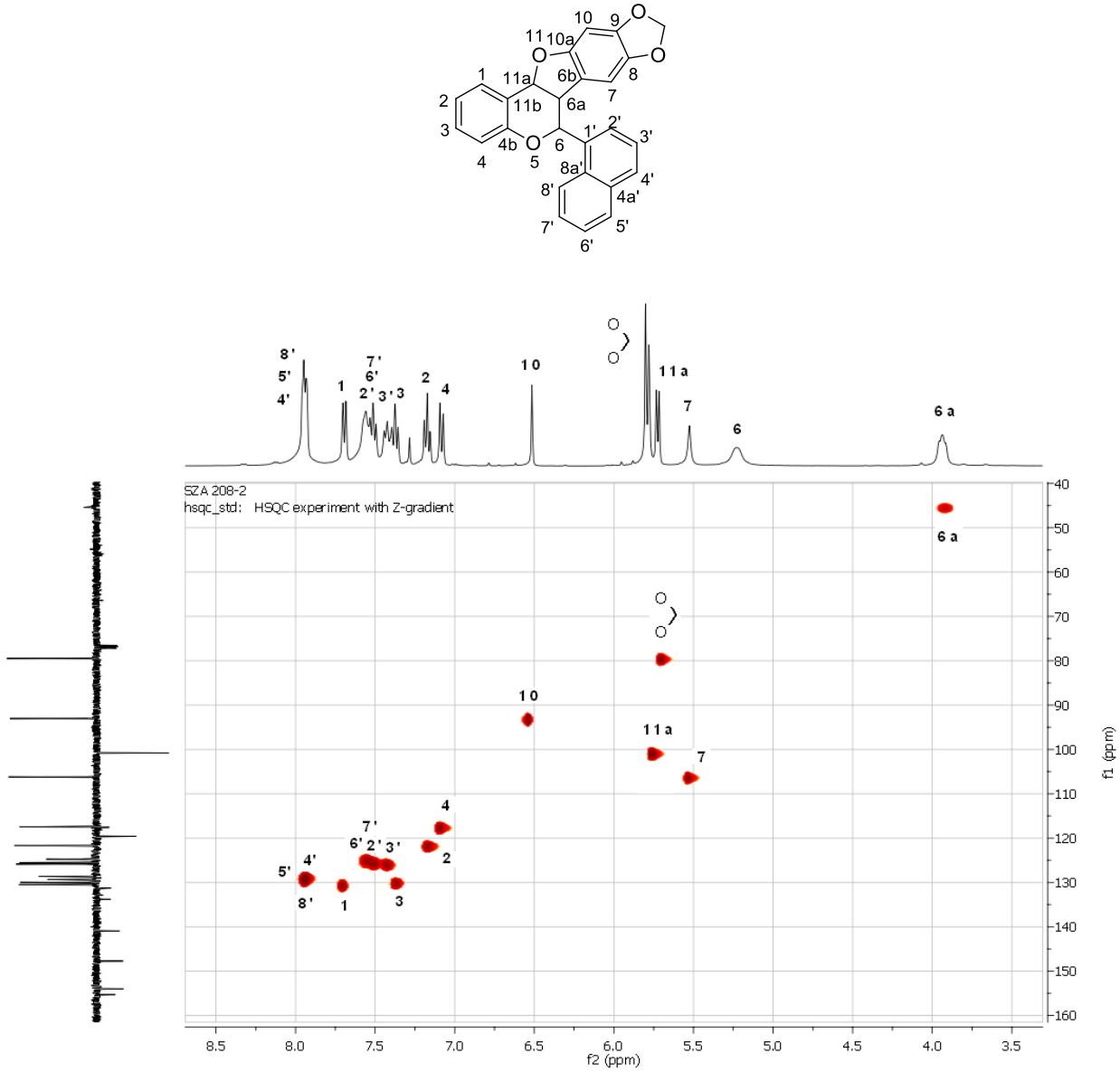

Figure S4. HSQC spectrum of **9a** in $CDCl_3$

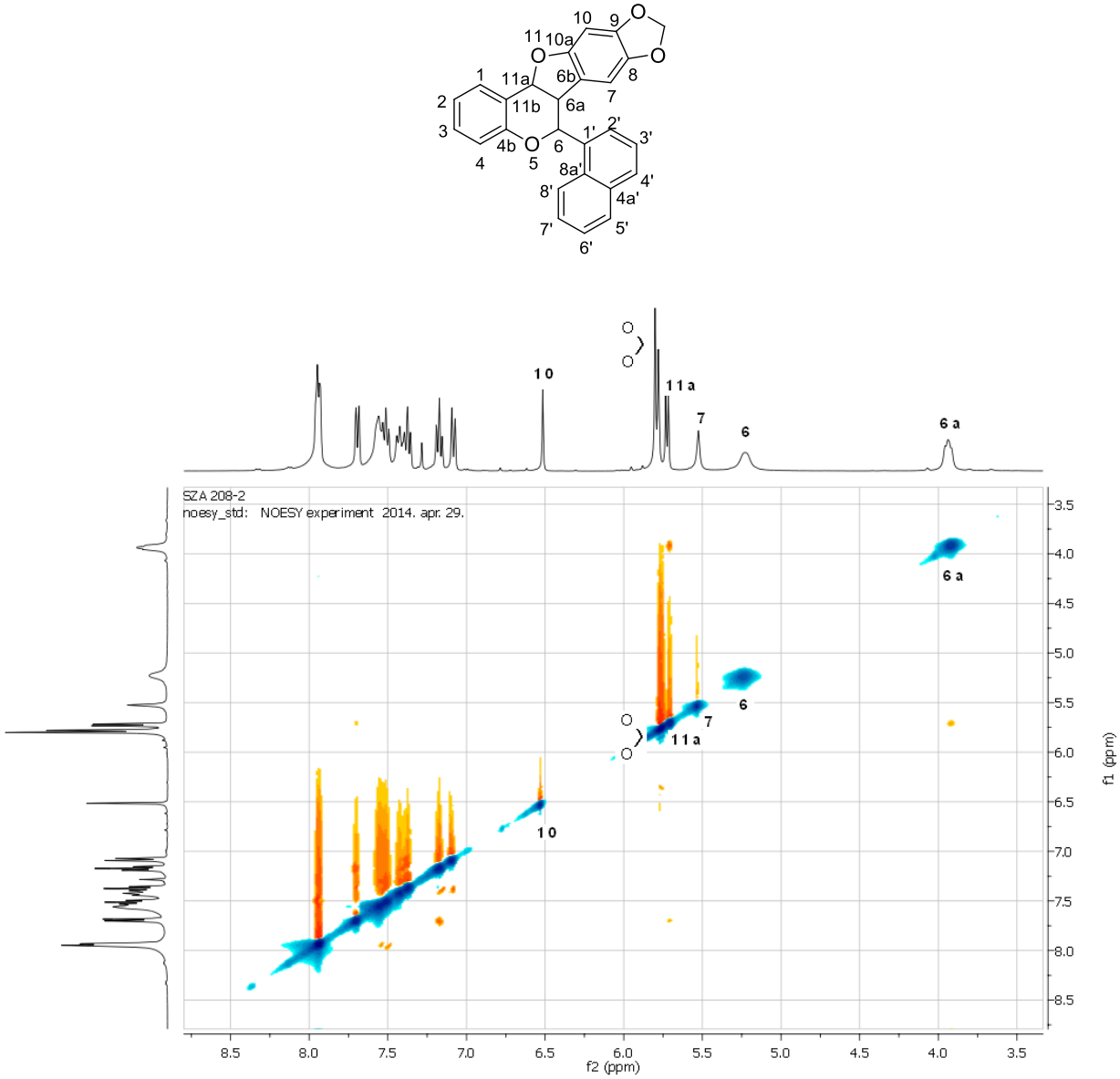

Figure S5. NOESY spectrum of **9a** in $CDCl_3$

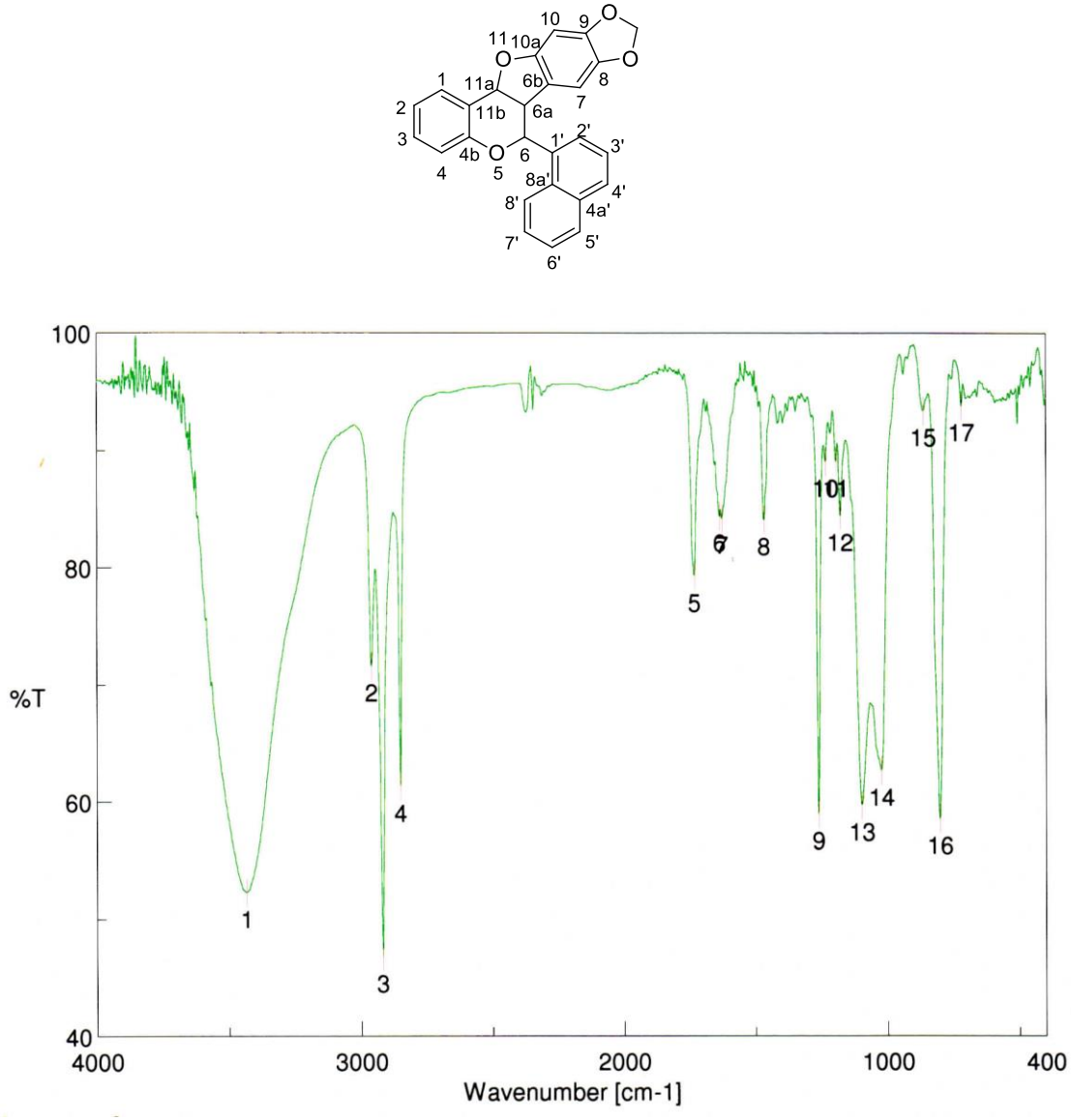

Figure S6. IR spectrum of **9a** recorded as KBr disc

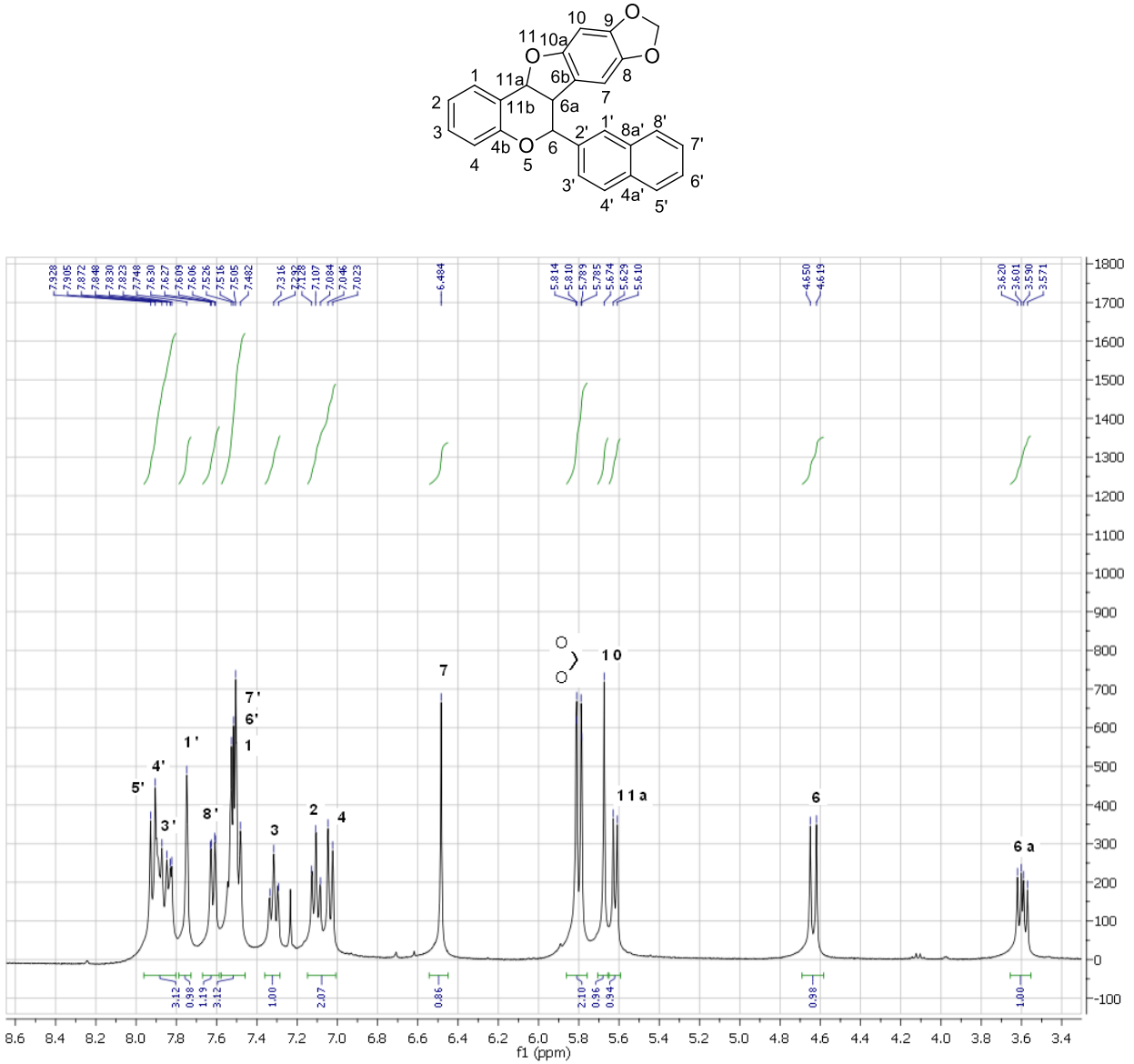

Figure S7. ^{1}H NMR (360 MHz) spectrum of **9b** in $CDCl_3$

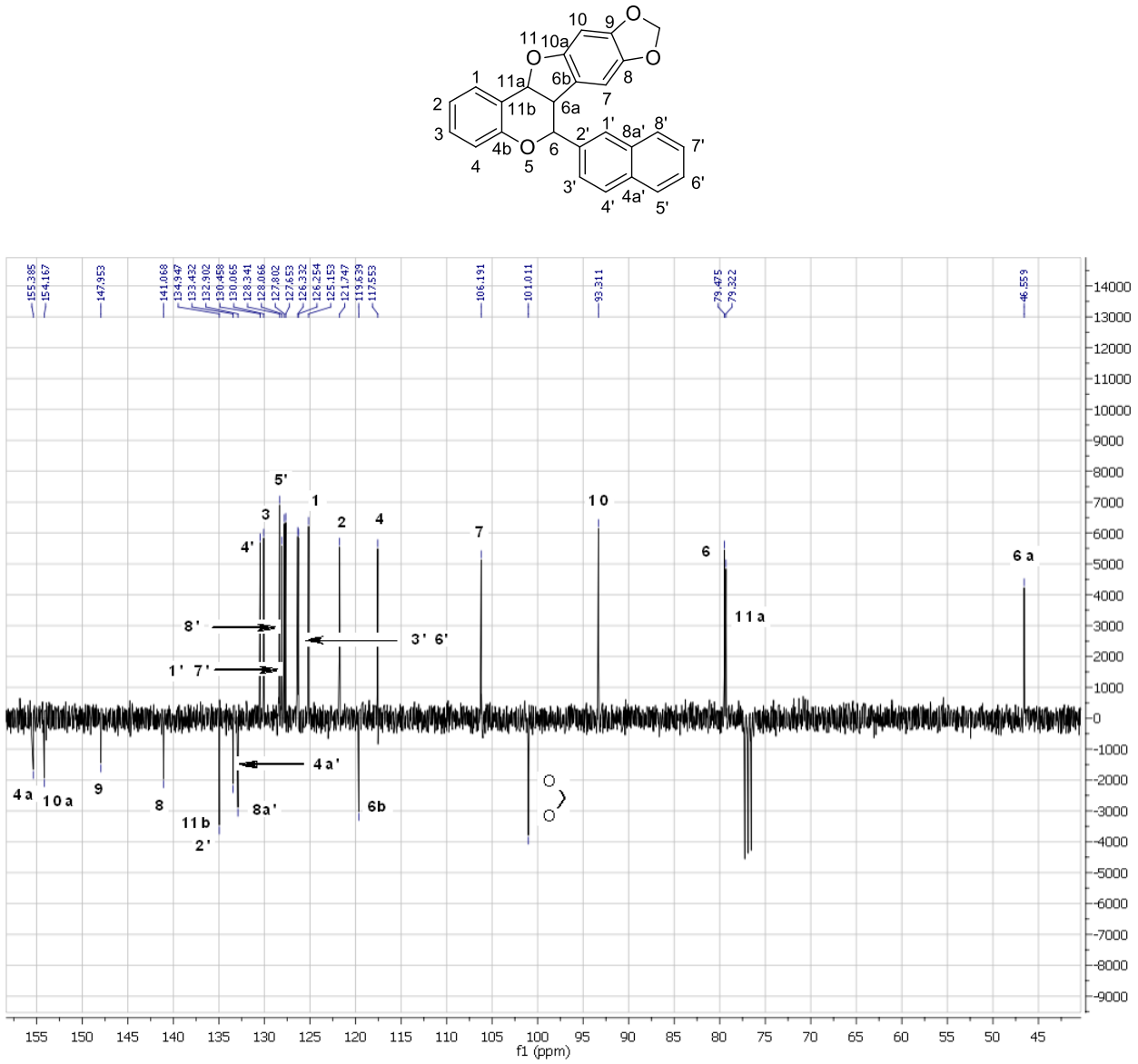

Figure S8. ^{13}C NMR (90 MHz) spectrum of **9b** in $CDCl_3$

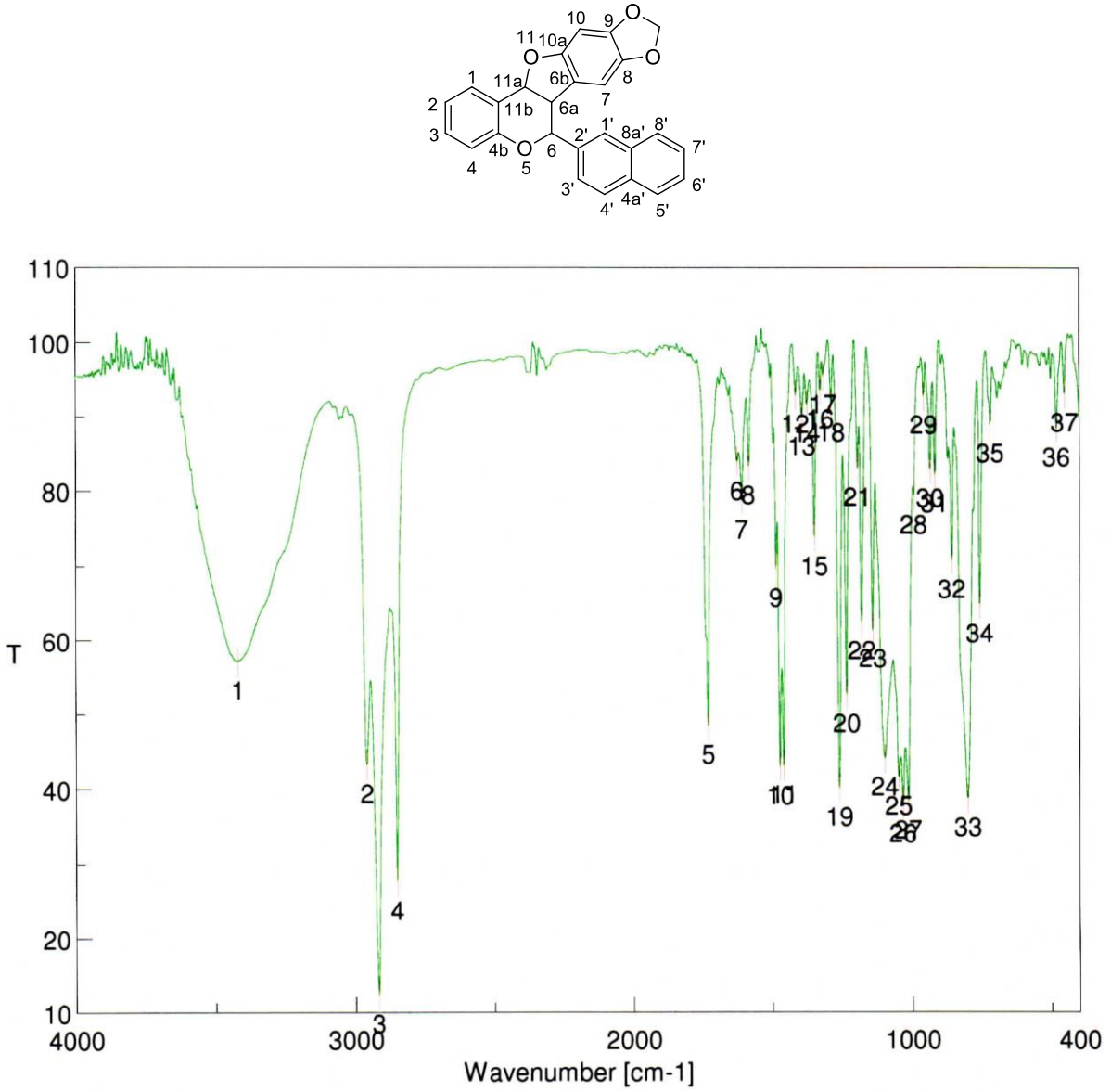

Figure S9. IR spectrum of **9b** recorded as KBr disc

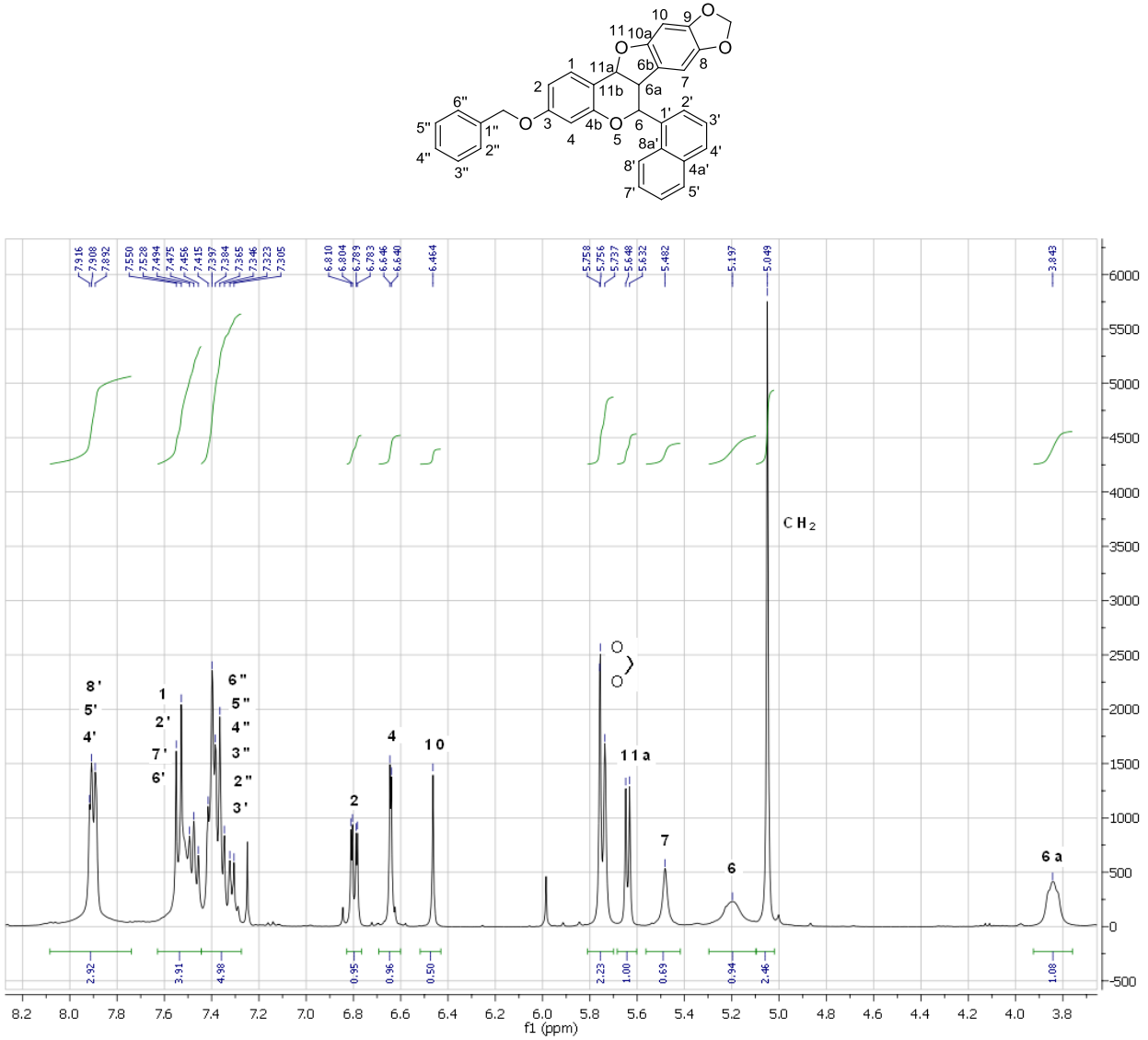

Figure S10. ^{1}H NMR (400 MHz) spectrum of **9c** in $CDCl_3$

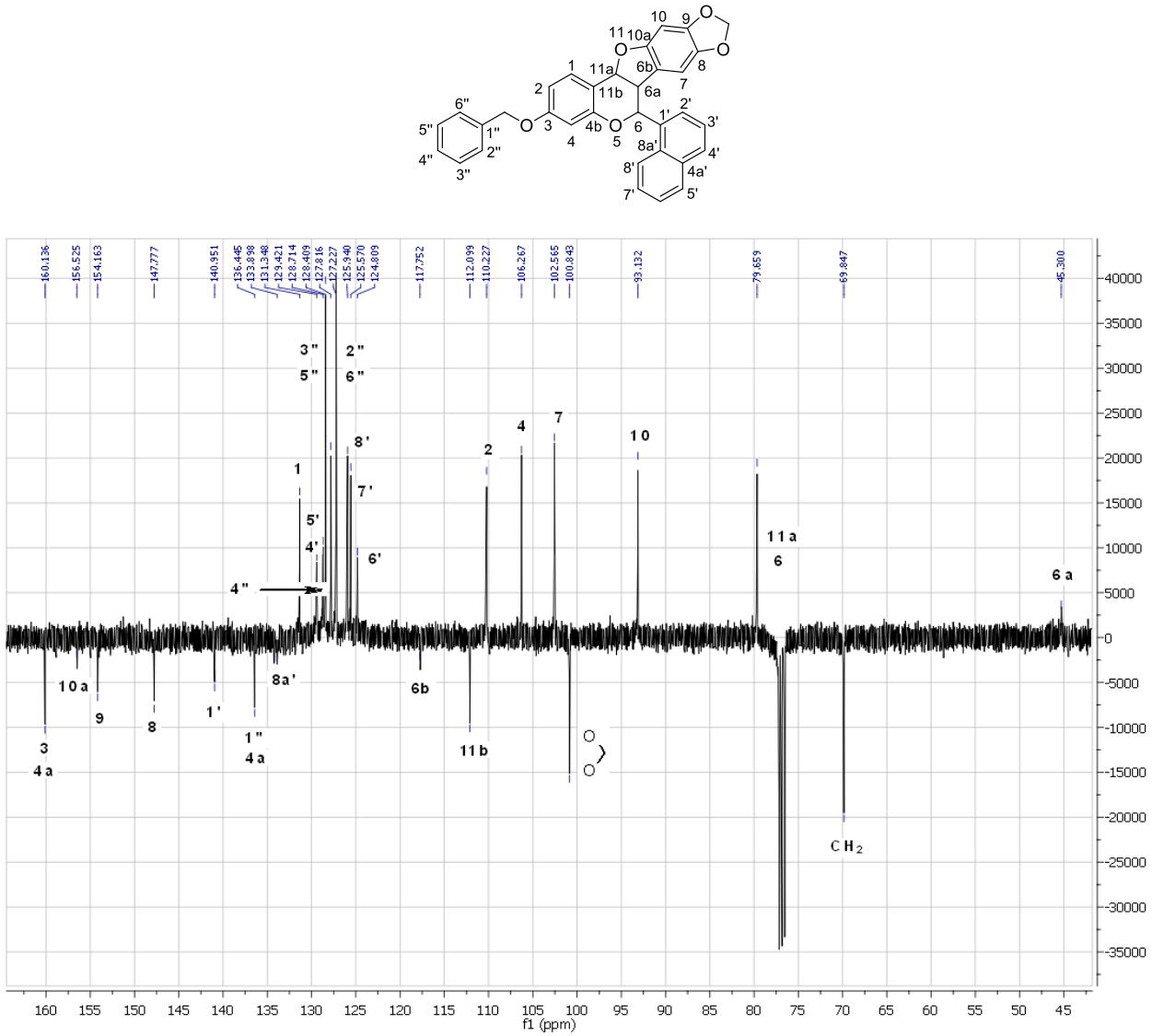

Figure S11. ^{13}C NMR (100 MHz) spectrum of **9c** in $CDCl_3$

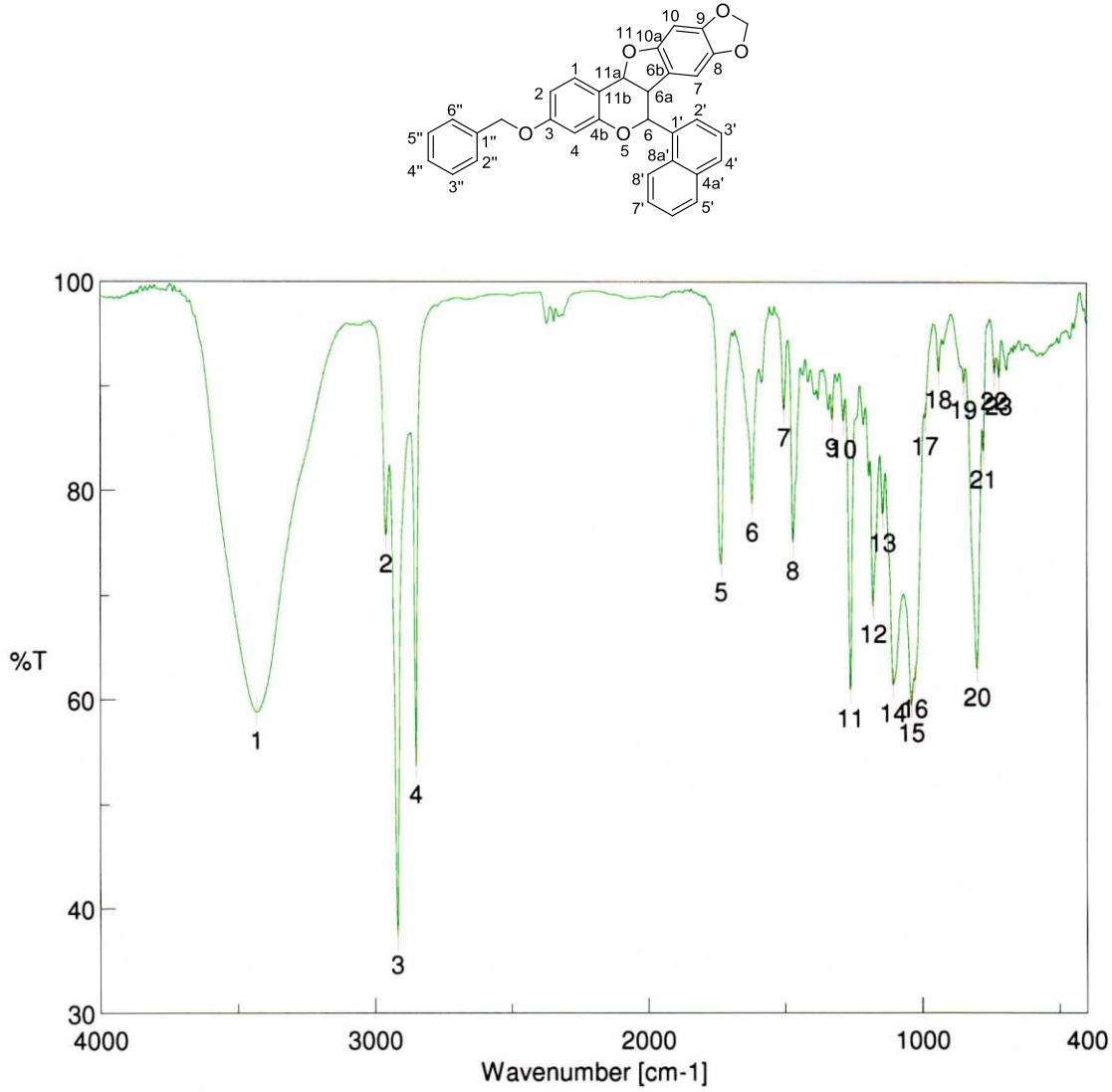

Figure S12. IR spectrum of **9c** recorded as KBr disc

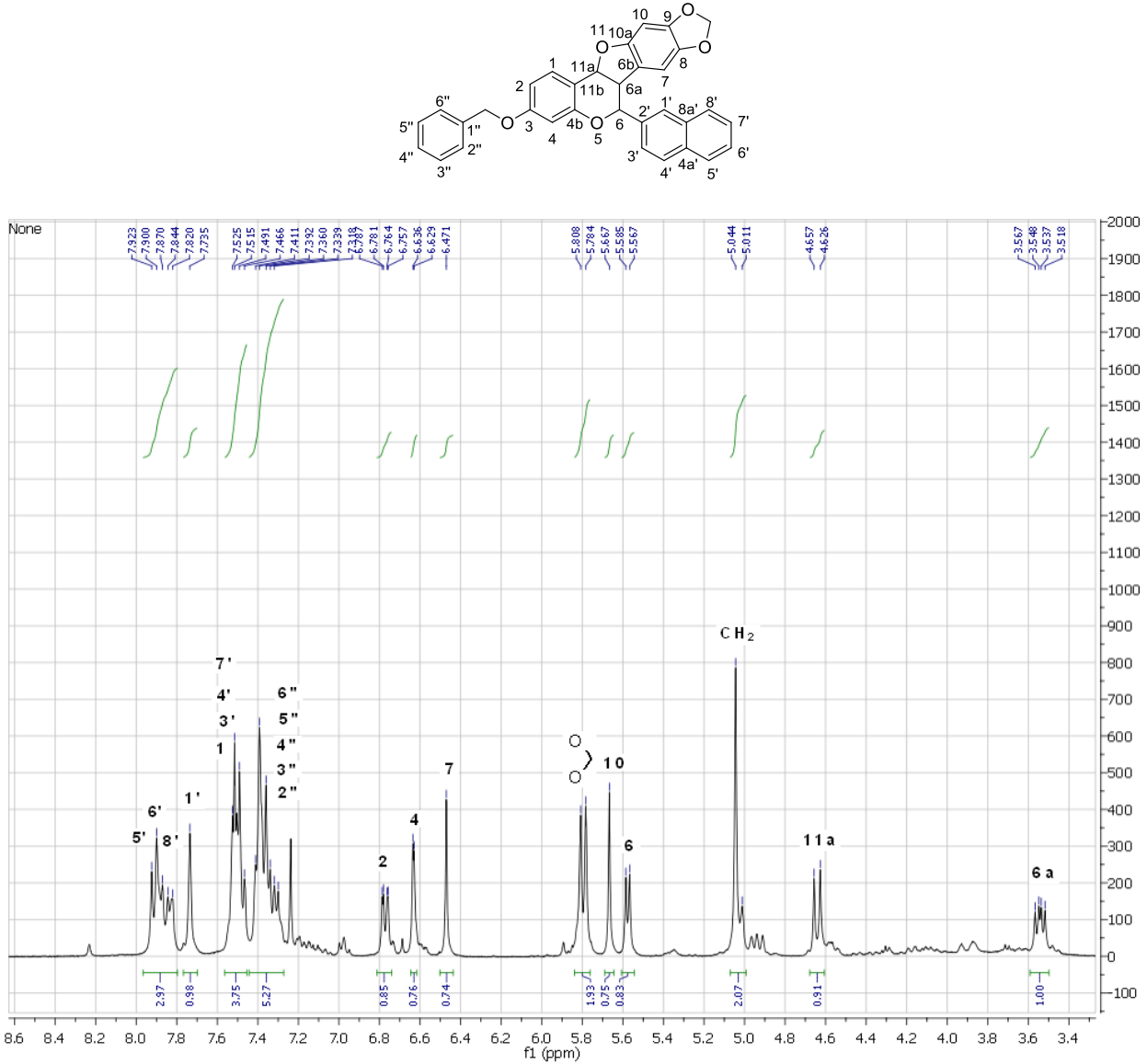

Figure S13. ^{1}H NMR (360 MHz) spectrum of **9d** in $CDCl_3$

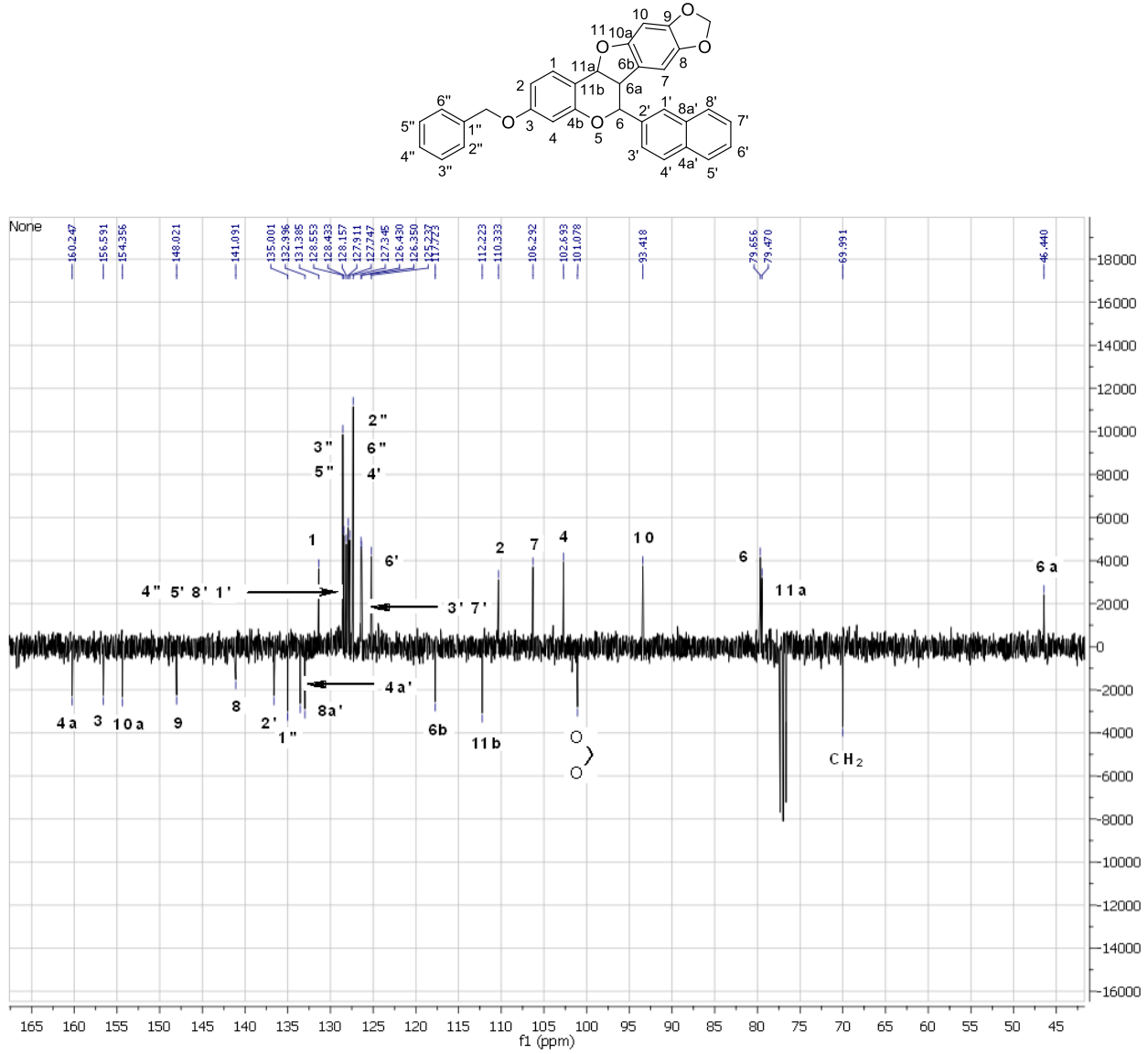

Figure S14. ^{13}C NMR (90 MHz) spectrum of **9d** in $CDCl_3$

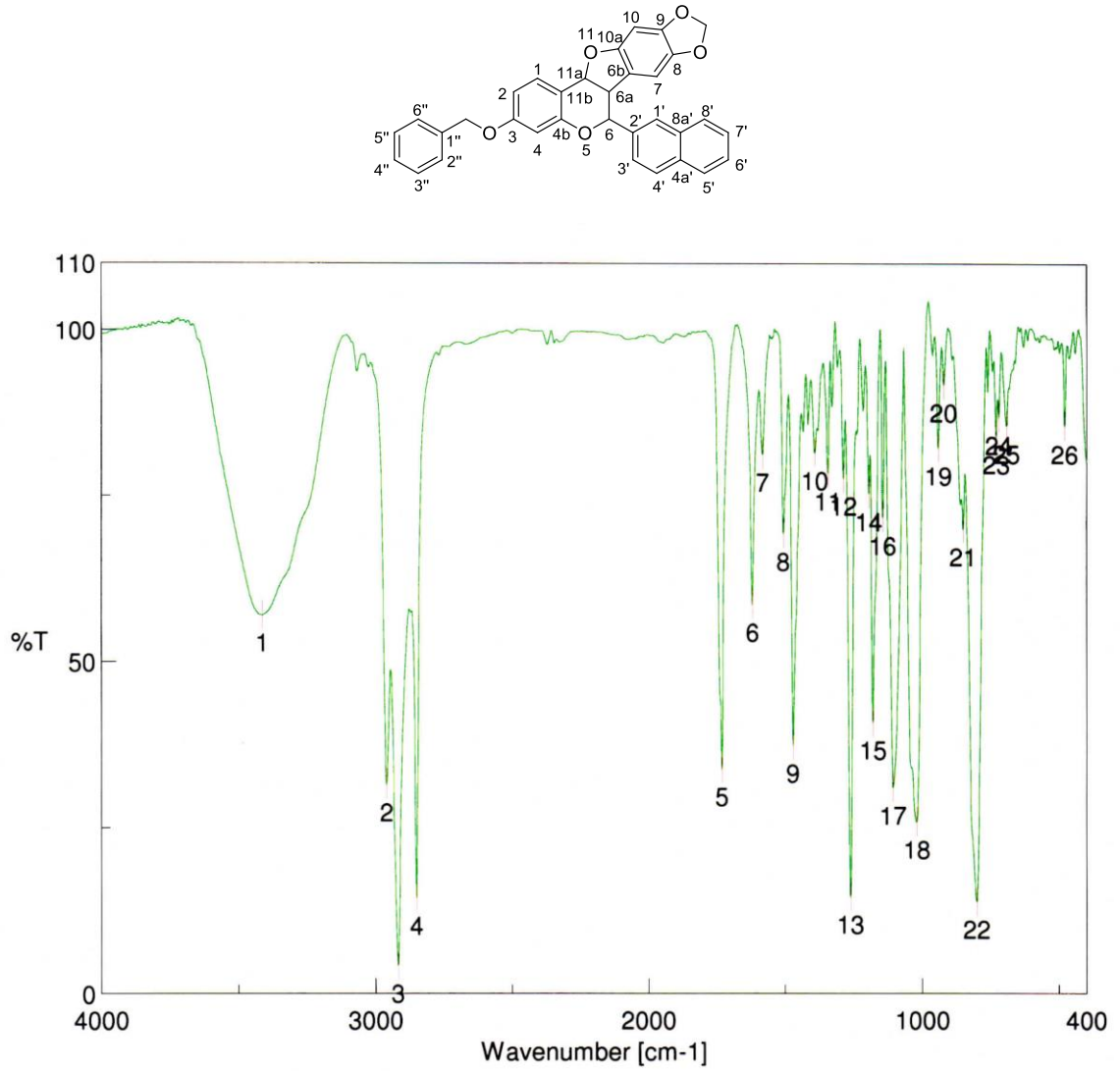

Figure S15. IR spectrum of **9d** recorded as KBr disc

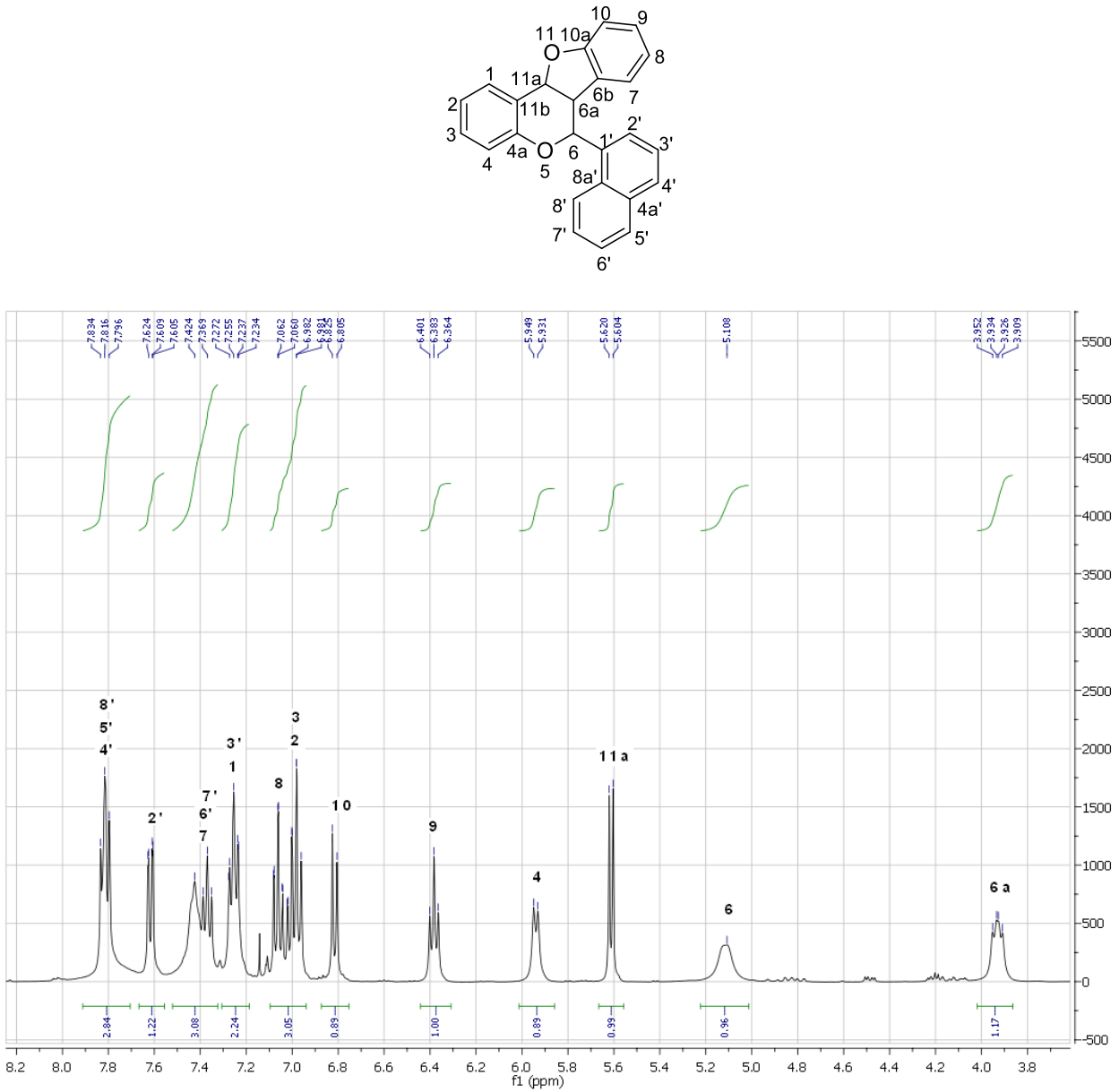

Figure S13. ^{1}H NMR (400 MHz) spectrum of **17** in $CDCl_3$

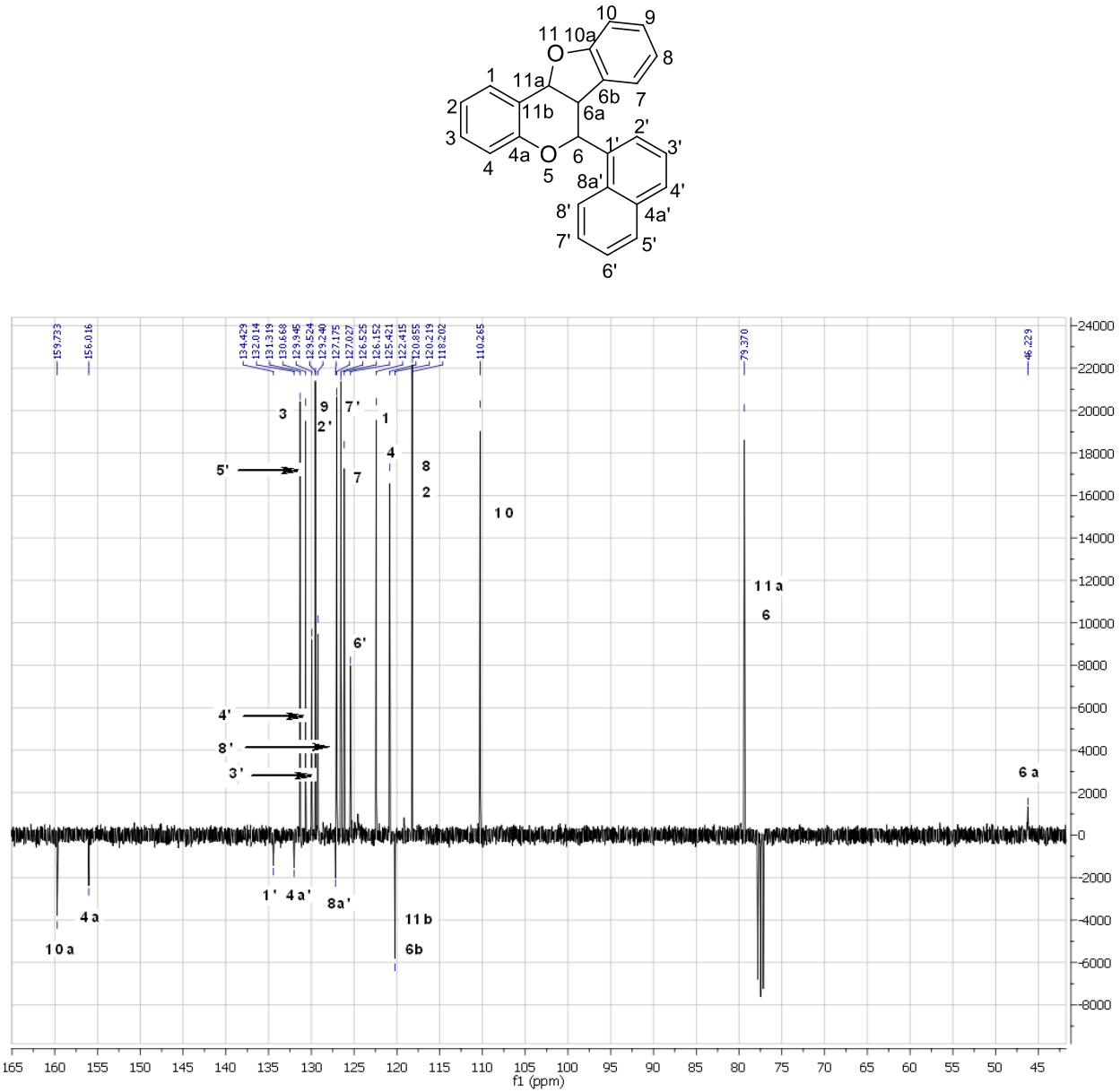

Figure S14. ^{13}C NMR (100 MHz) spectrum of **17** in $CDCl_3$

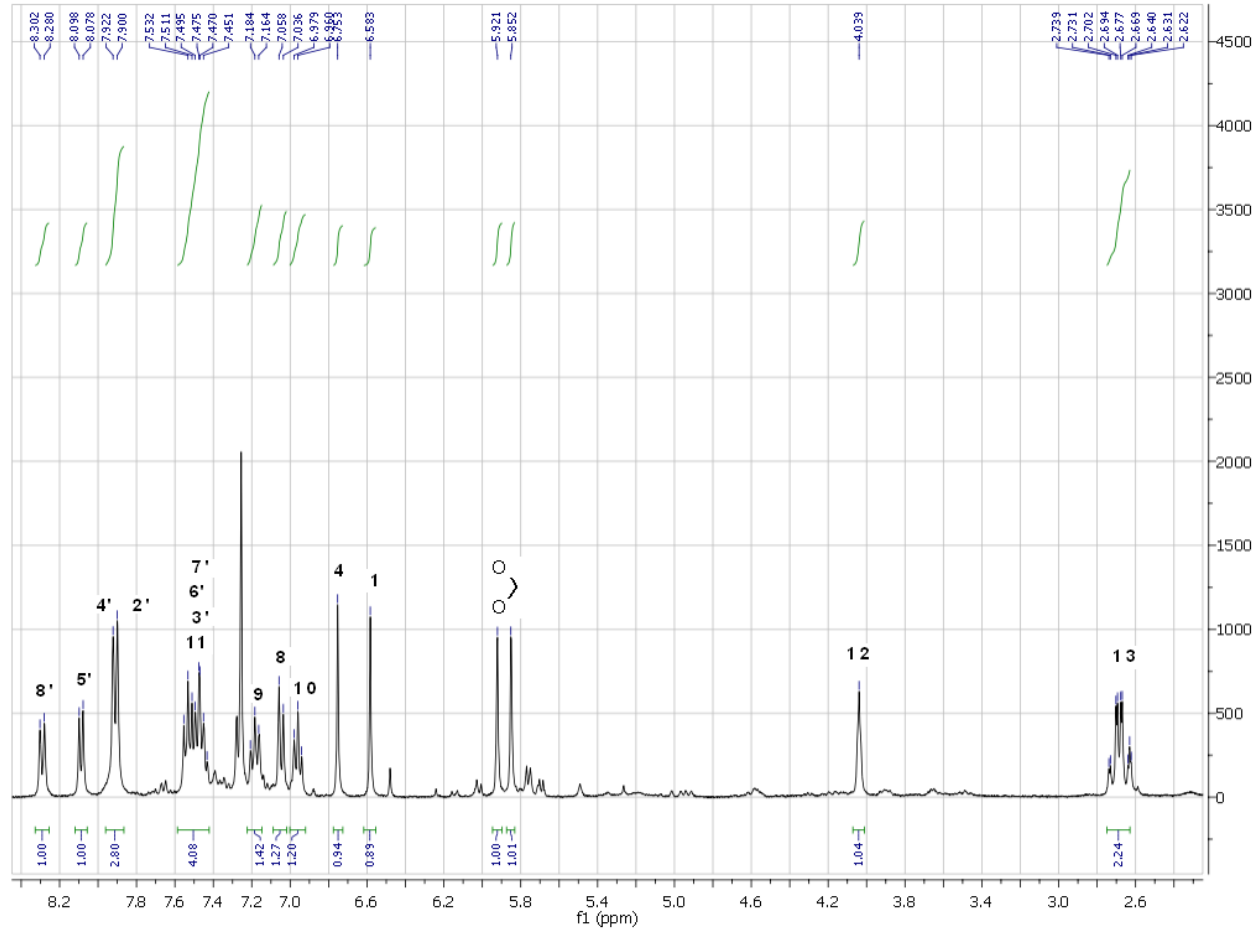

Figure S16. ^{1}H NMR (360 MHz) spectrum of **10a** in $CDCl_3$

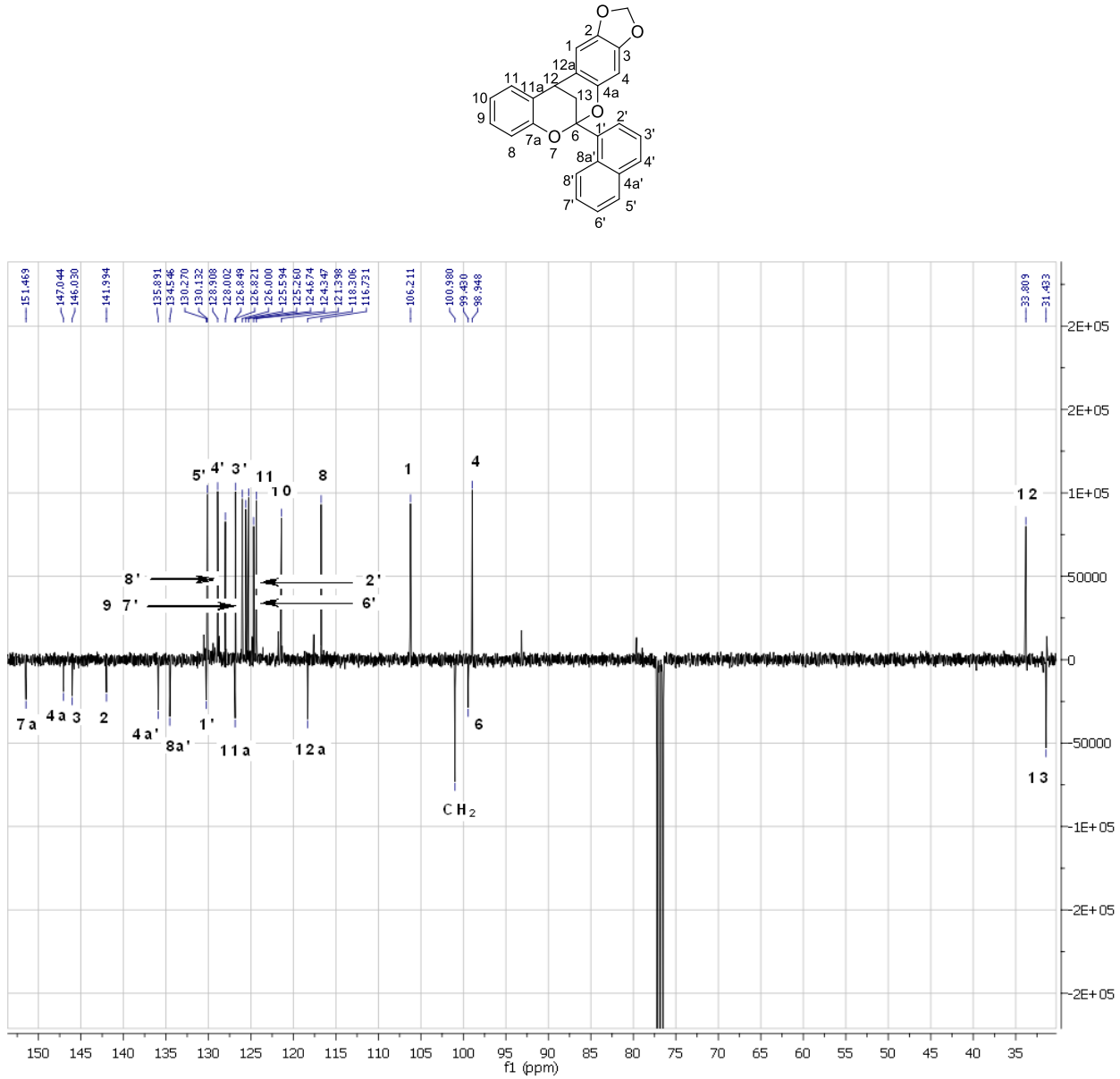

Figure S17. ^{13}C NMR (90 MHz) spectrum of **10a** in $CDCl_3$

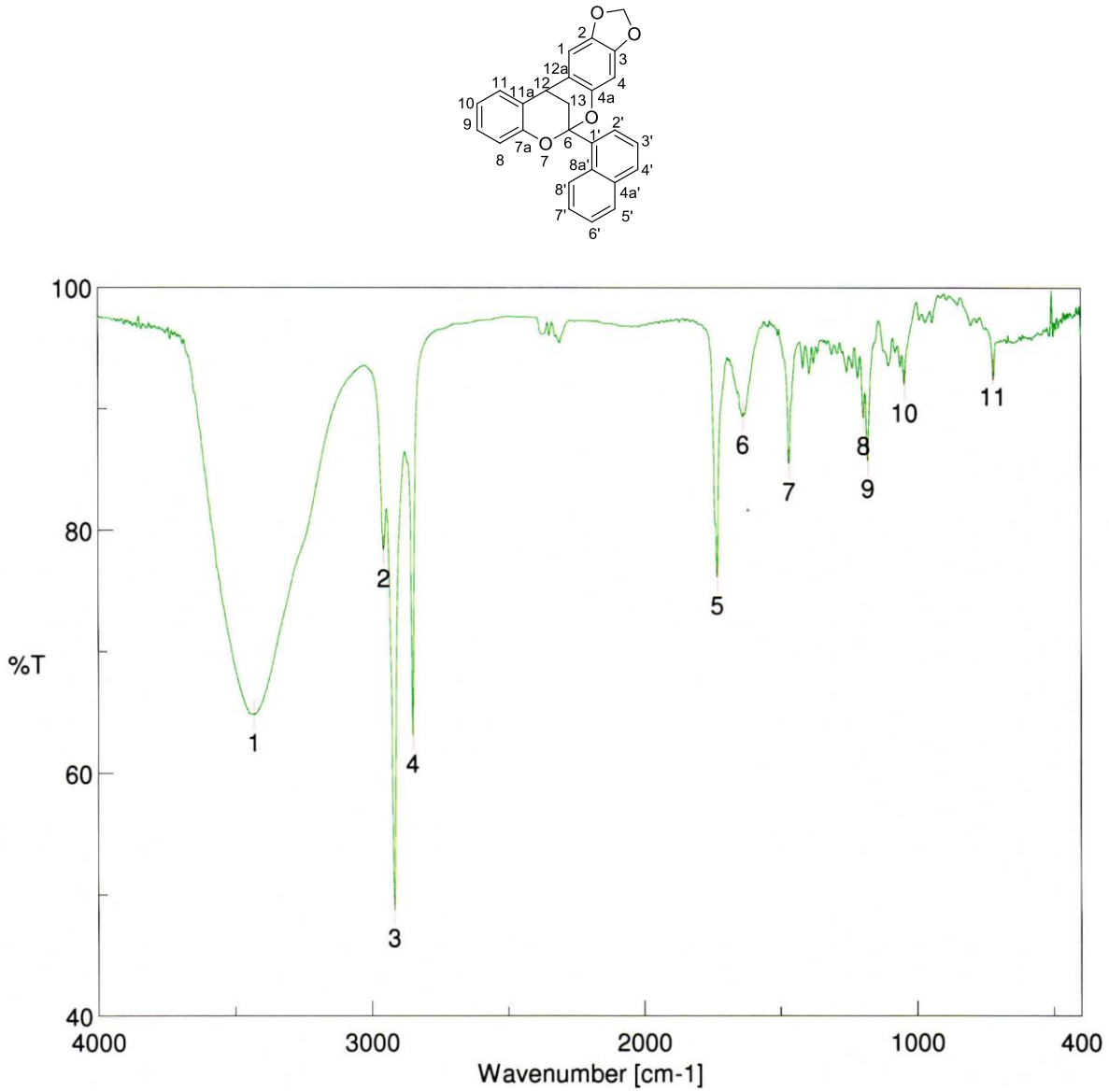

Figure S18. IR spectrum of **10a** recorded as KBr disc

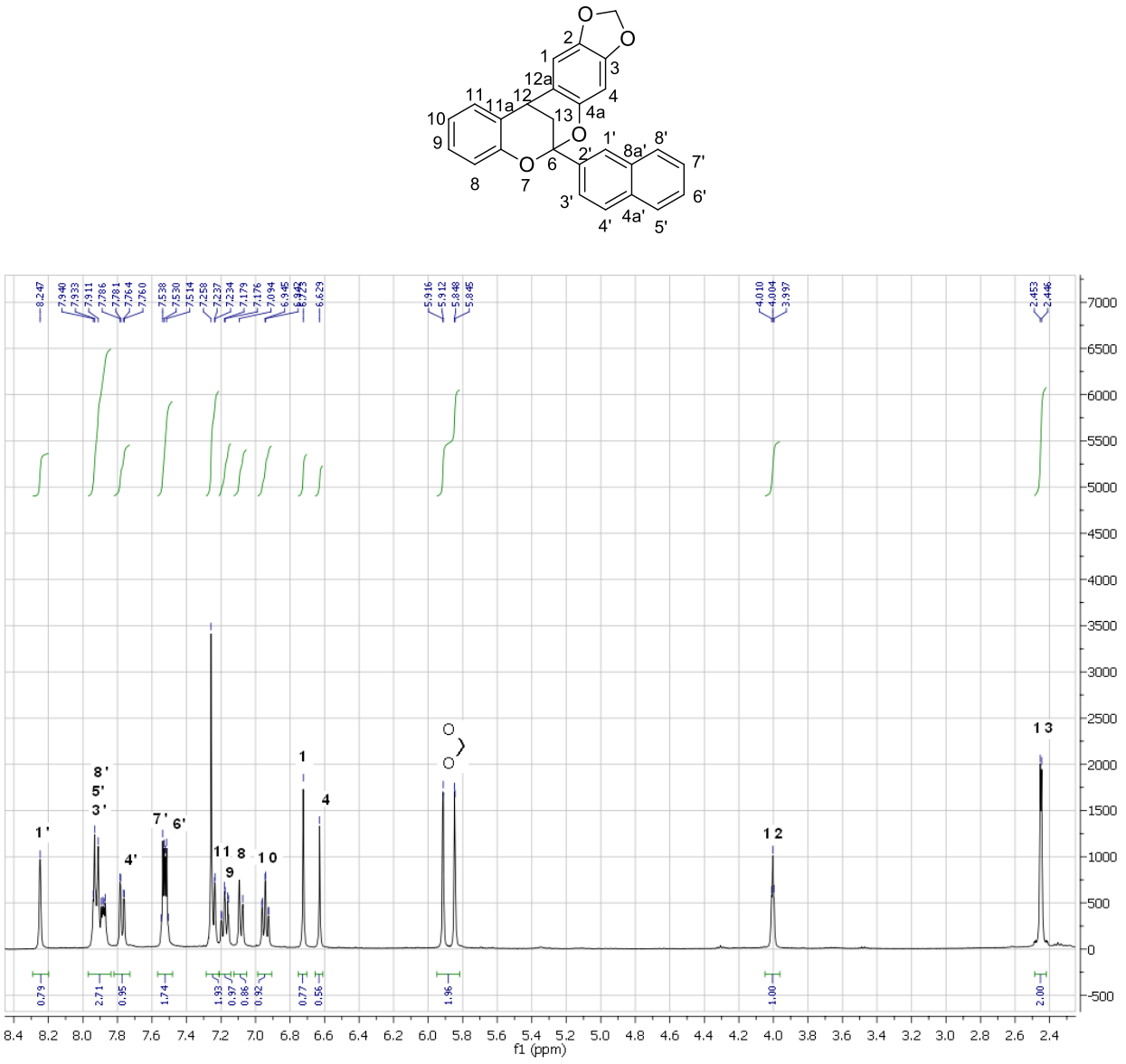

Figure S19. ^{1}H NMR (400 MHz) spectrum of **10b** in $CDCl_3$

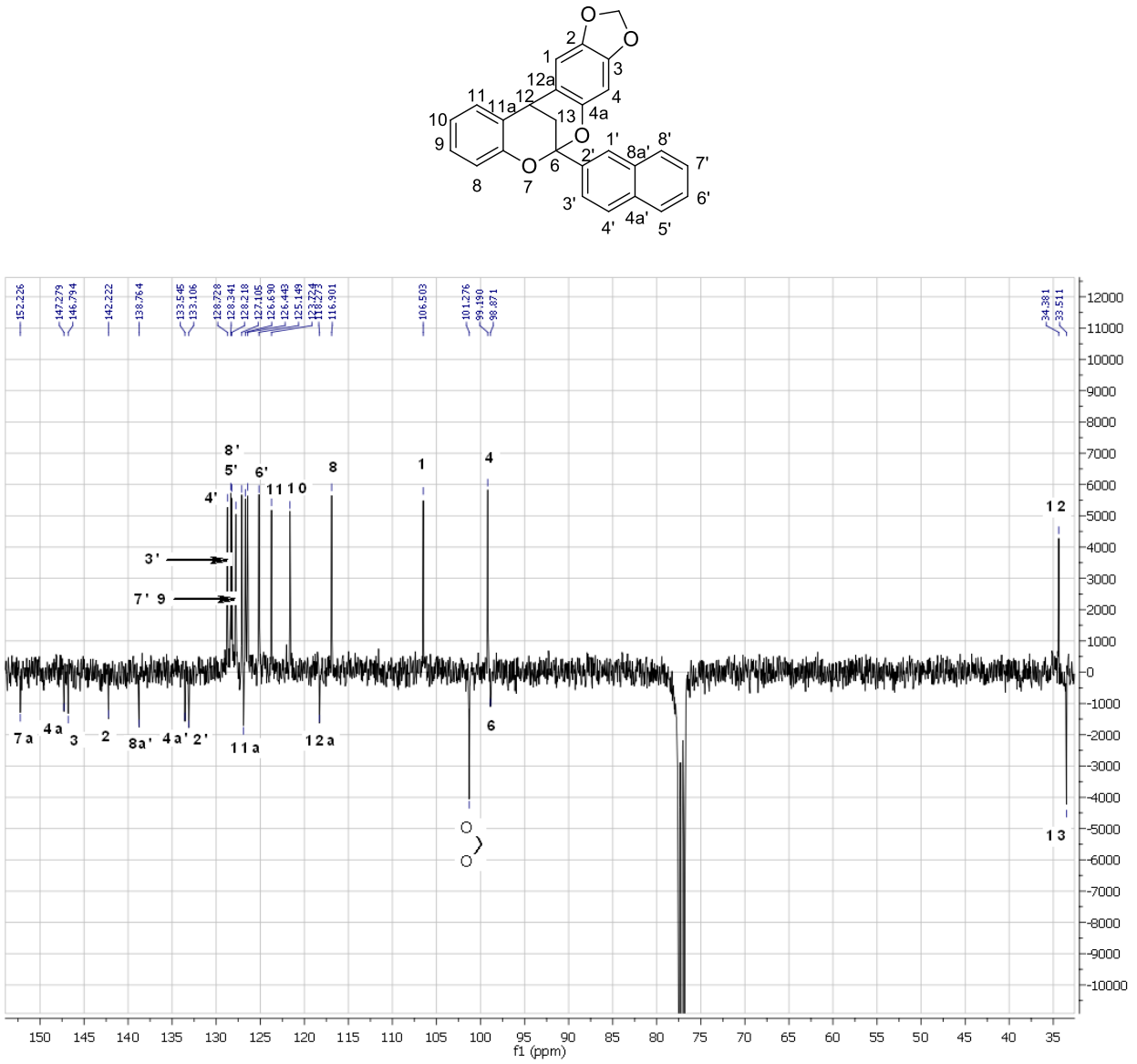

Figure S20. ^{13}C NMR (100 MHz) spectrum of **10b** in $CDCl_3$

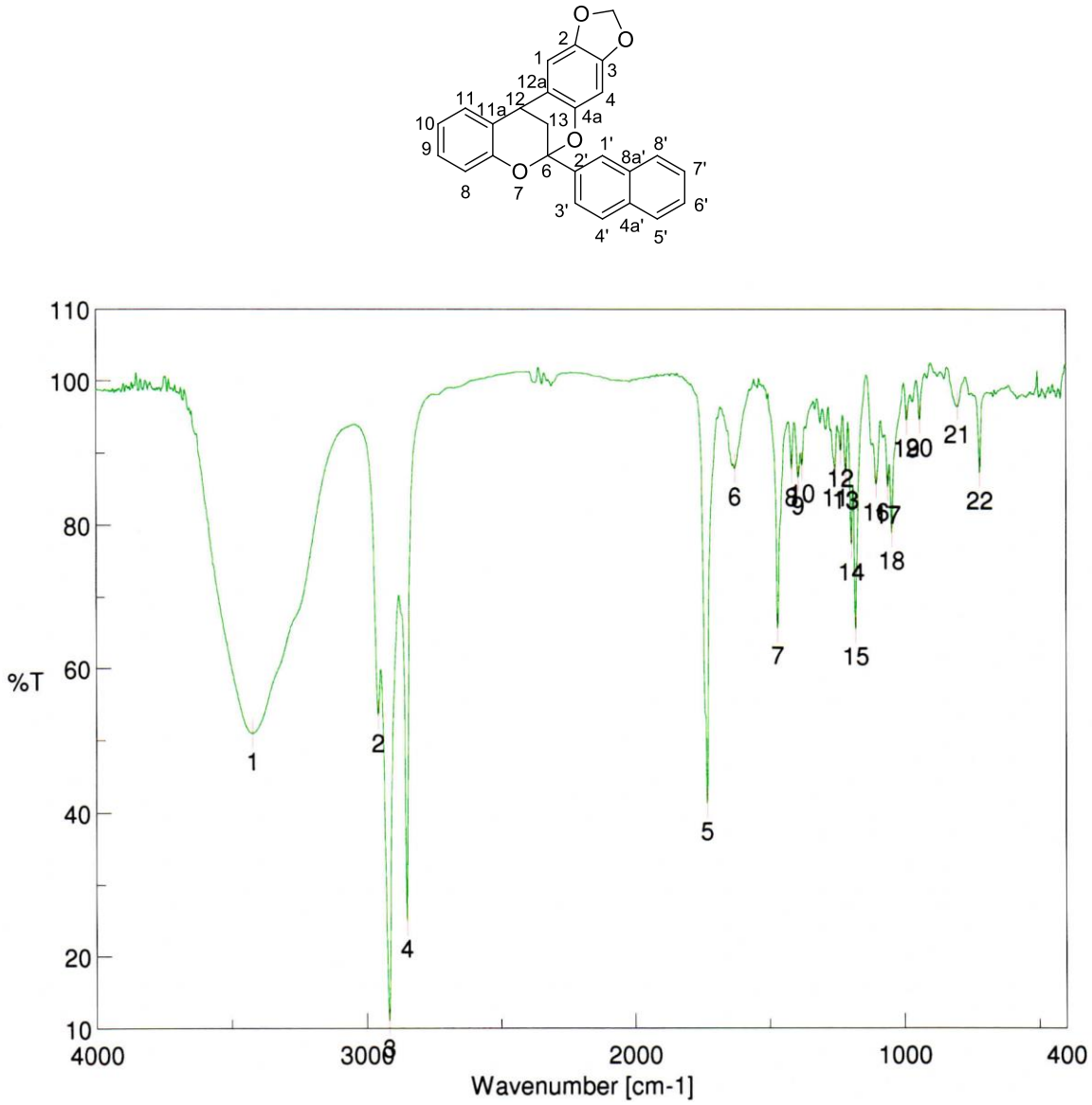

Figure S21. IR spectrum of **10b** recorded as KBr disc

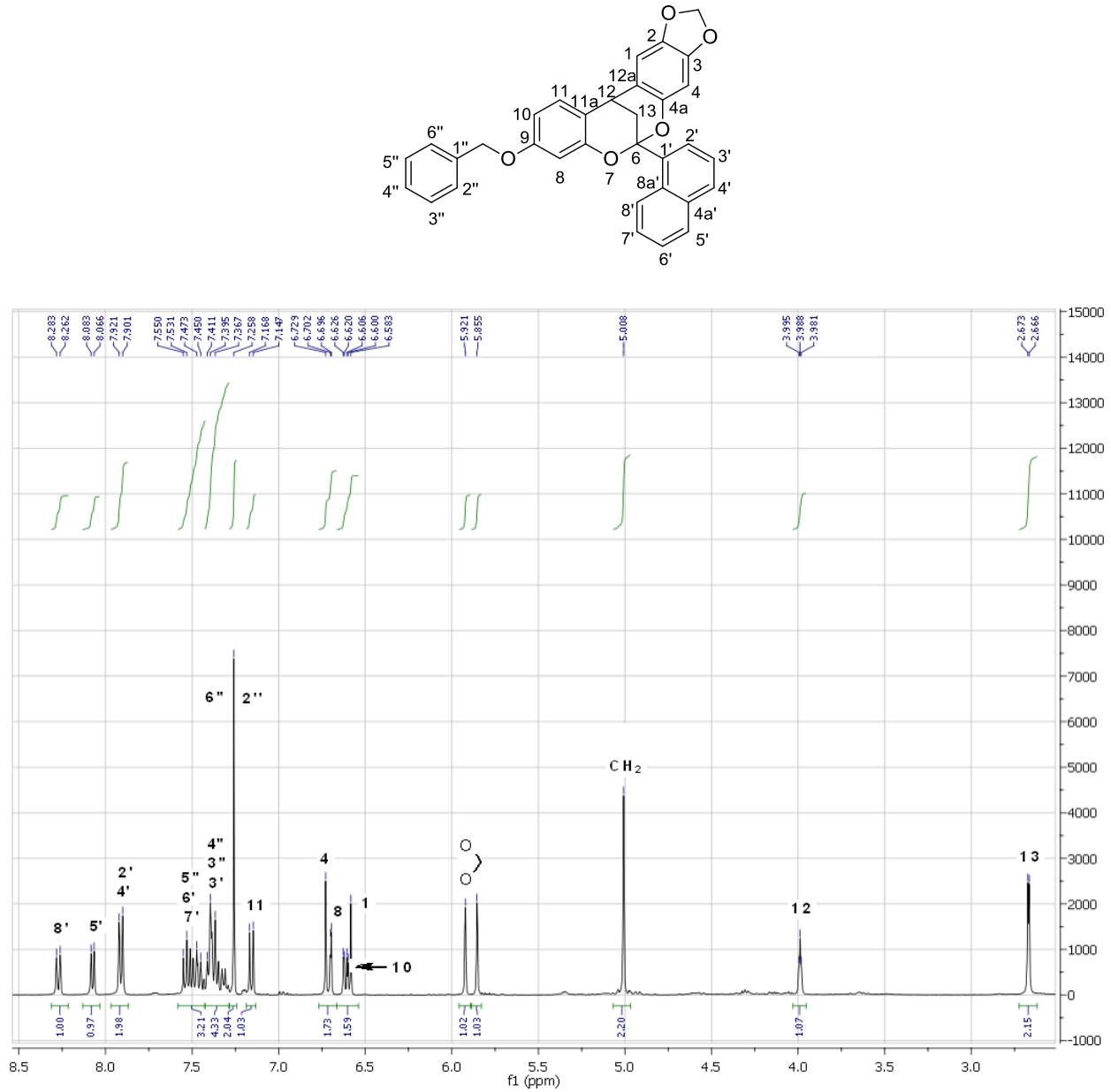

Figure S22. ^{1}H NMR (360 MHz) spectrum of **10c** in $CDCl_3$

Figure S23. ^{13}C NMR (90 MHz) spectrum of **10c** in $CDCl_3$

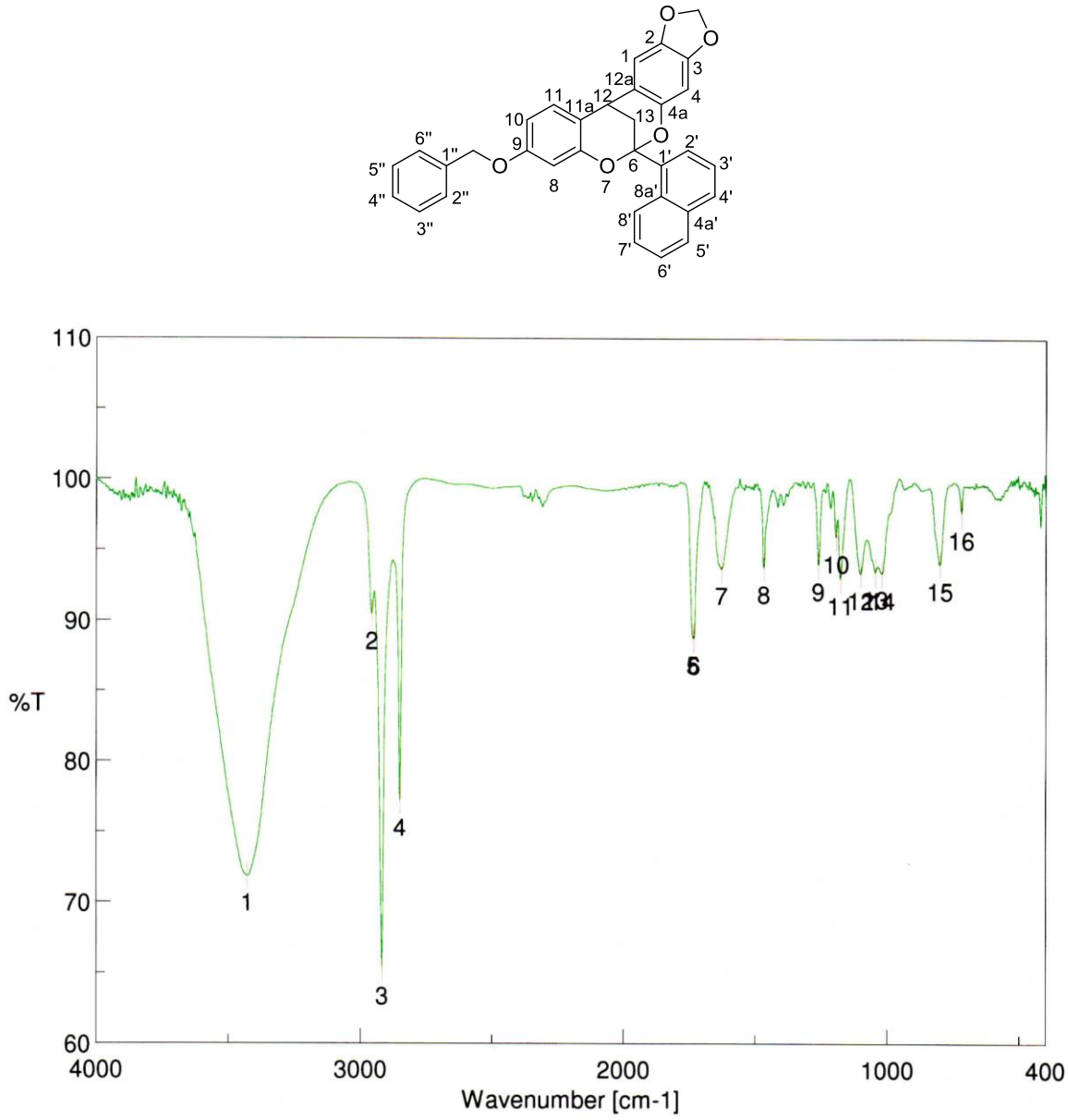

Figure S24. IR spectrum of **10c** recorded as KBr disc

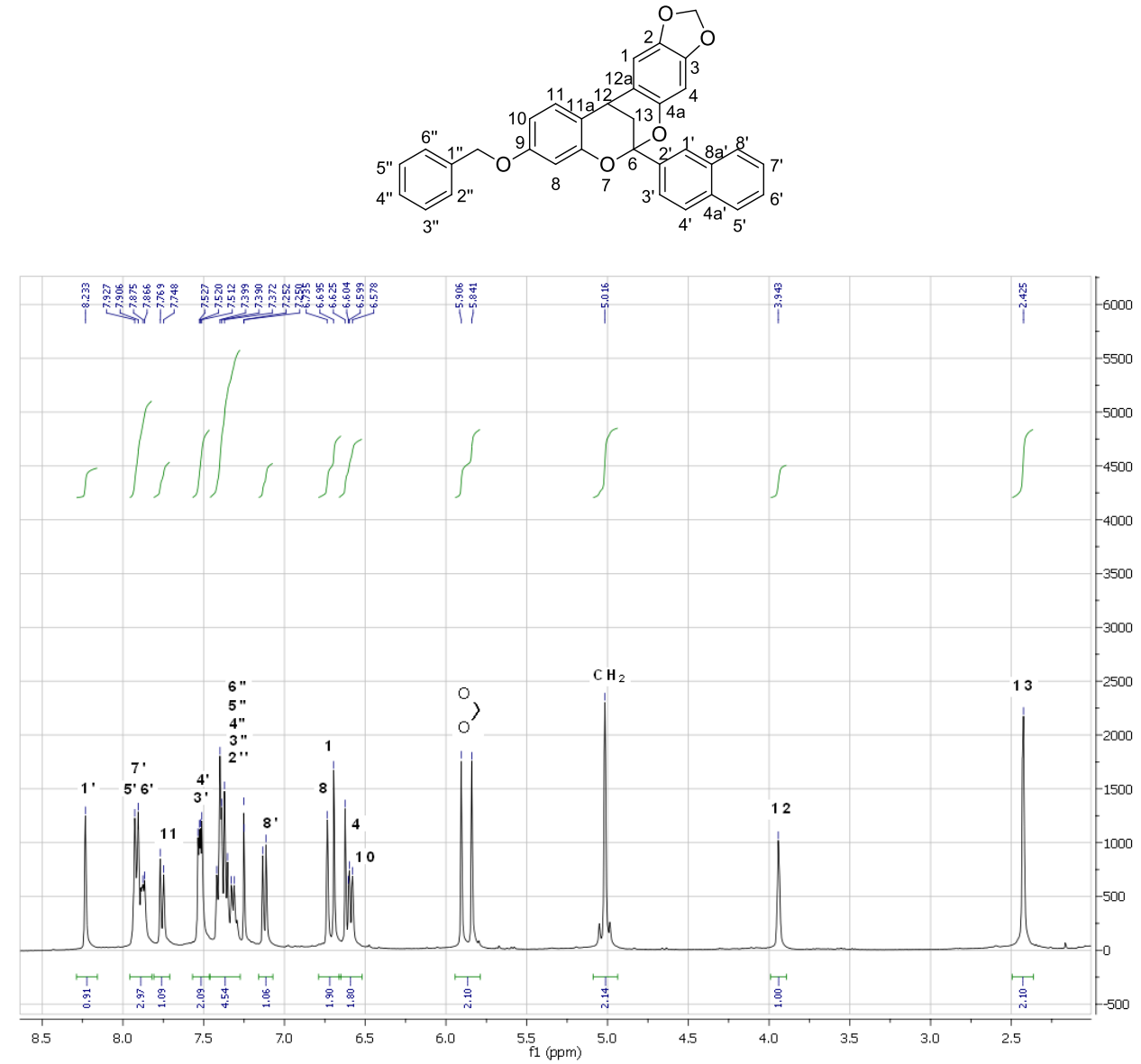

Figure S25. ^{1}H NMR (400 MHz) spectrum of **10d** in $CDCl_3$

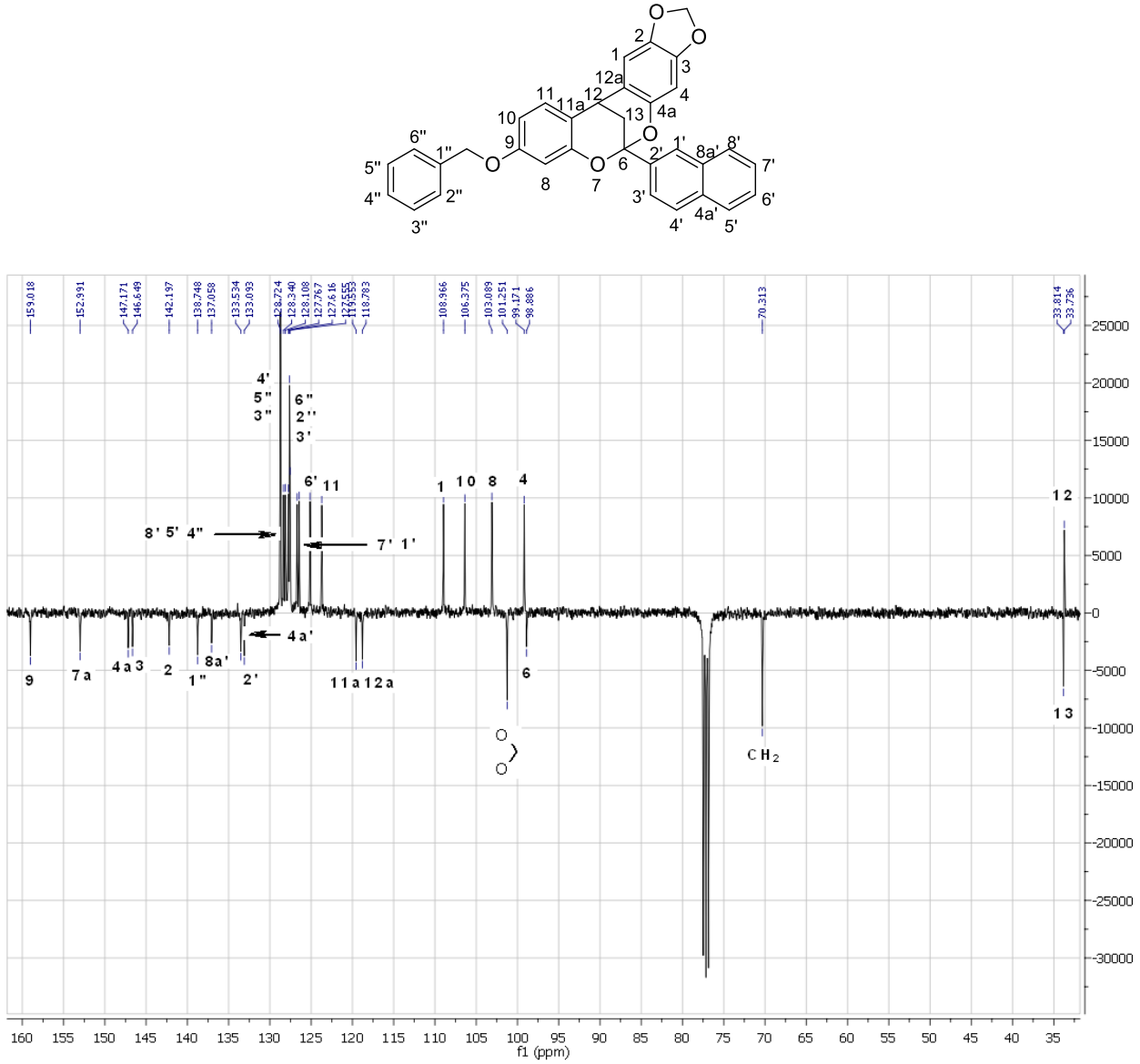

Figure S26. ^{13}C NMR (100 MHz) spectrum of **10d** in $CDCl_3$

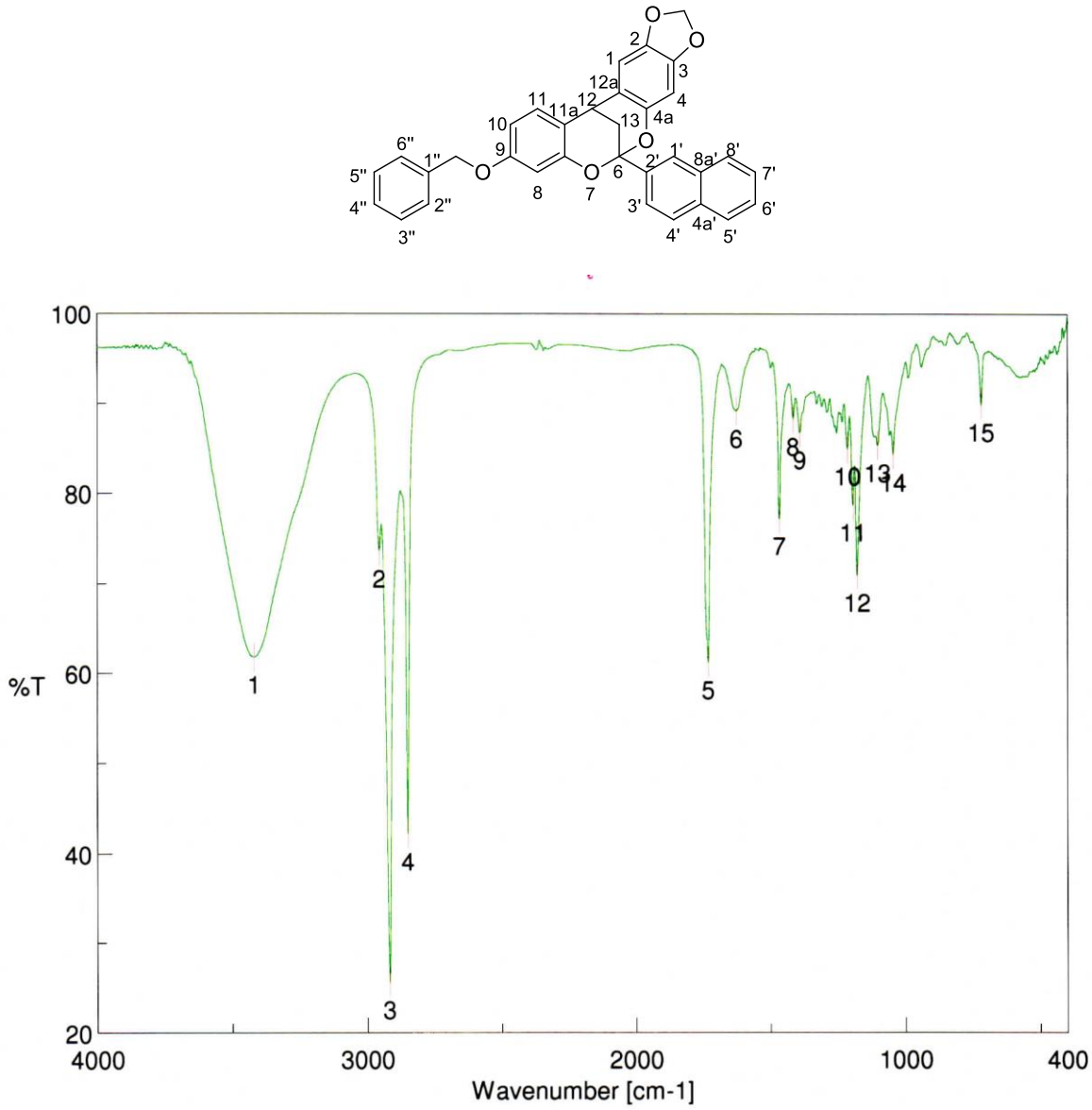

Figure S27. IR spectrum of **10d** recorded as KBr disc

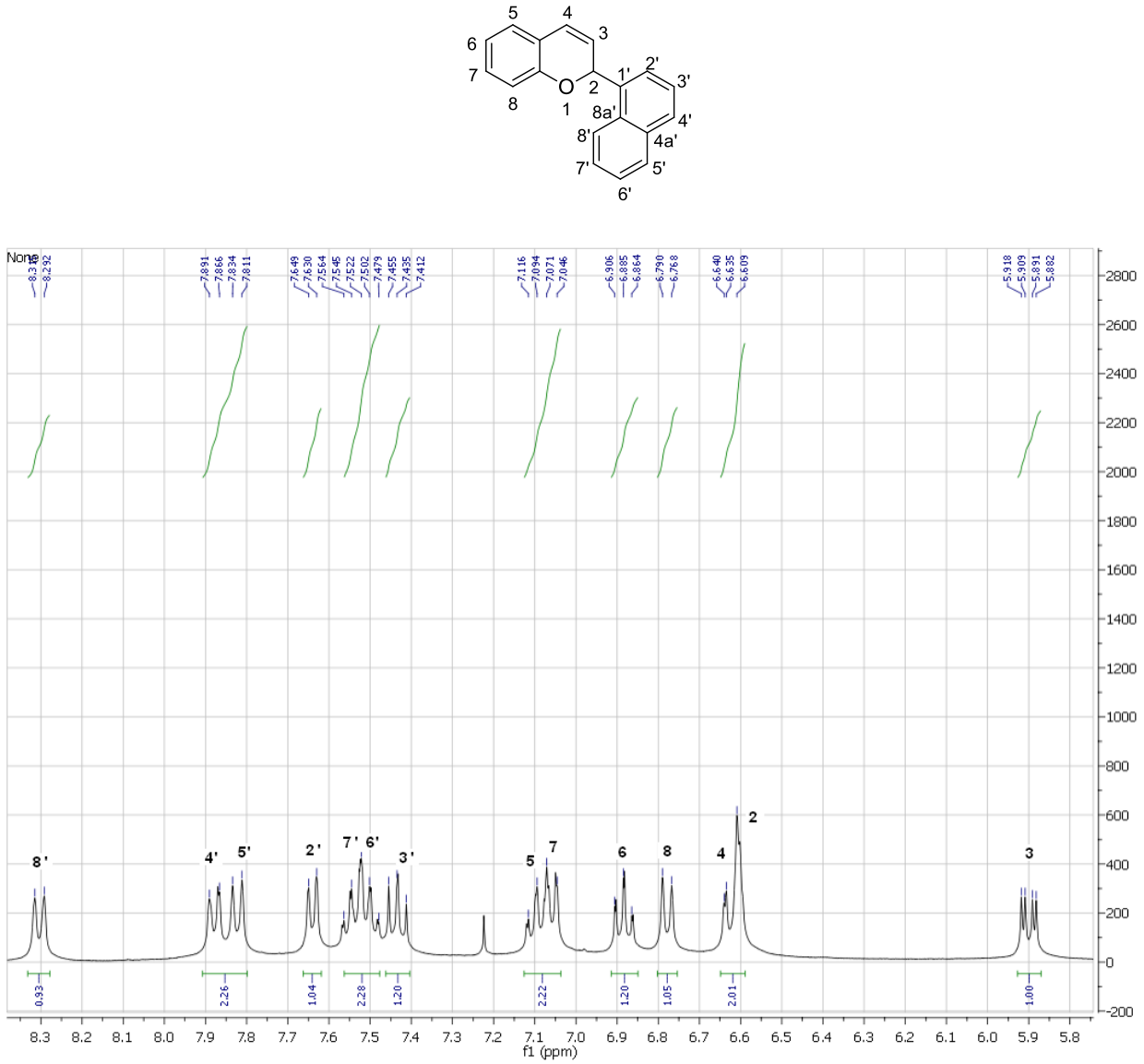

Figure S28. ^{1}H NMR (360 MHz) spectrum of **7a** in $CDCl_3$

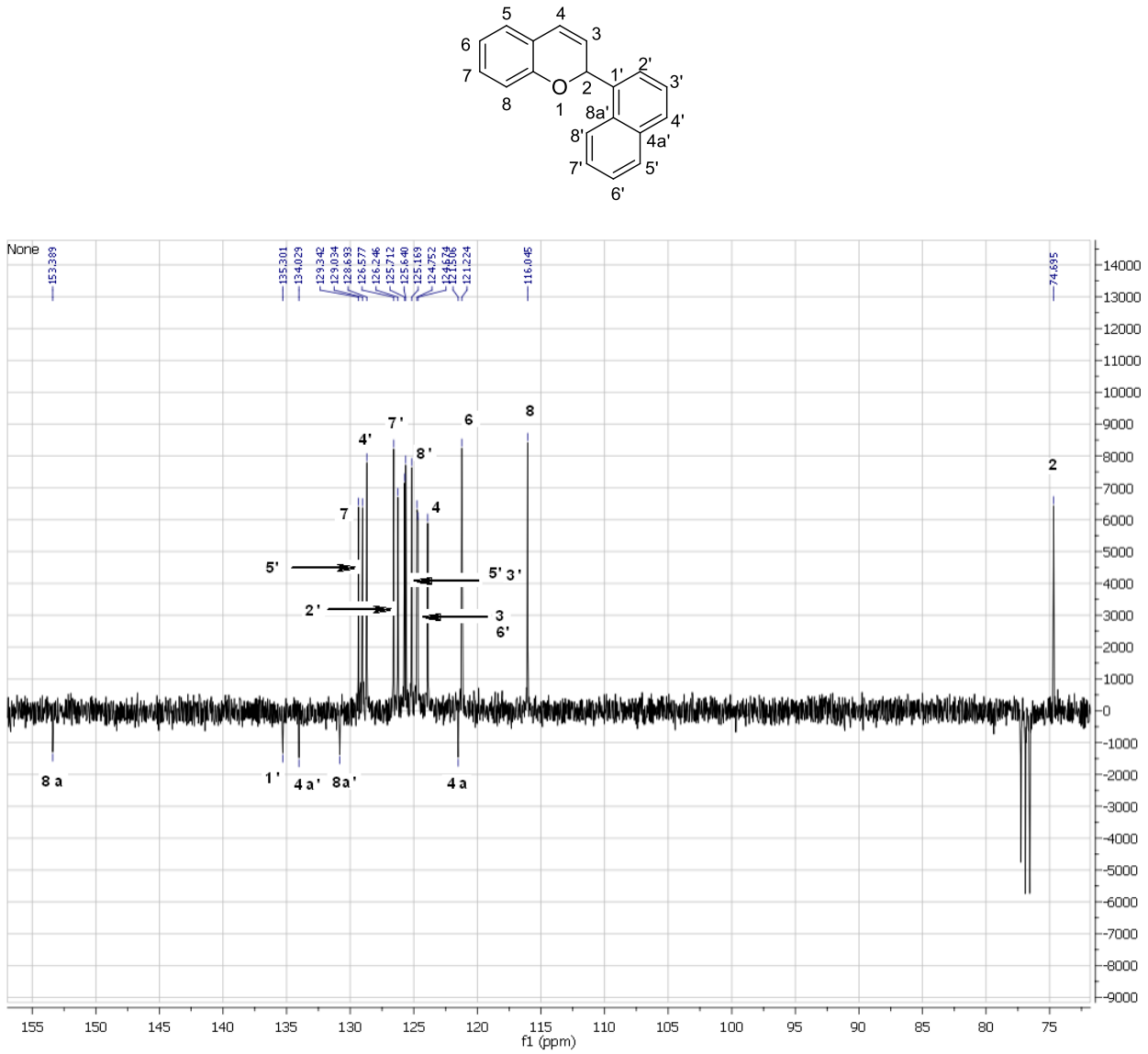

Figure S29. ^{13}C NMR (90 MHz) spectrum of **7a** in $CDCl_3$

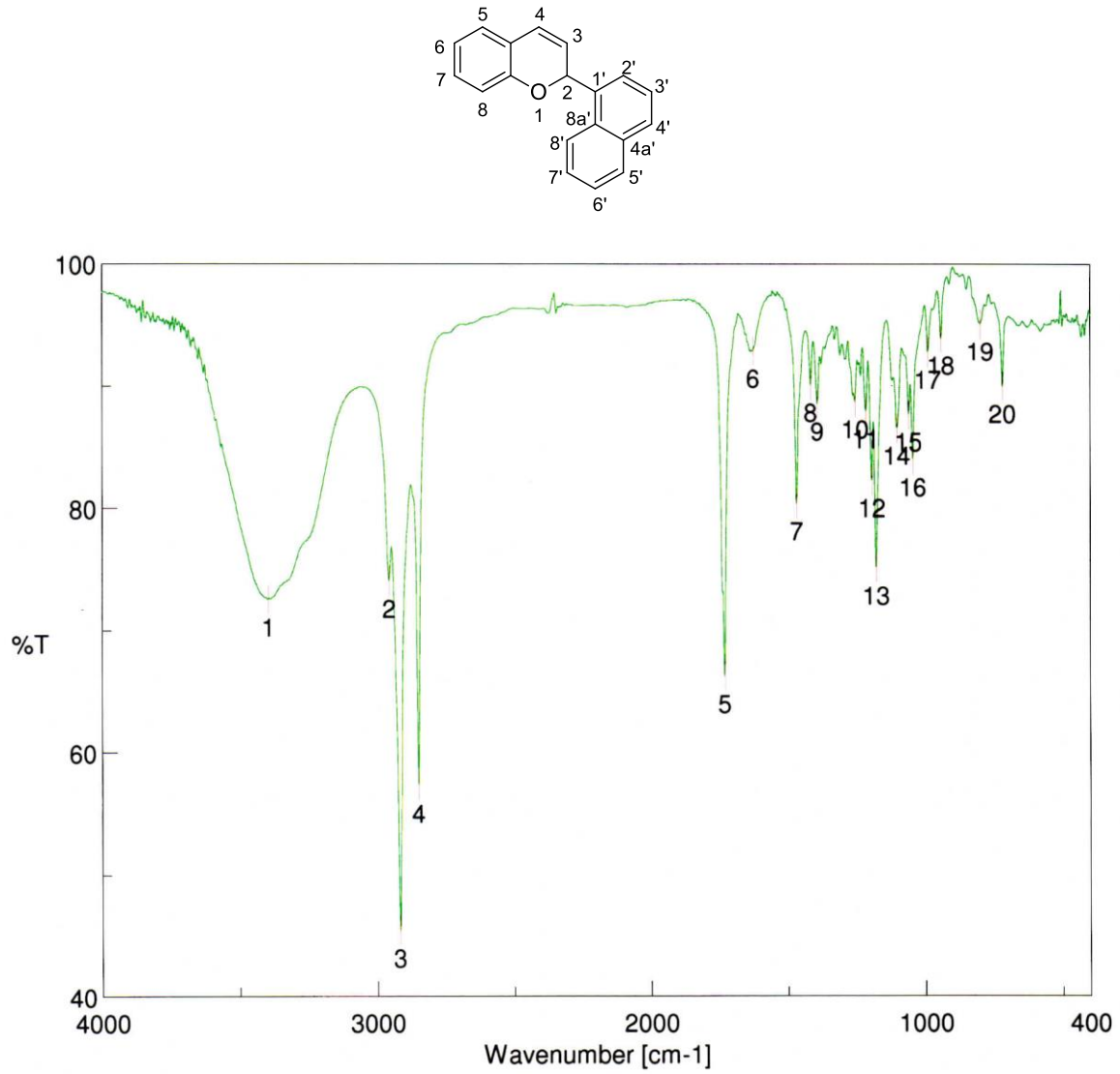

Figure S30. IR spectrum of **7a** recorded as KBr disc

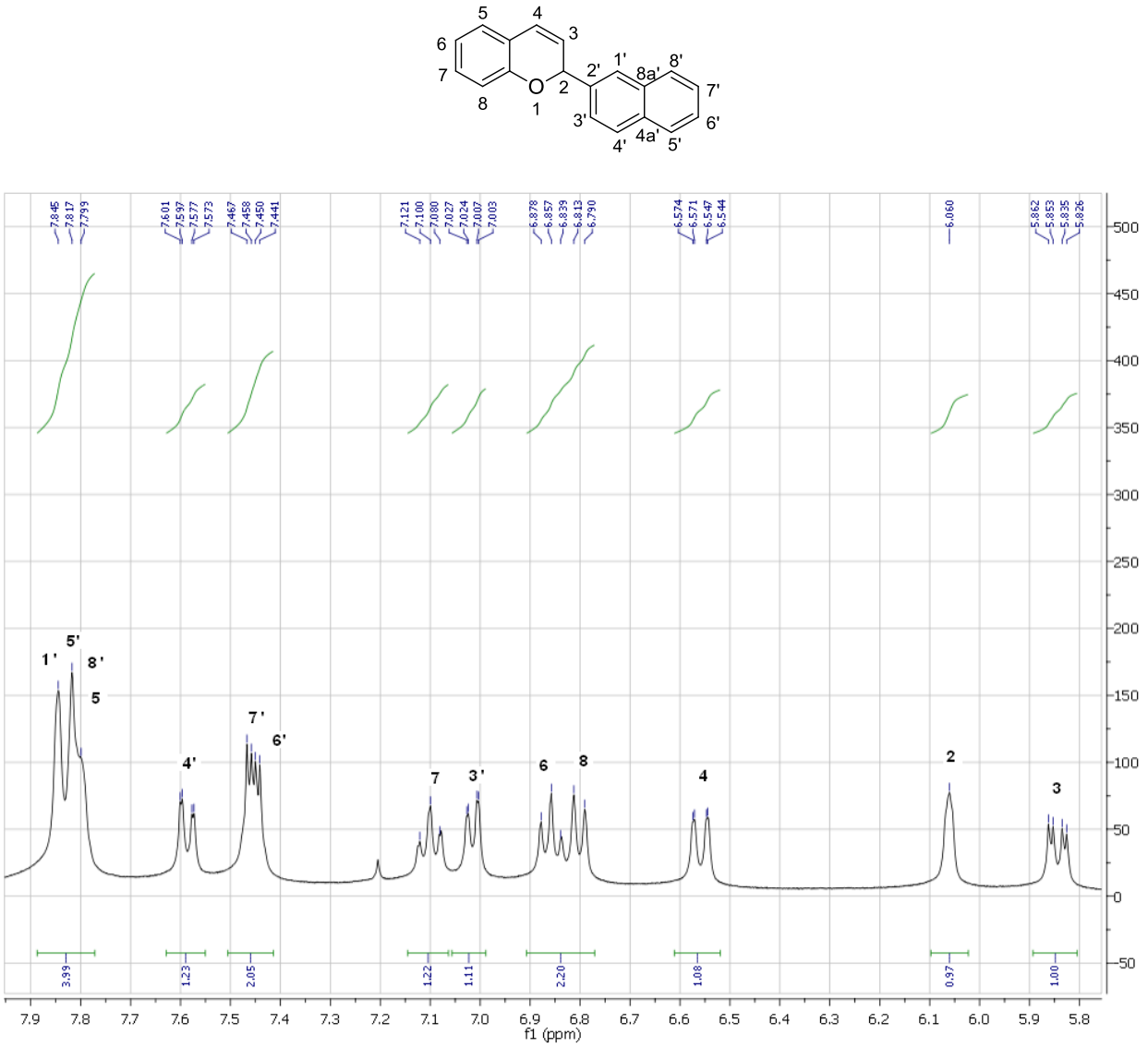

Figure S31. ^{1}H NMR (360 MHz) spectrum of **7b** in $CDCl_3$

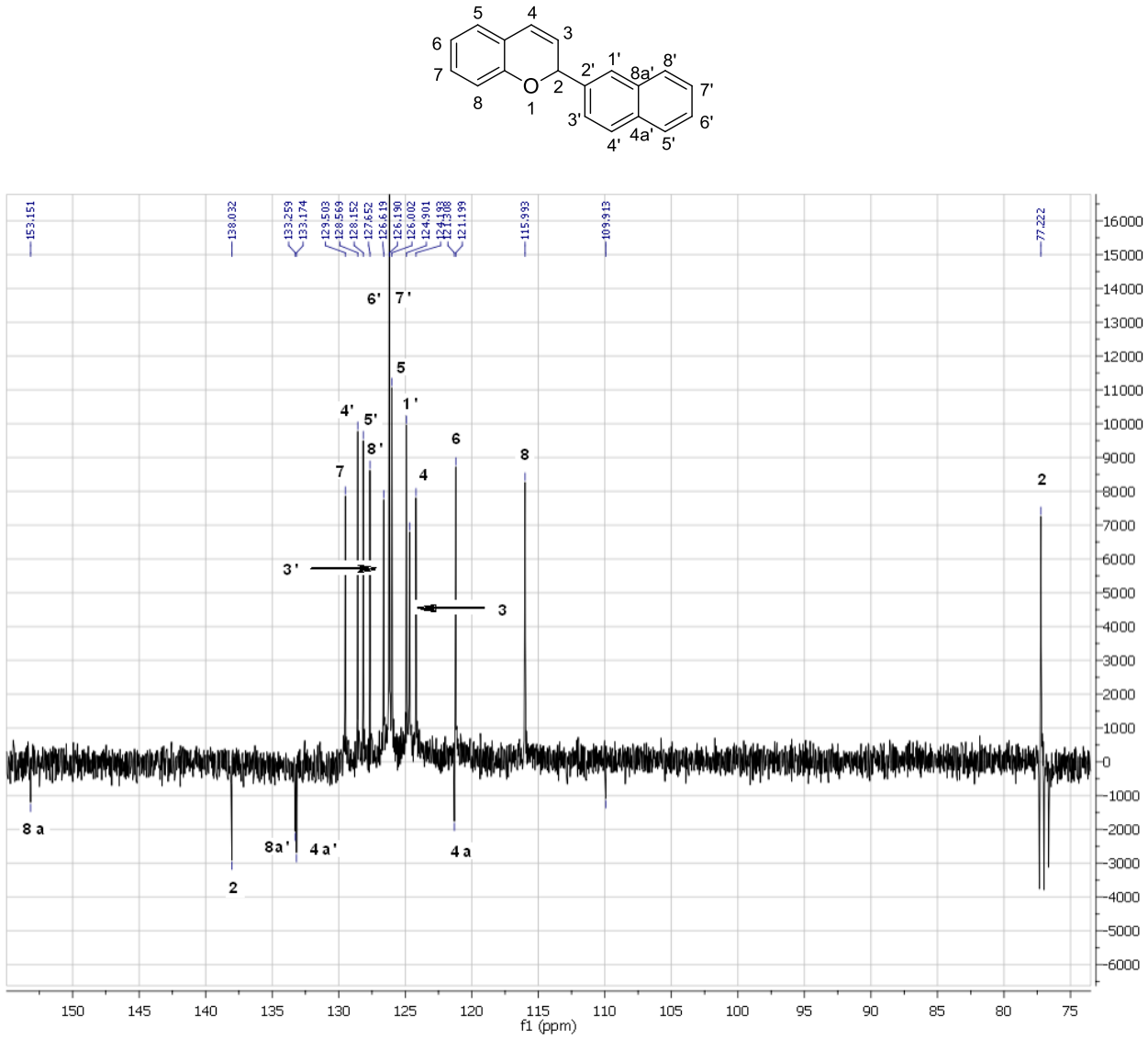

Figure S32. ^{13}C NMR (90 MHz) spectrum of **7b** in $CDCl_3$

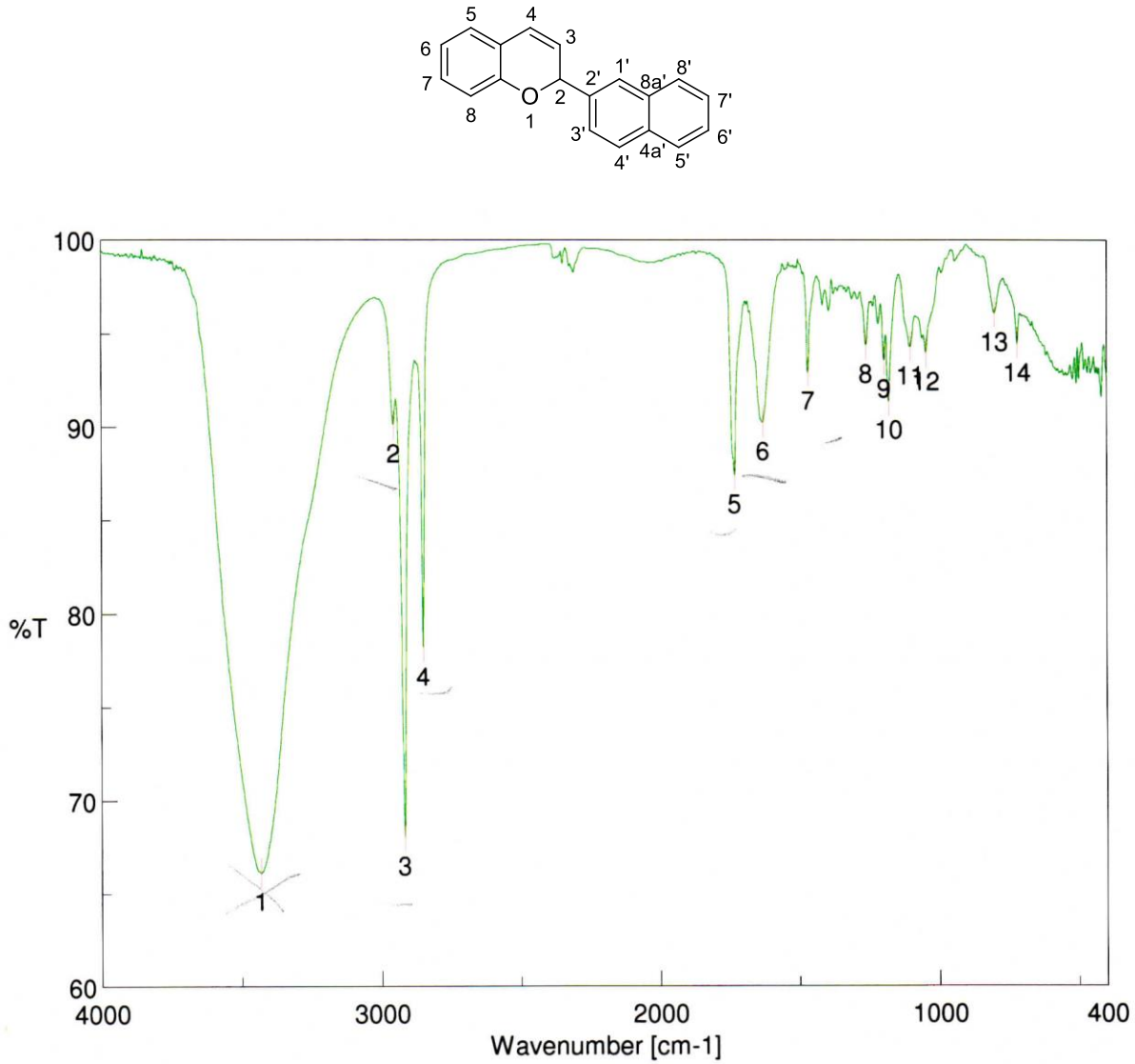

Figure S33. IR spectrum of **7b** recorded as KBr disc

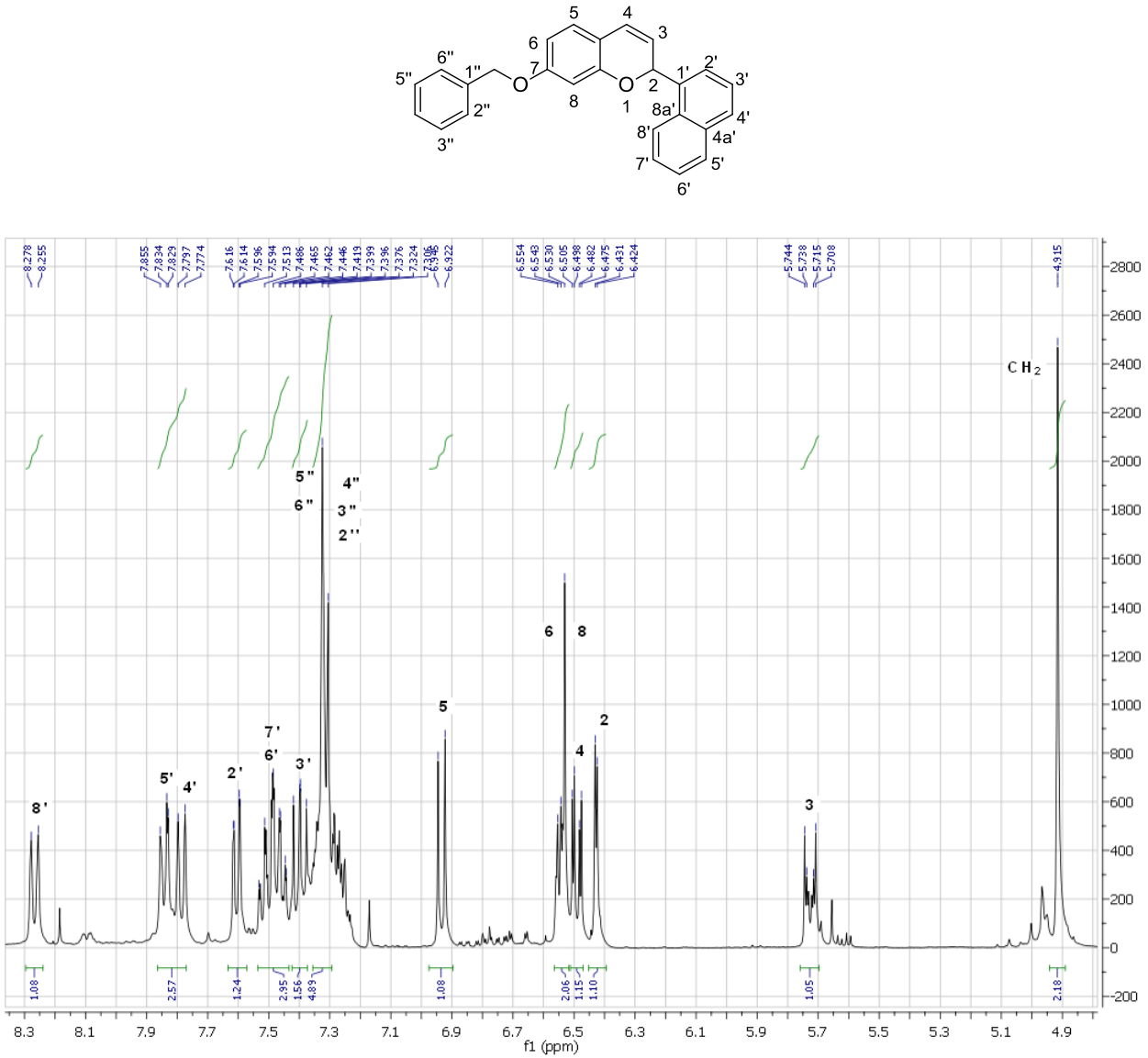

Figure S34. ^{1}H NMR (360 MHz) spectrum of **7c** in $CDCl_3$

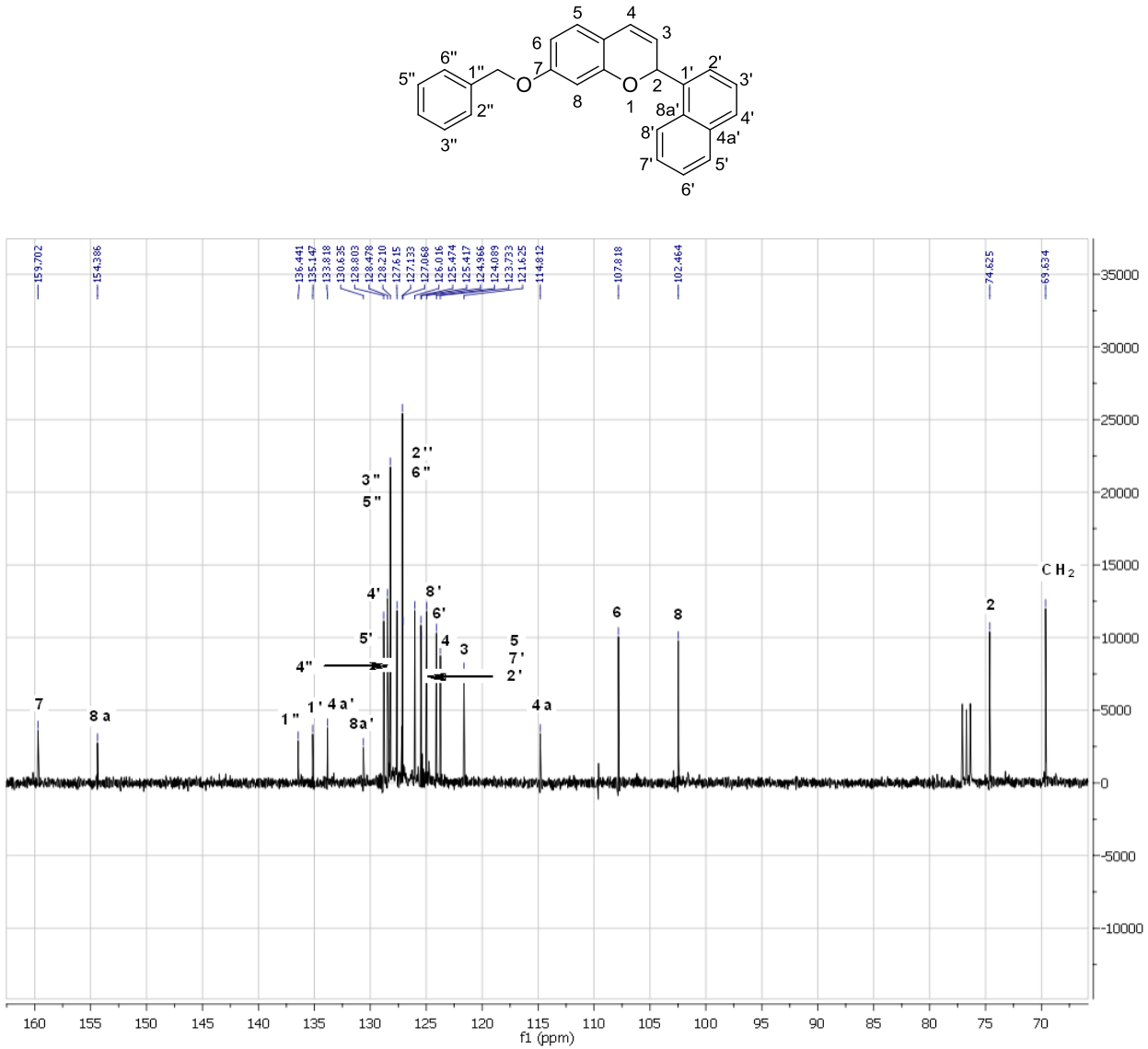

Figure S35. ^{13}C NMR (90 MHz) spectrum of **7c** in $CDCl_3$

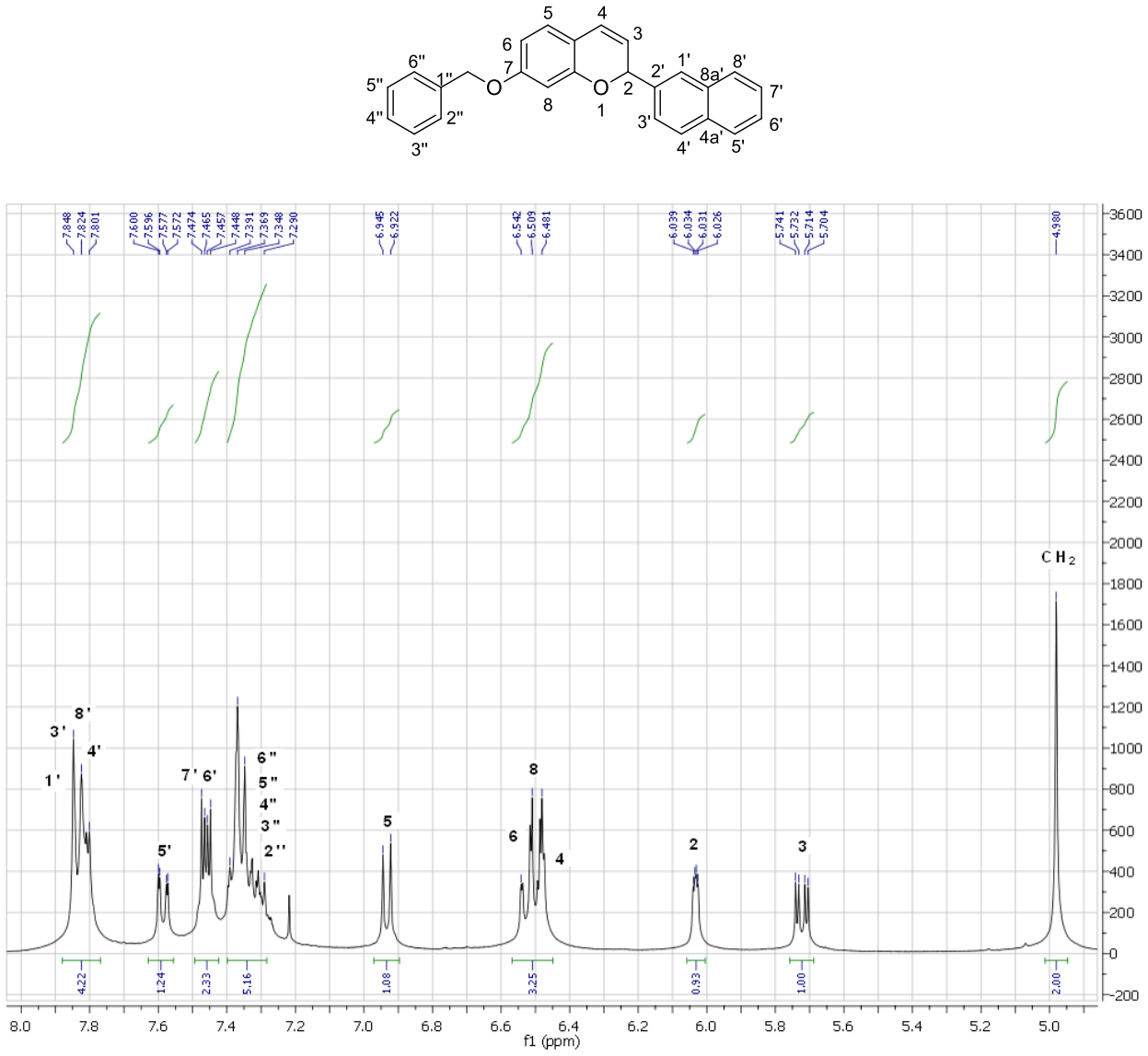

Figure S36. ^{1}H NMR (360 MHz) spectrum of **7d** in $CDCl_3$

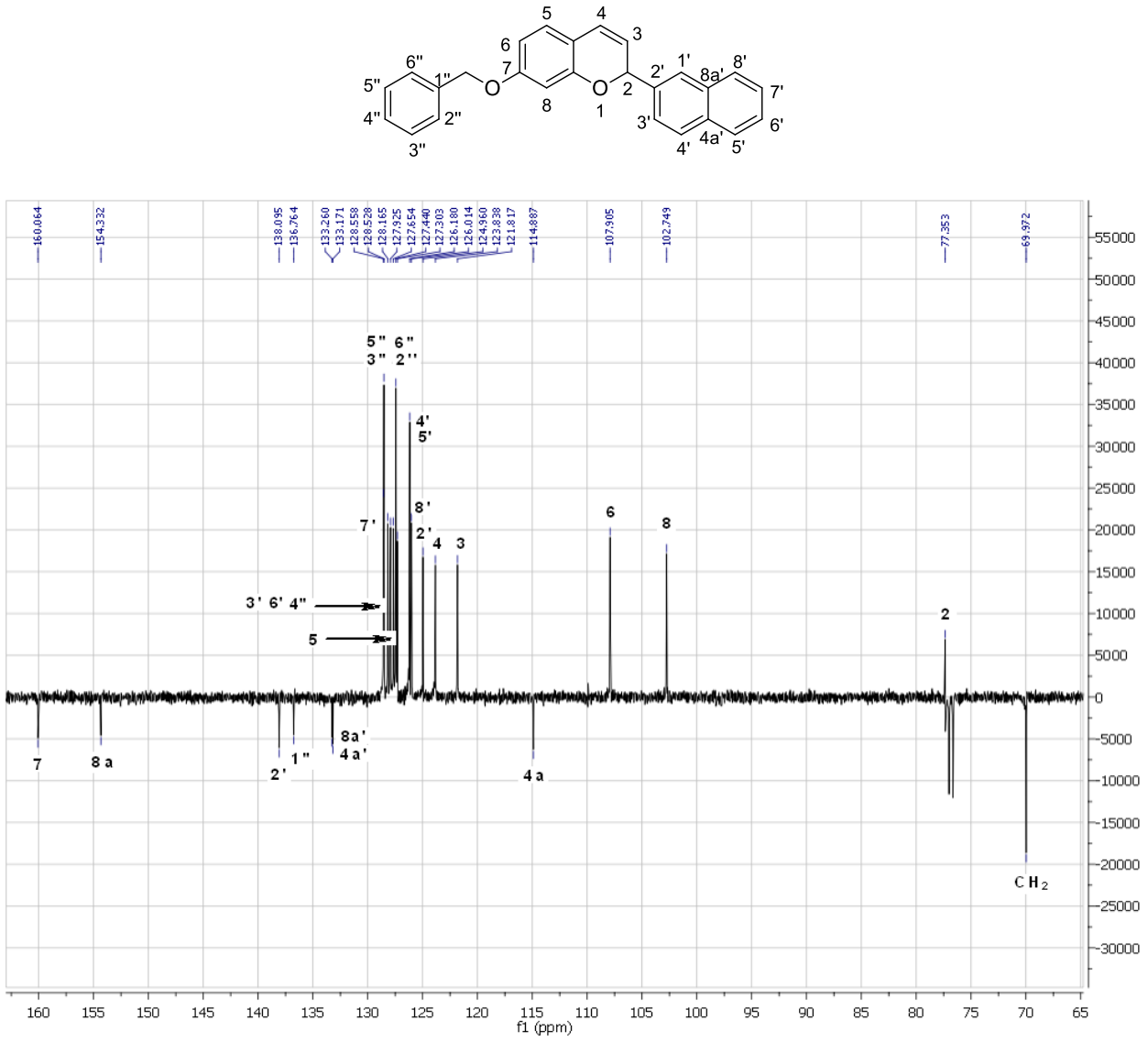

Figure S37. ^{13}C NMR (90 MHz) spectrum of **7d** in $CDCl_3$

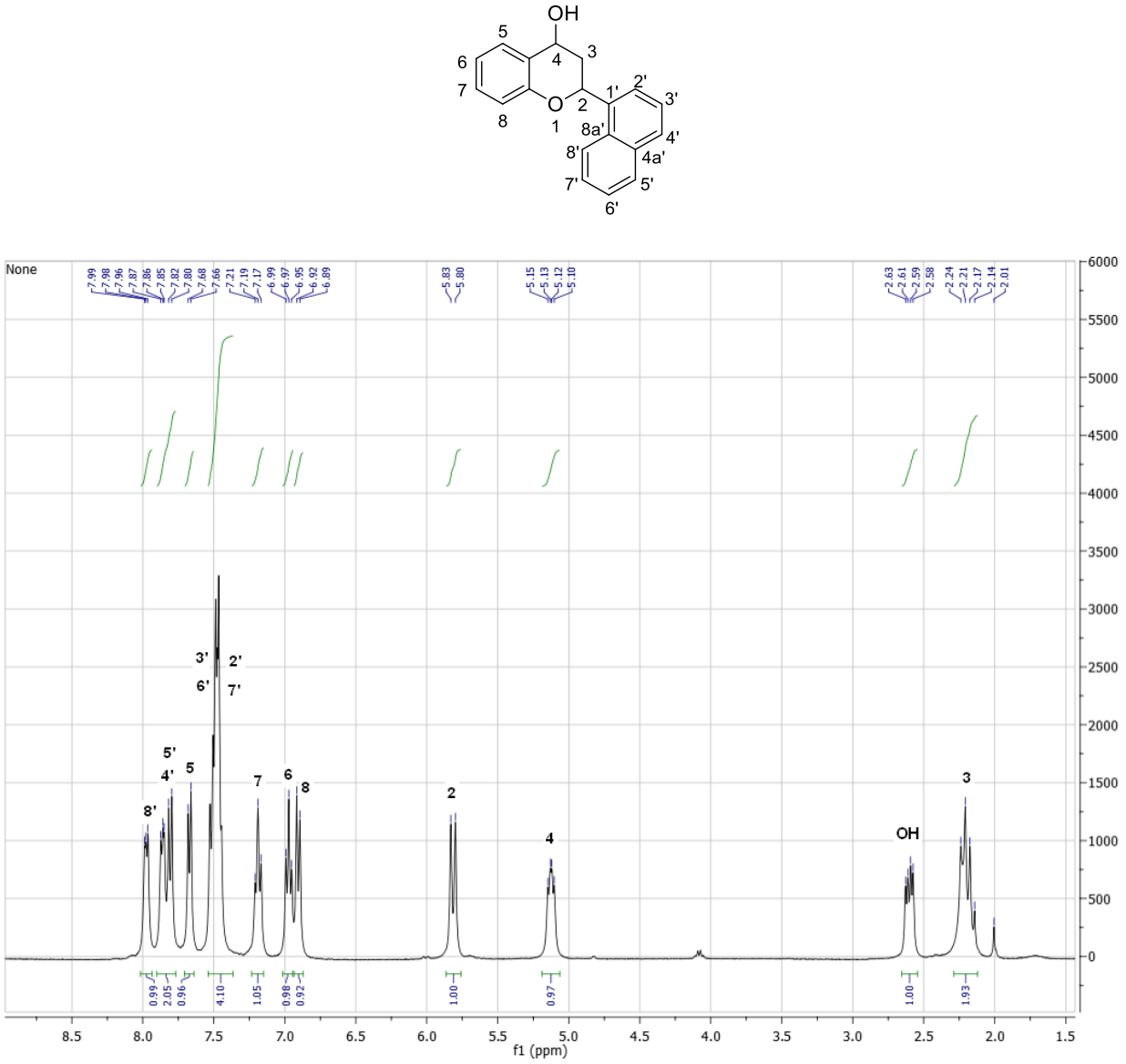

Figure S38. ^{1}H NMR (360 MHz) spectrum of **14a** in $CDCl_3$

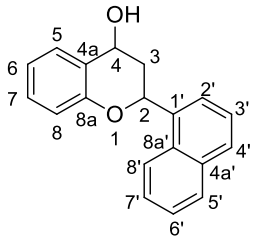

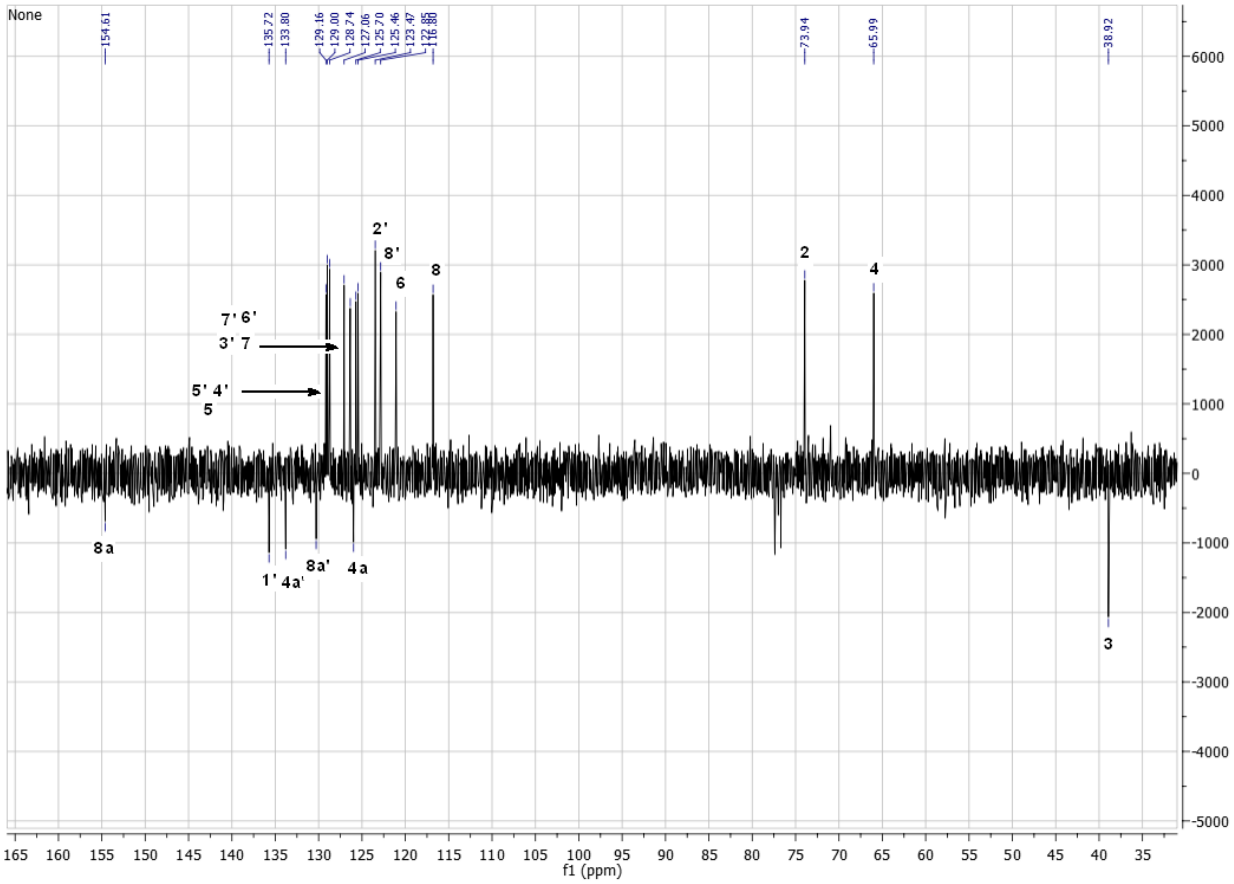

Figure S39. ^{13}C NMR (90 MHz) spectrum of **14a** in $CDCl_3$

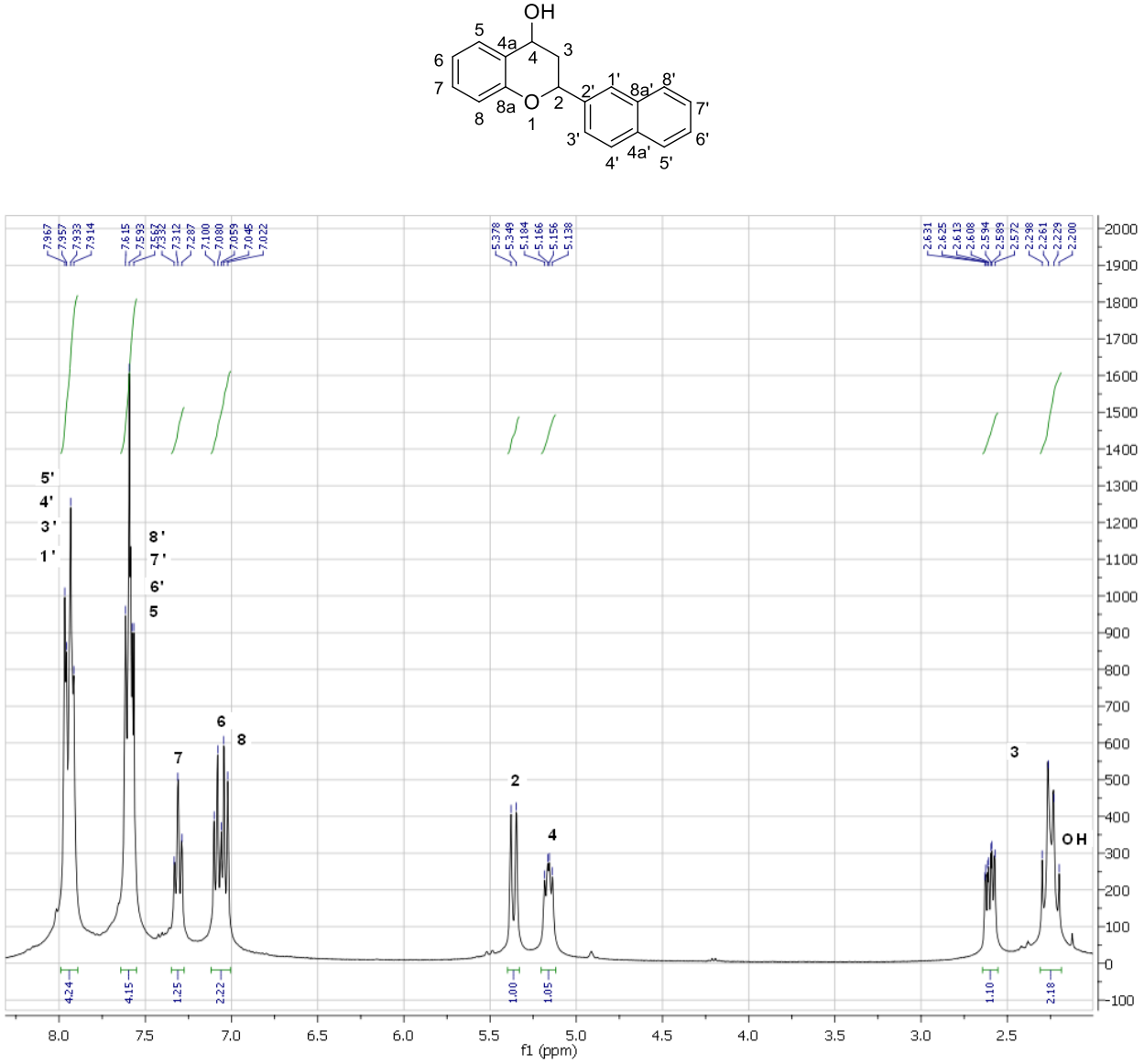

Figure S40. ^{1}H NMR (360 MHz) spectrum of **14b** in $CDCl_3$

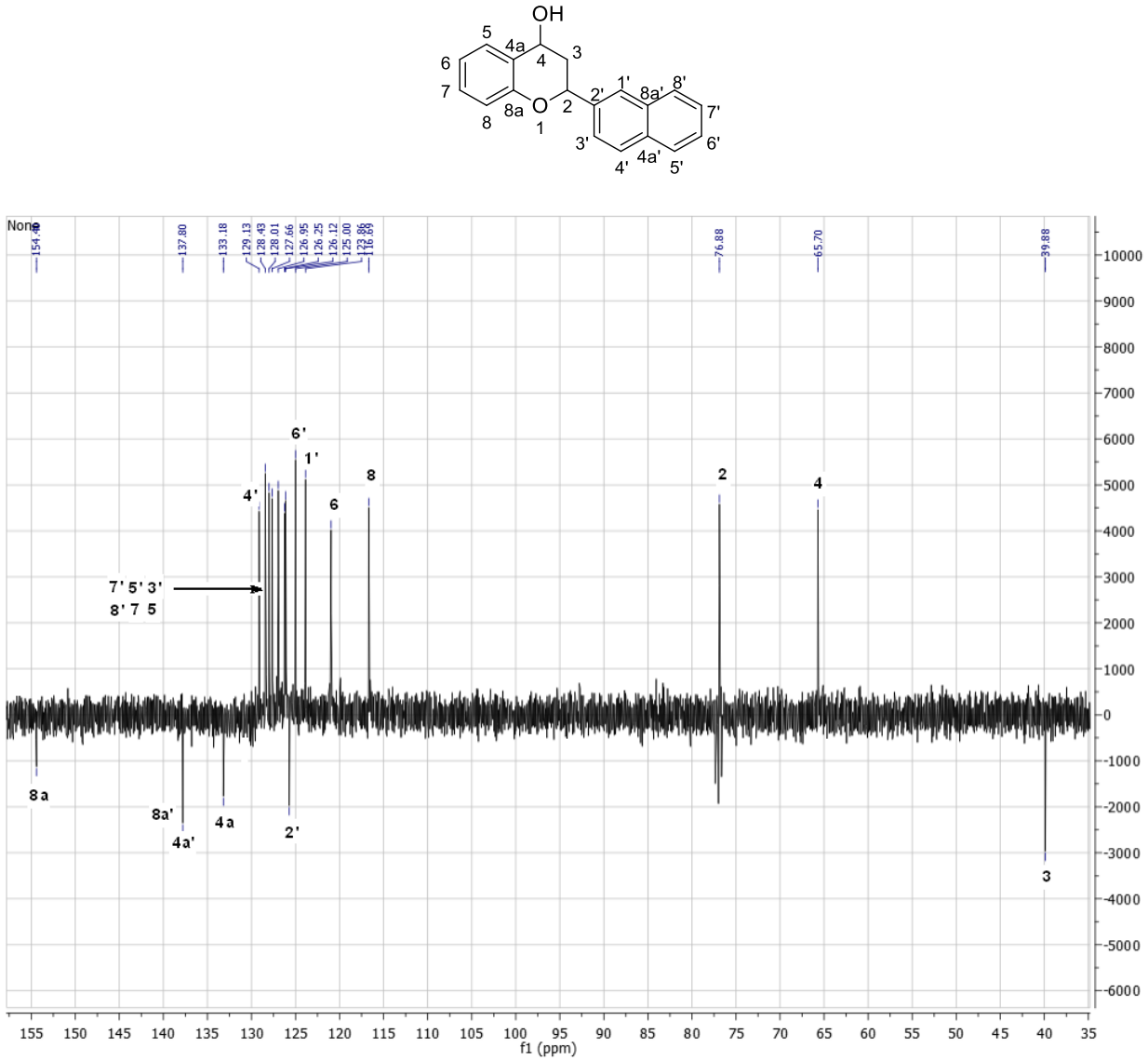

Figure S41. ^{13}C NMR (90 MHz) spectrum of **14b** in $CDCl_3$

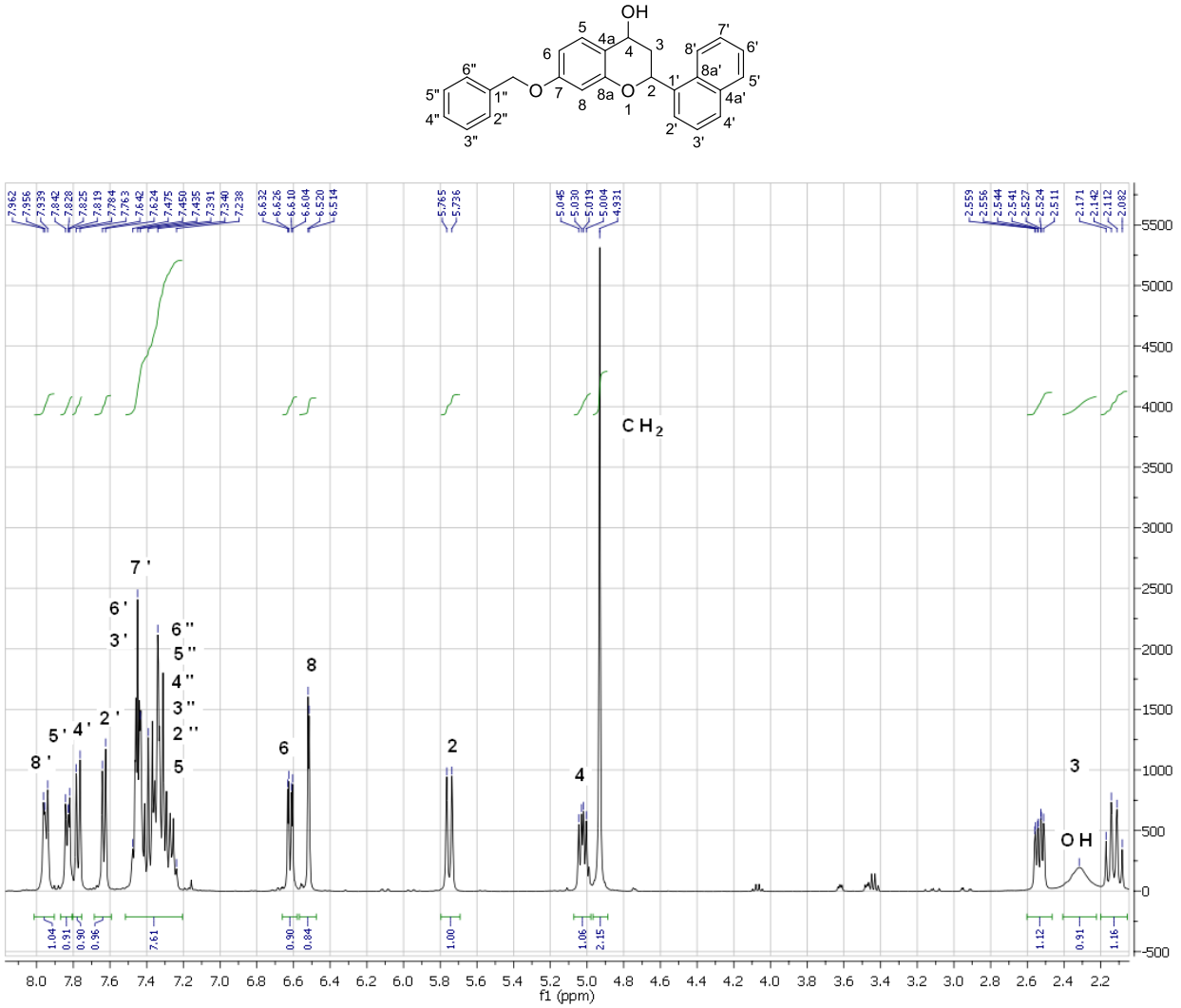

Figure S42. ^{1}H NMR (400 MHz) spectrum of **14c** in $CDCl_3$

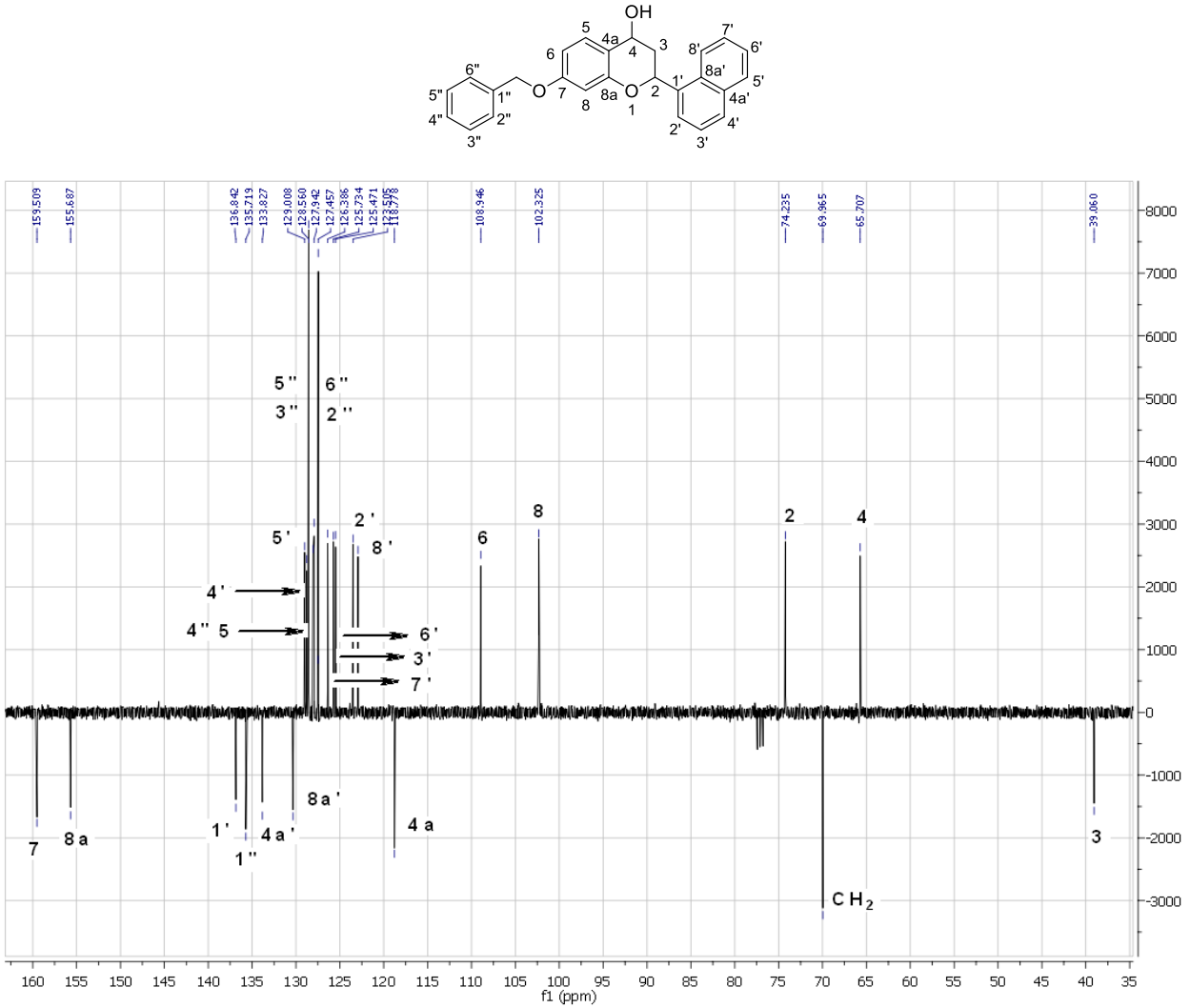

Figure S43. ^{13}C NMR (100 MHz) spectrum of **14c** in $CDCl_3$

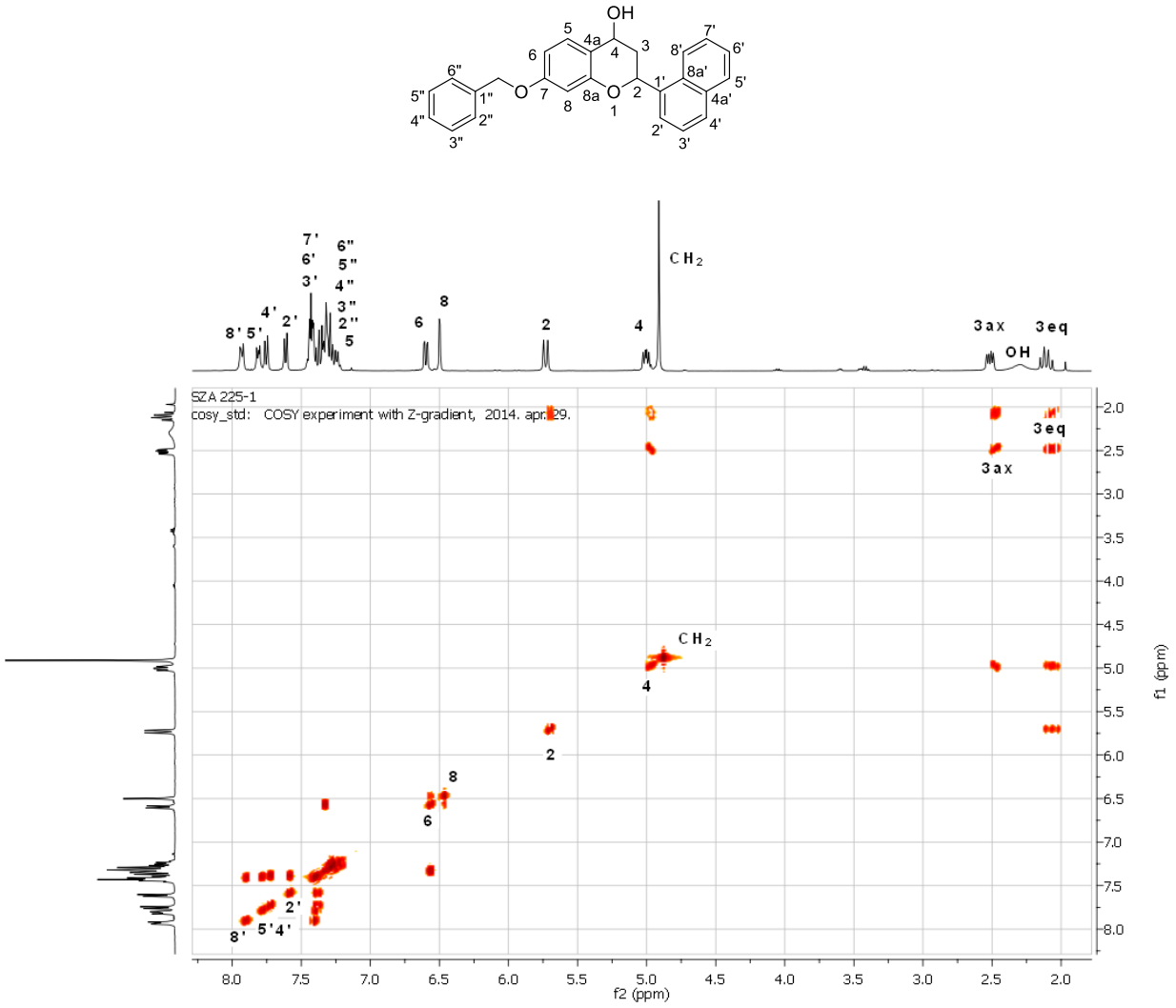

Figure S44. COSY spectrum of **14c** in $CDCl_3$

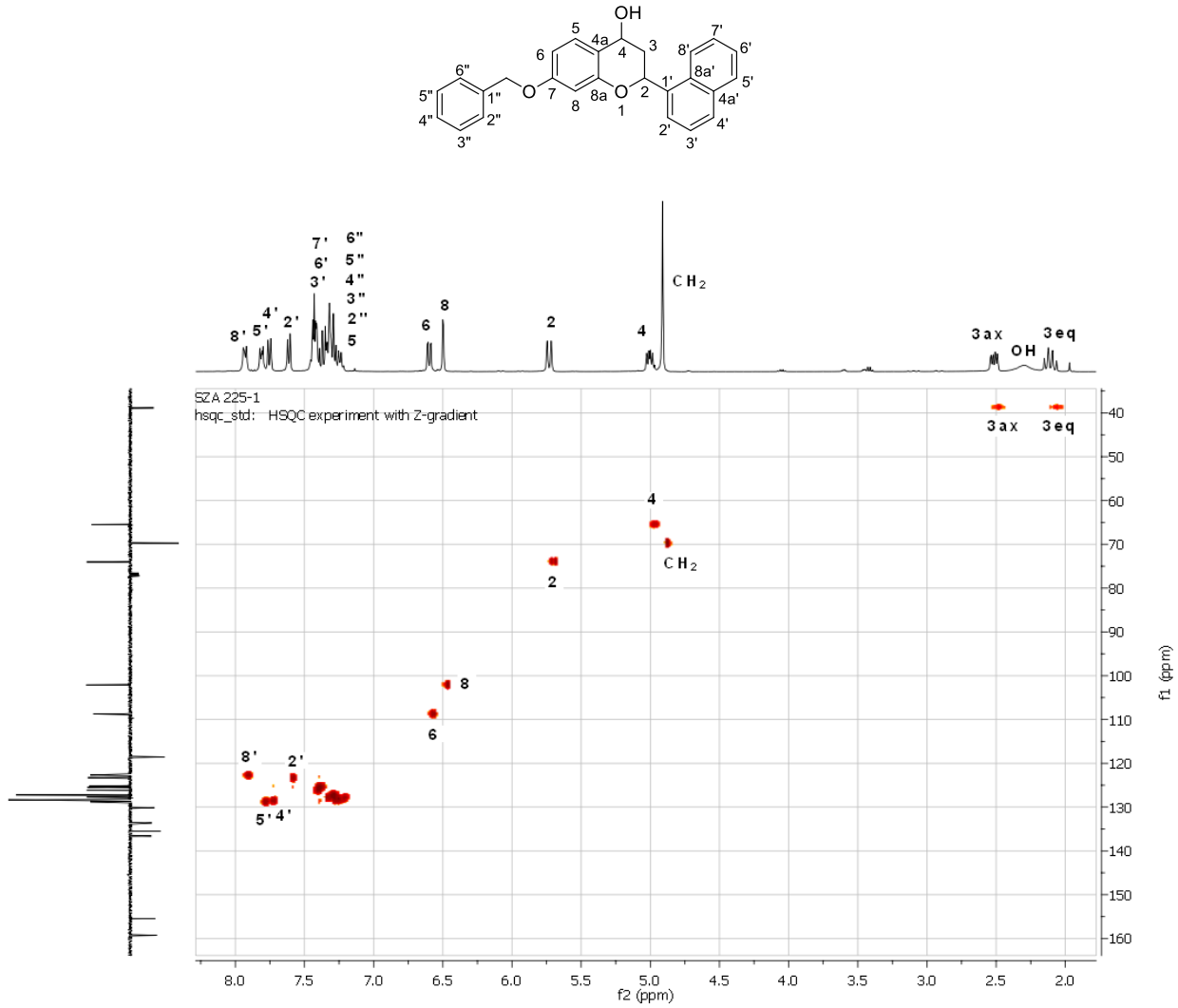

Figure S45. HSQC spectrum of **14c** in $CDCl_3$

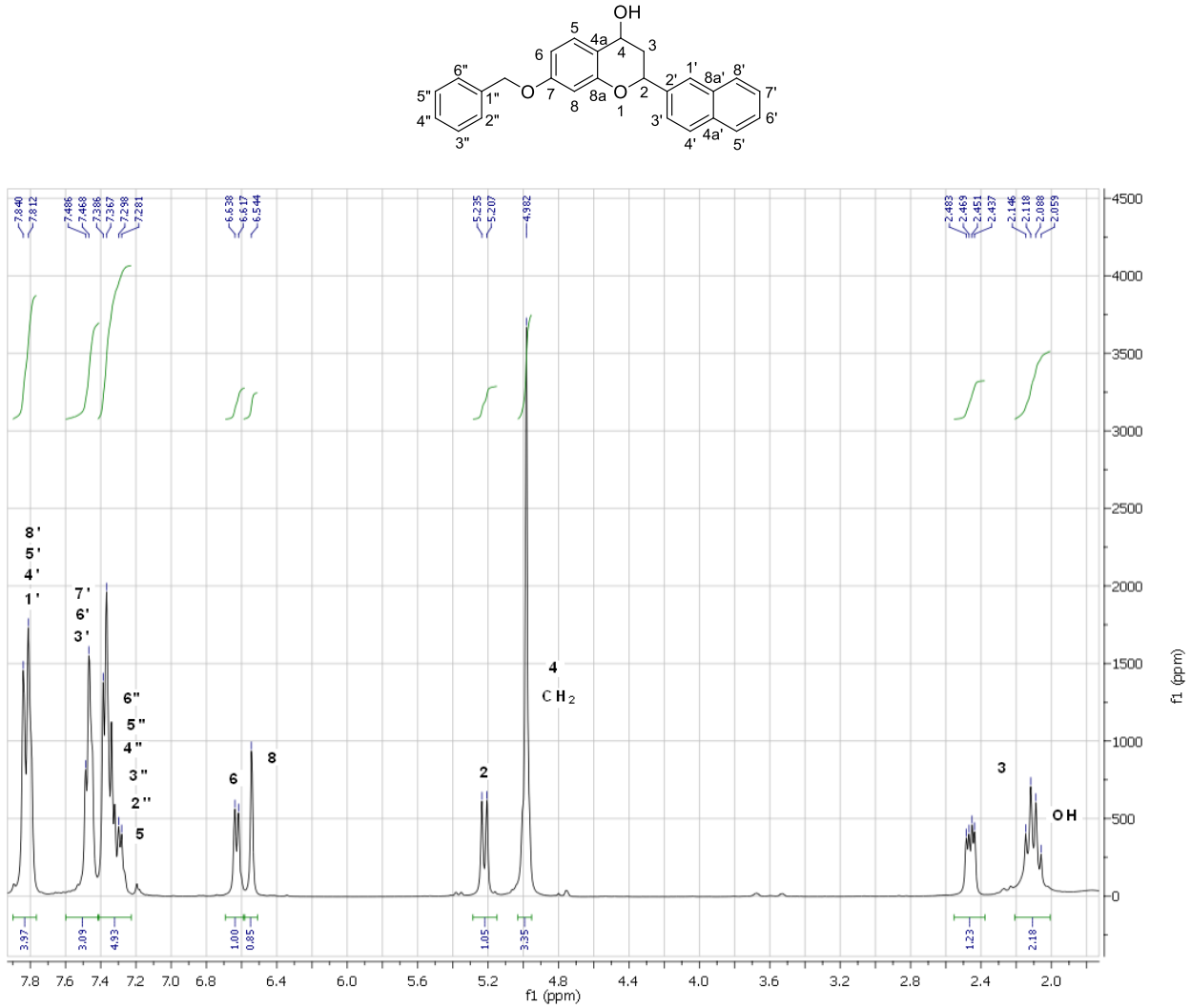

Figure S46. ^{1}H NMR (360 MHz) spectrum of **14d** in $CDCl_3$

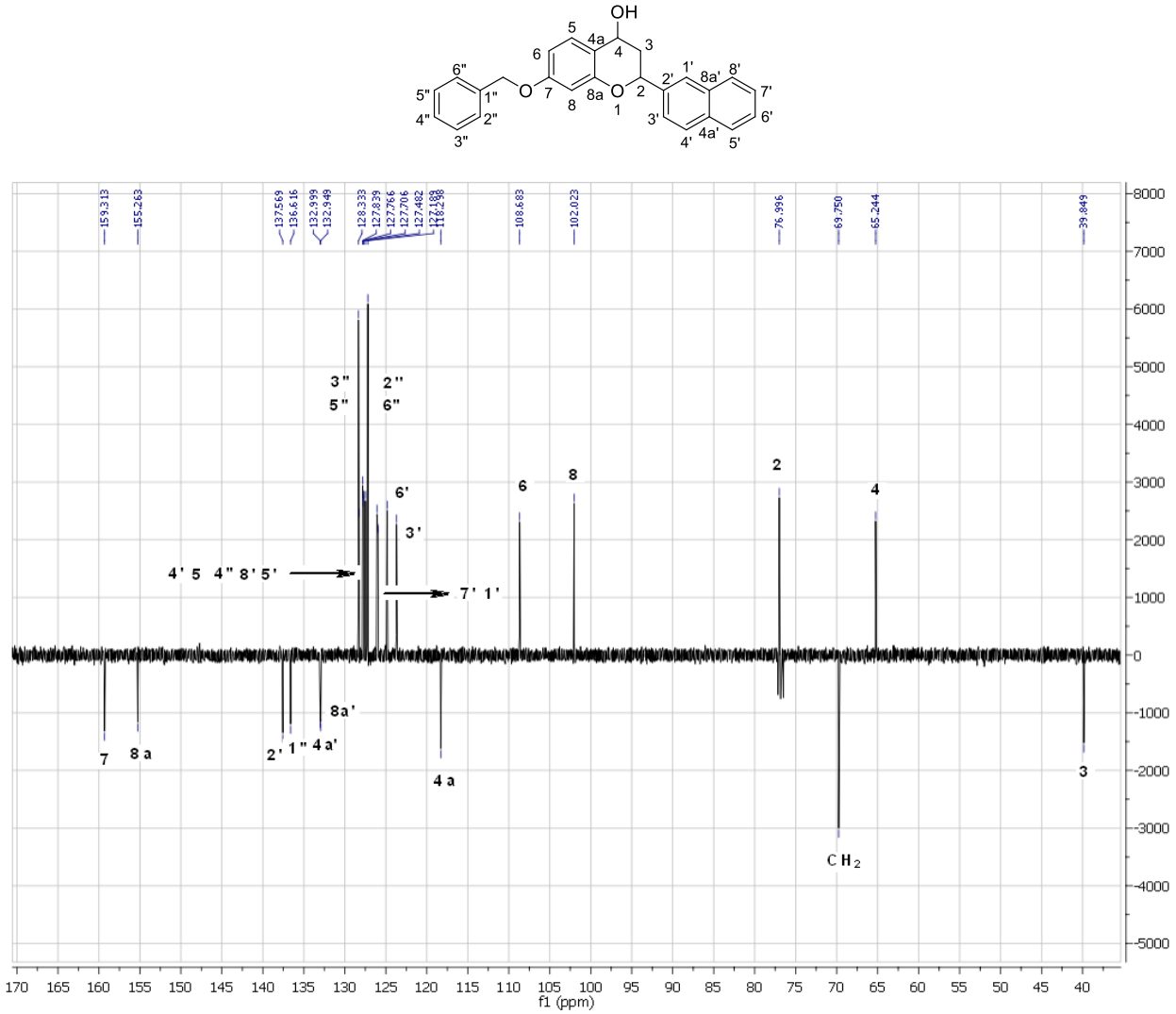

Figure S47. ^{13}C NMR (90 MHz) spectrum of **14d** in $CDCl_3$

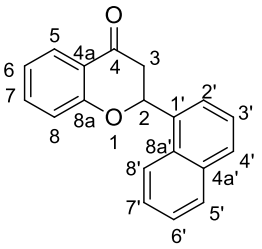

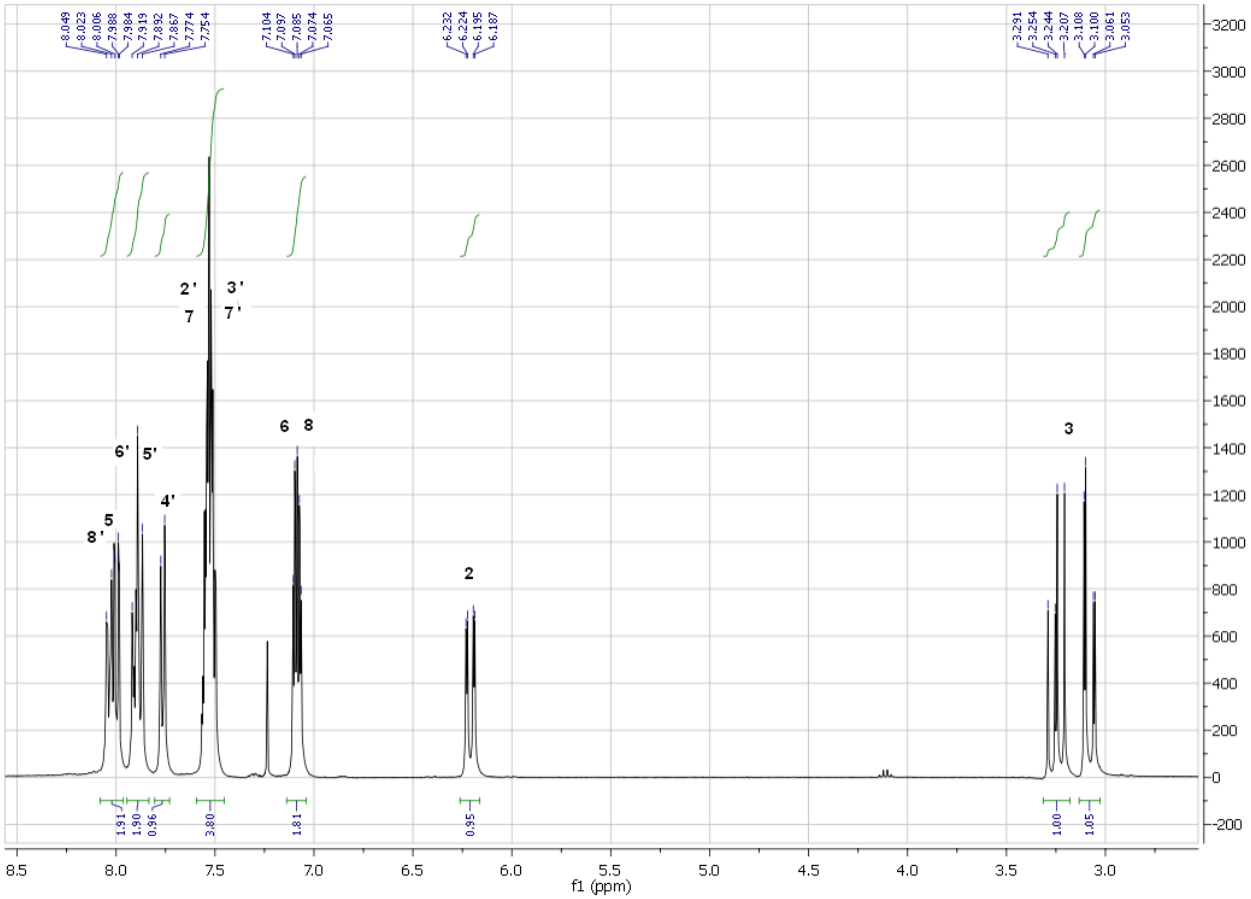

Figure S48. ^{1}H NMR (360 MHz) spectrum of **13a** in $CDCl_3$

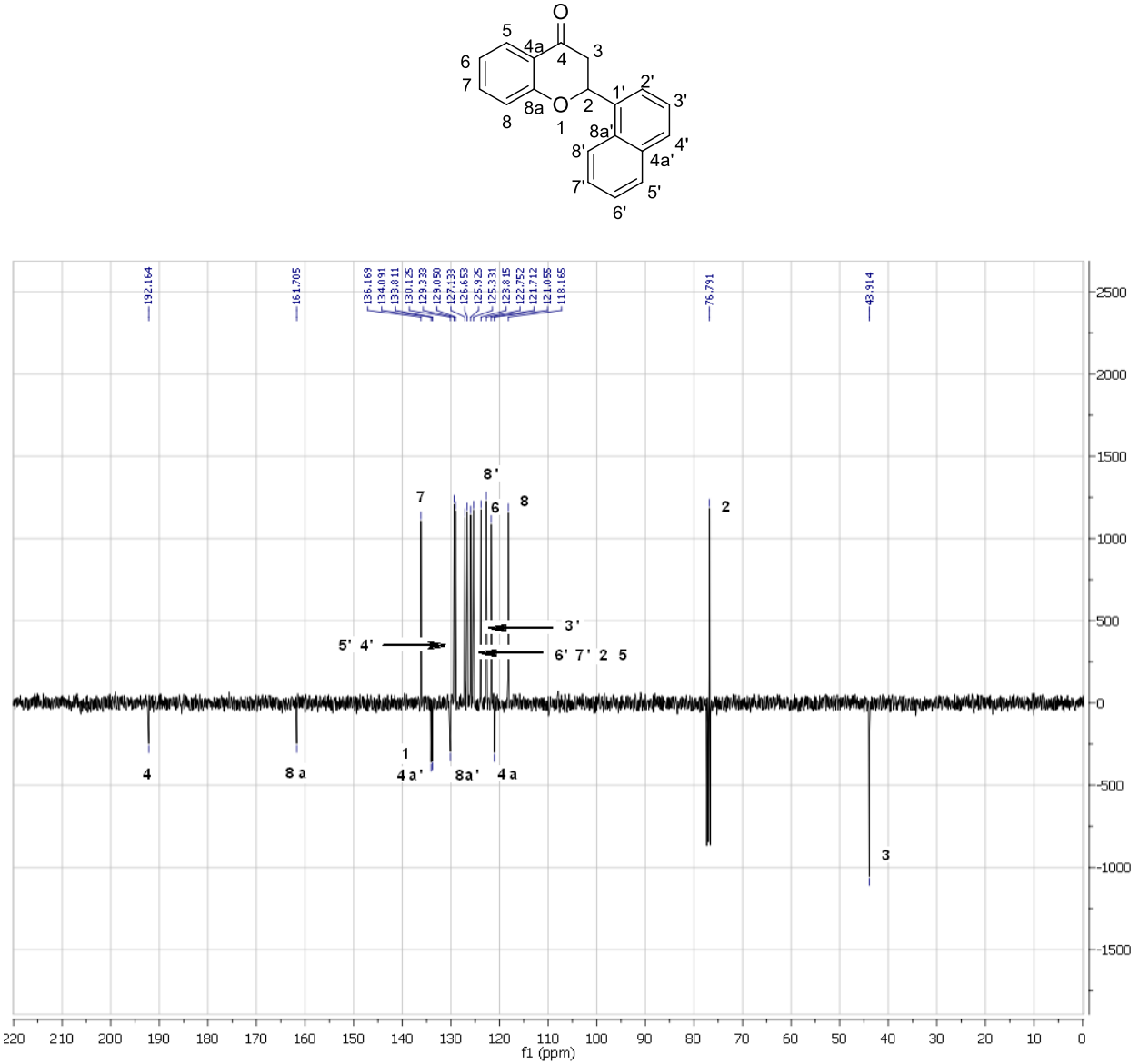

Figure S49. ^{13}C NMR (90 MHz) spectrum of **13a** in $CDCl_3$

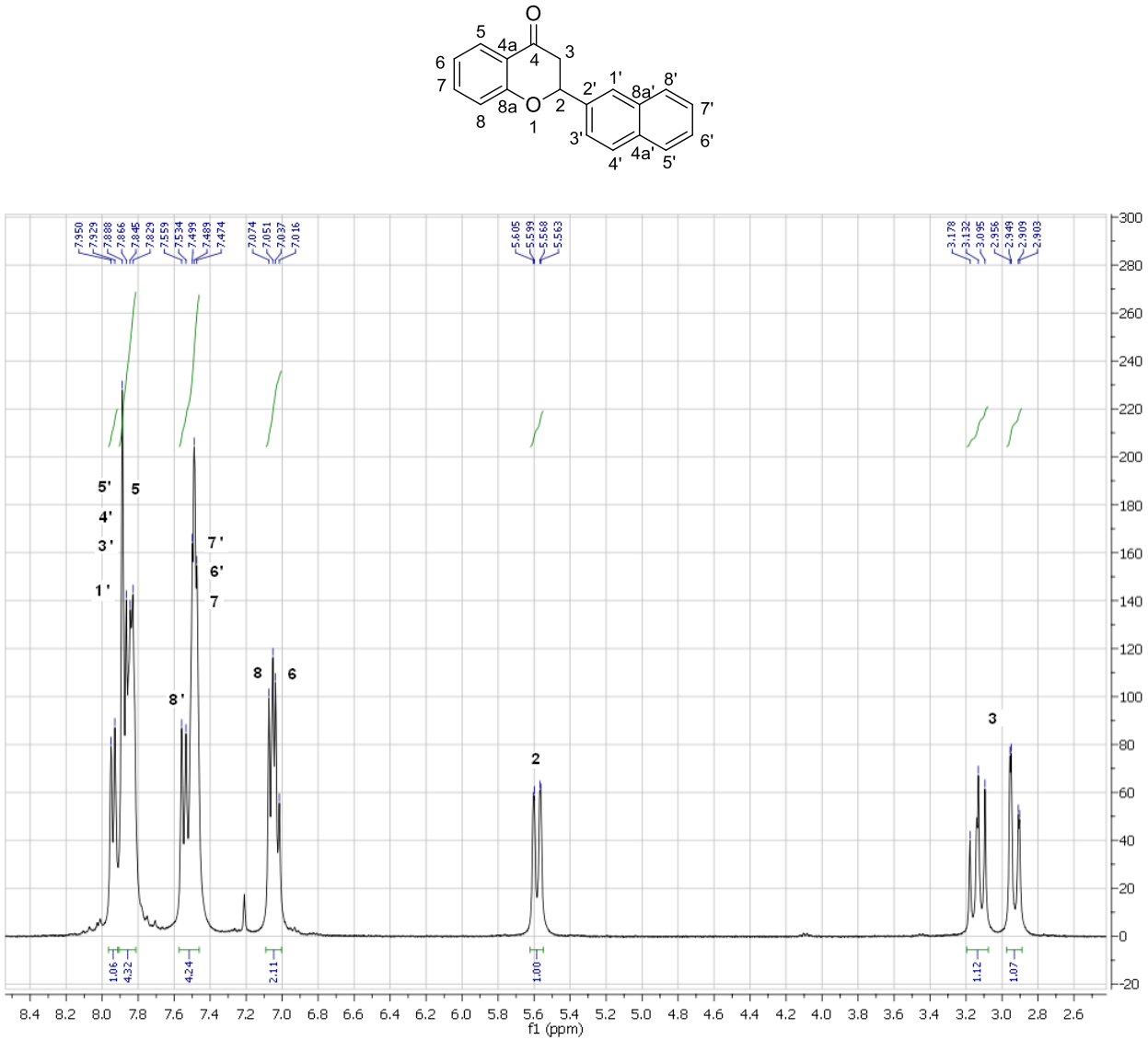

Figure S50. ^{1}H NMR (360 MHz) spectrum of **13b** in $CDCl_3$

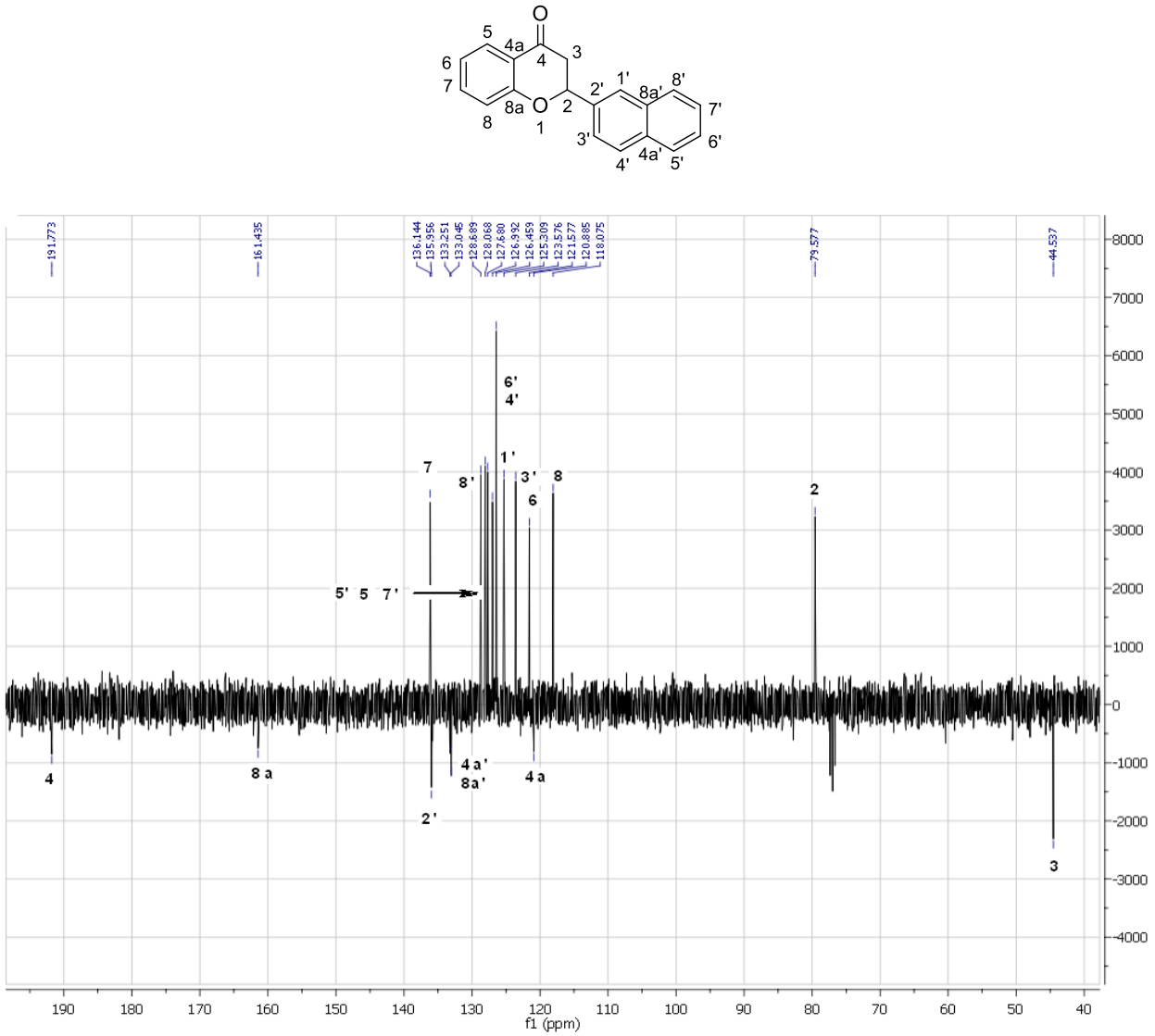

Figure S51. ^{13}C NMR (90 MHz) spectrum of **13b** in $CDCl_3$

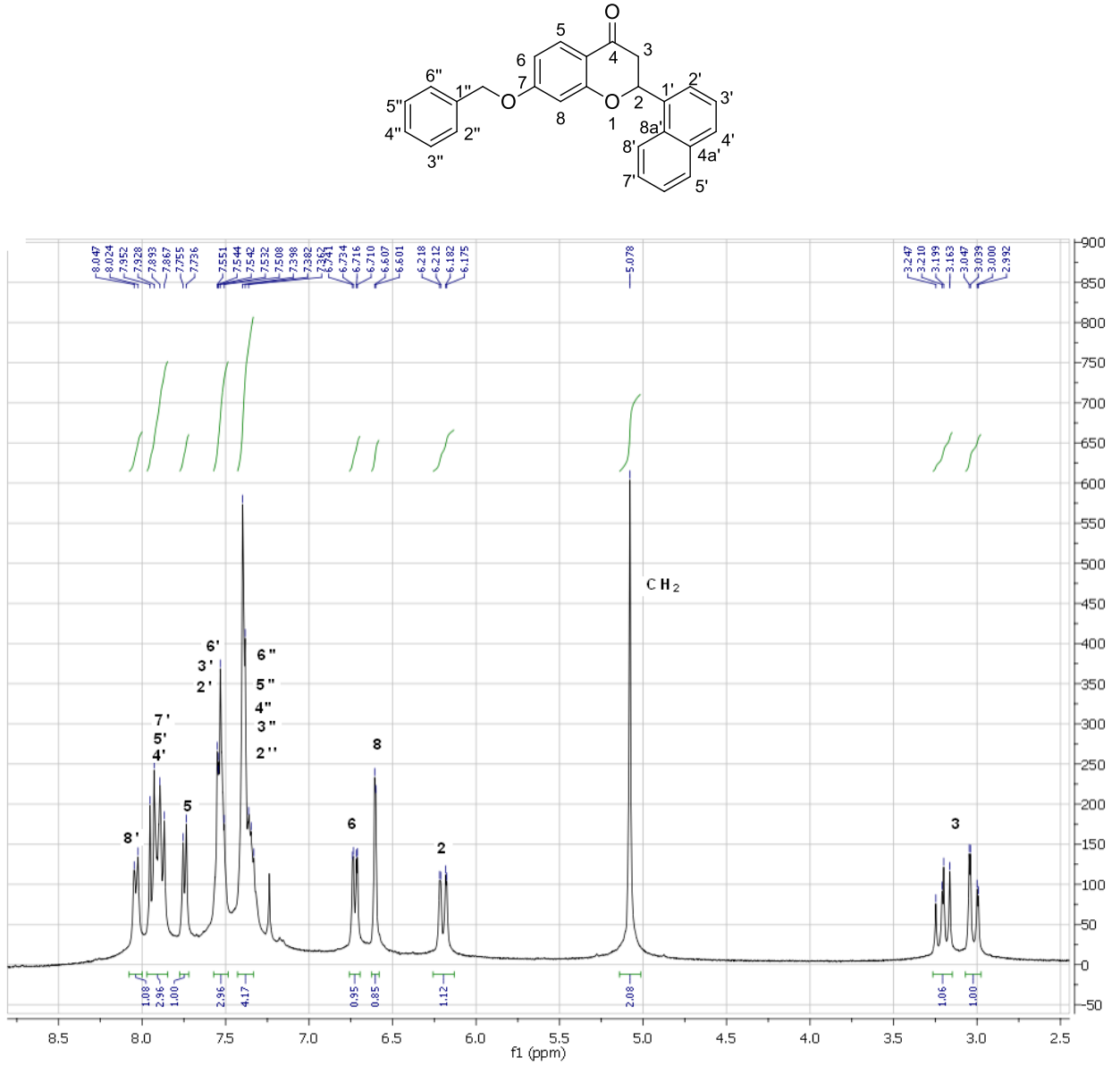

Figure S52. ^{1}H NMR (360 MHz) spectrum of **13c** in $CDCl_3$

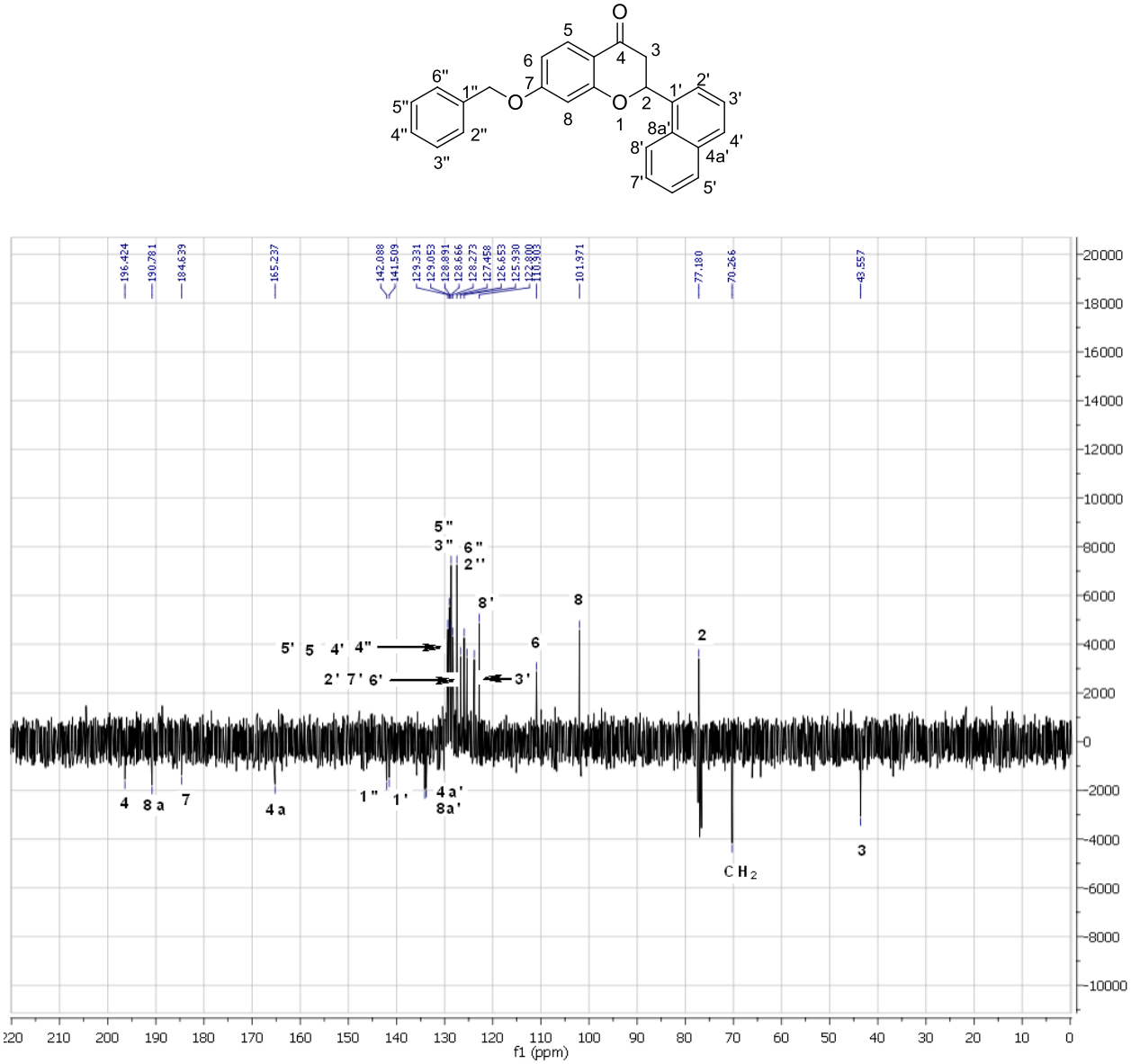

Figure S53. ^{13}C NMR (90 MHz) spectrum of **13c** in $CDCl_3$

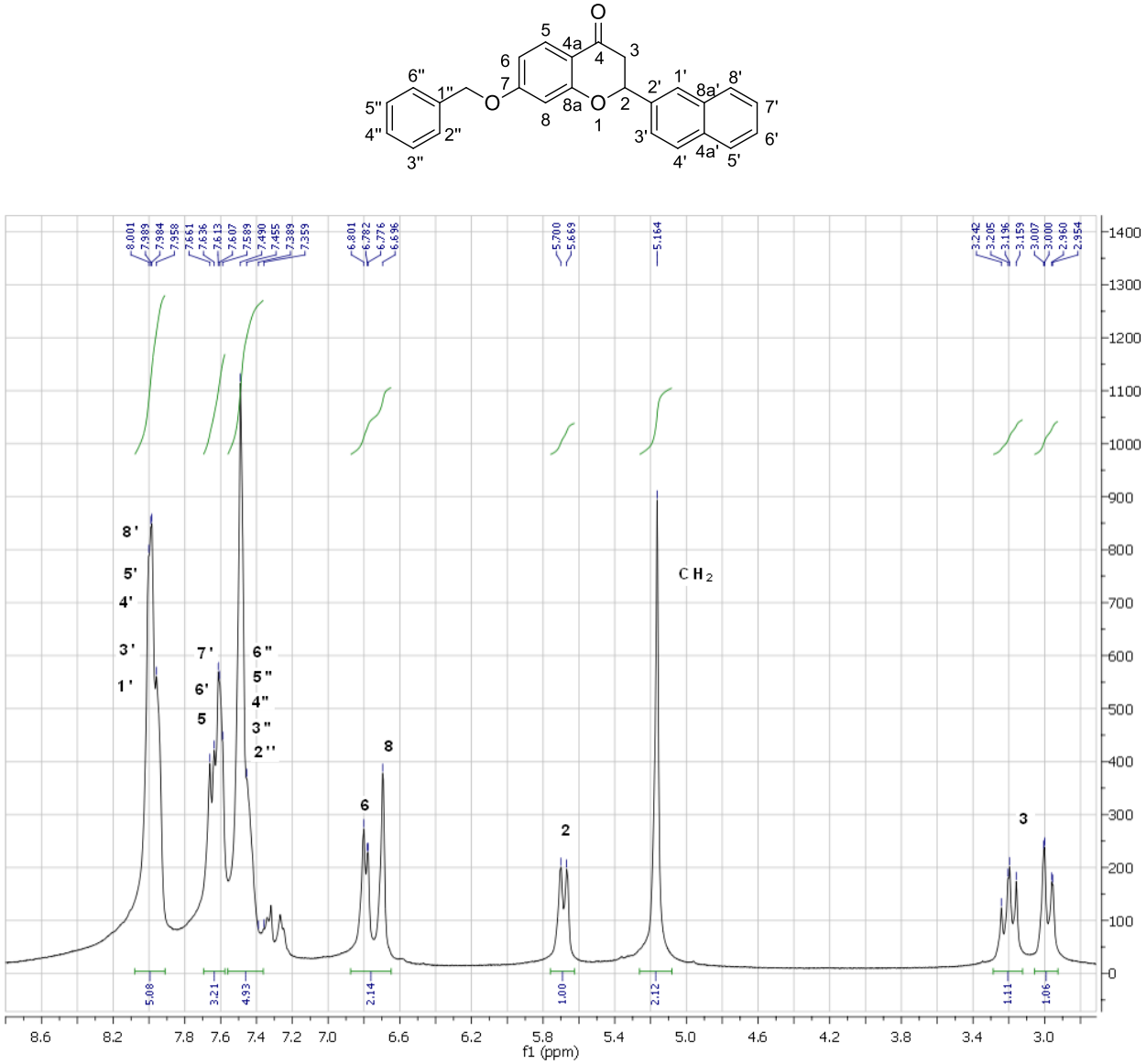

Figure S54. ^{1}H NMR (360 MHz) spectrum of **13d** in $CDCl_3$

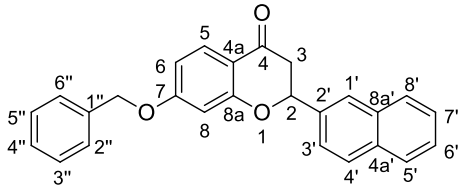

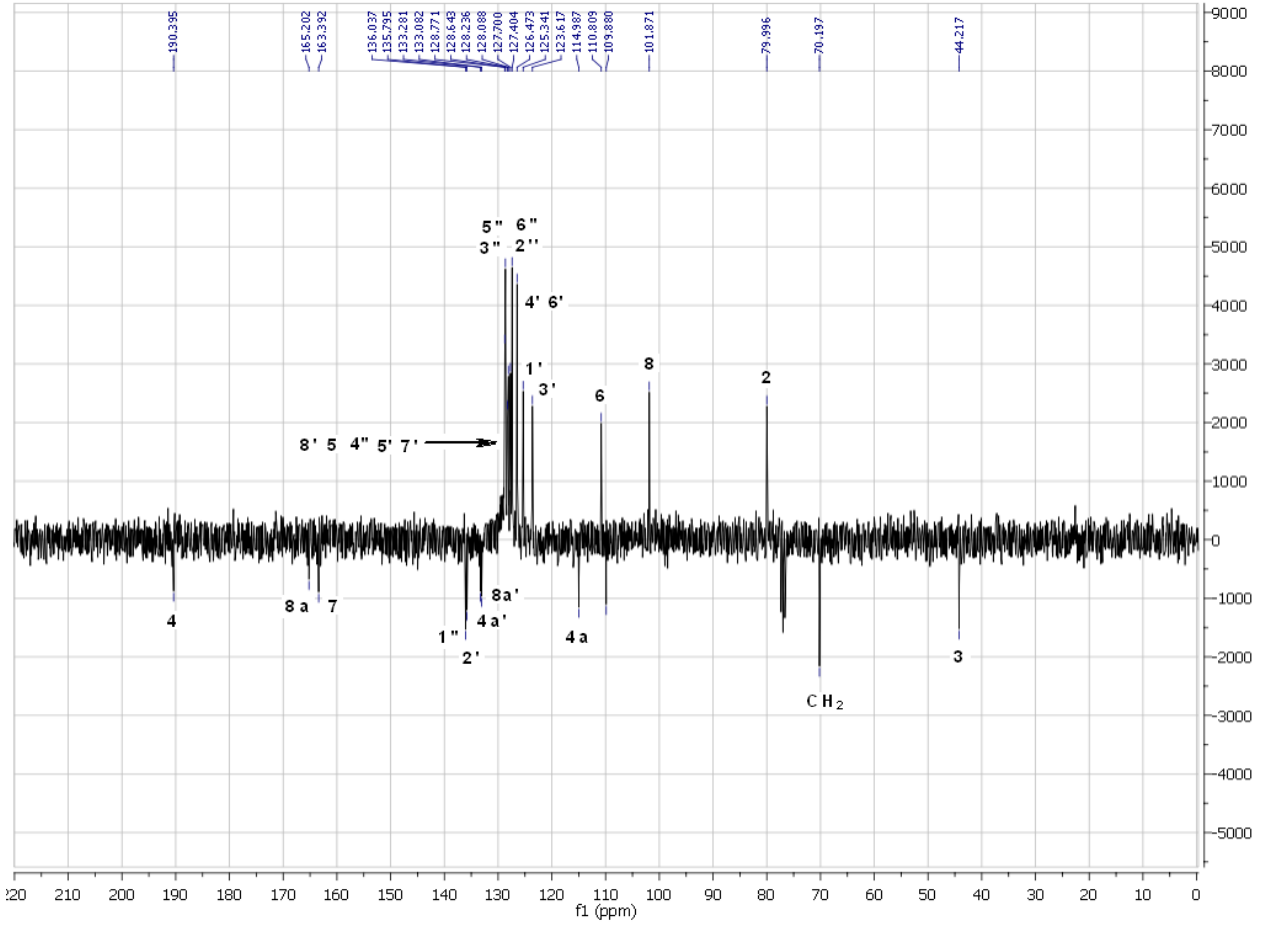

Figure S55. ^{13}C NMR (90 MHz) spectrum of **13d** in $CDCl_3$

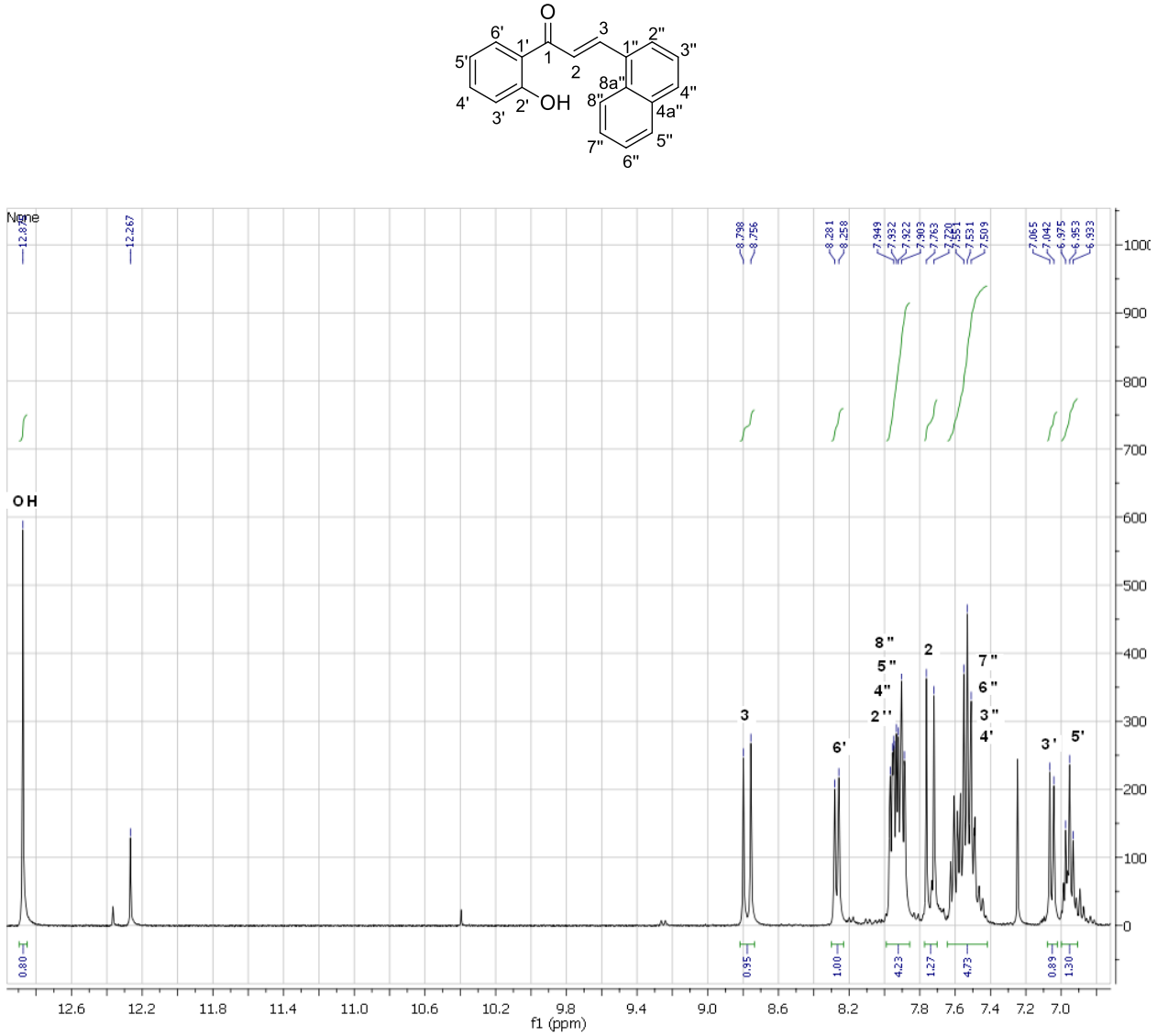

Figure S56. ^{1}H NMR (360 MHz) spectrum of **12a** in $CDCl_3$

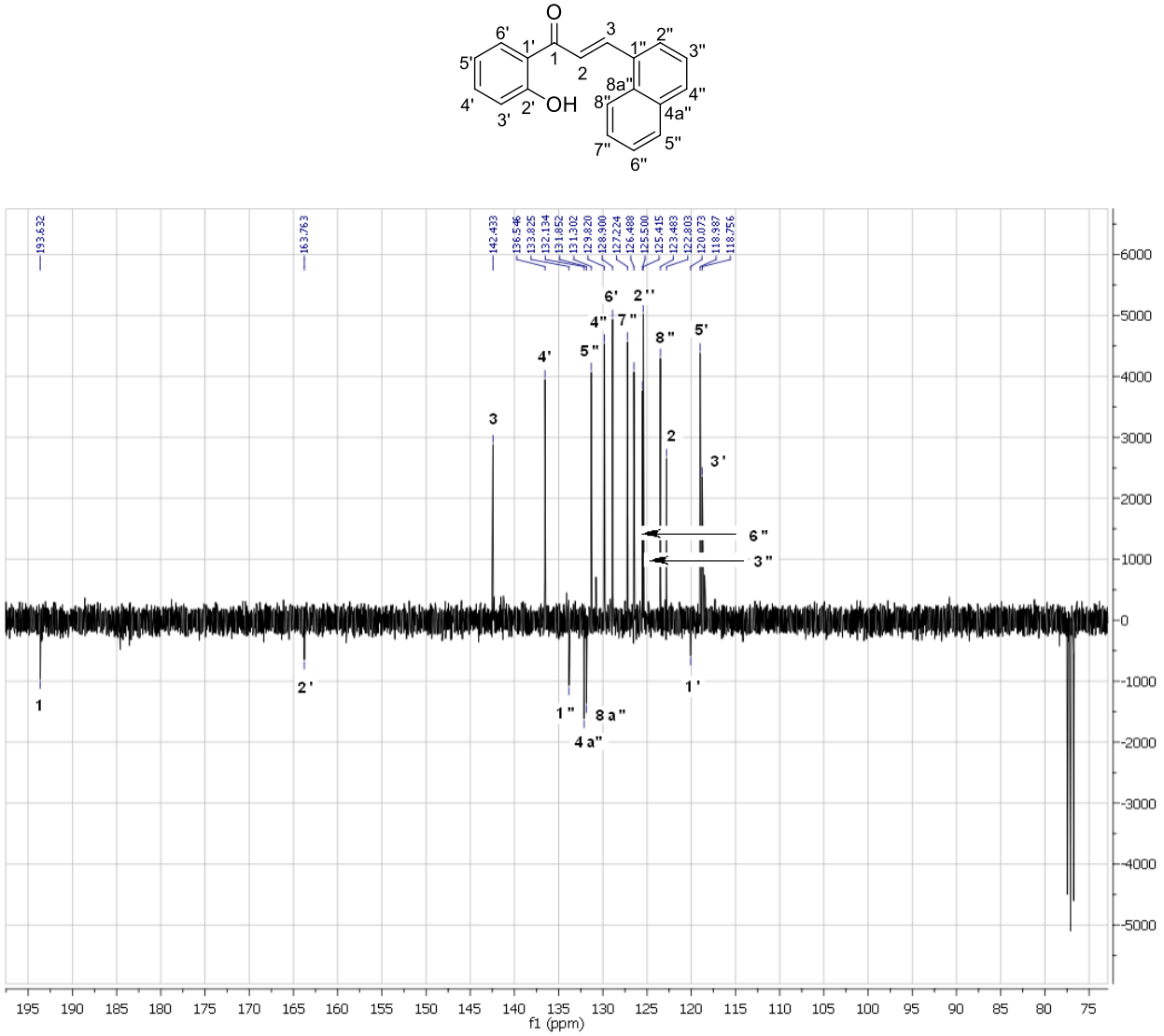

Figure S57. ^{13}C NMR (90 MHz) spectrum of **12a** in $CDCl_3$

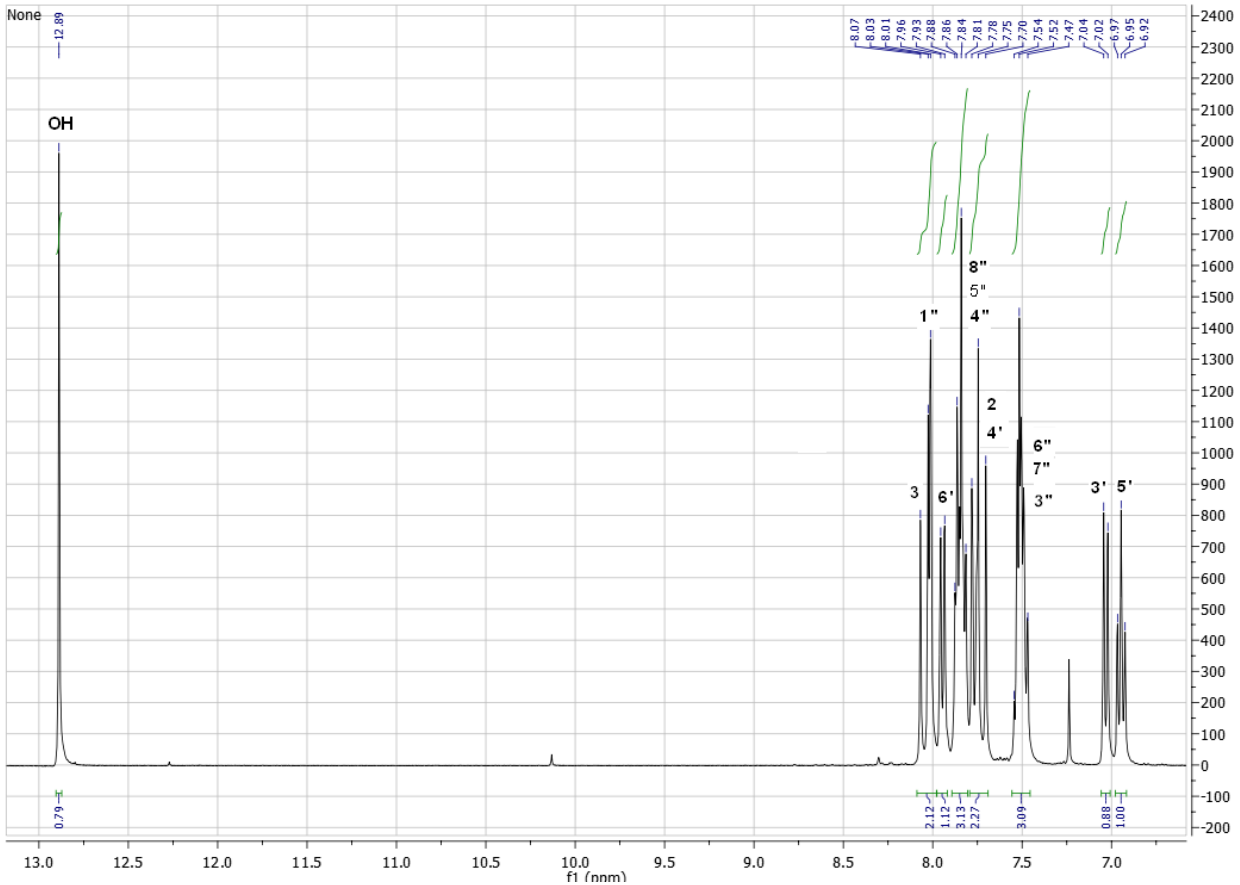

Figure S58. ^{1}H NMR (360 MHz) spectrum of **12b** in $CDCl_3$

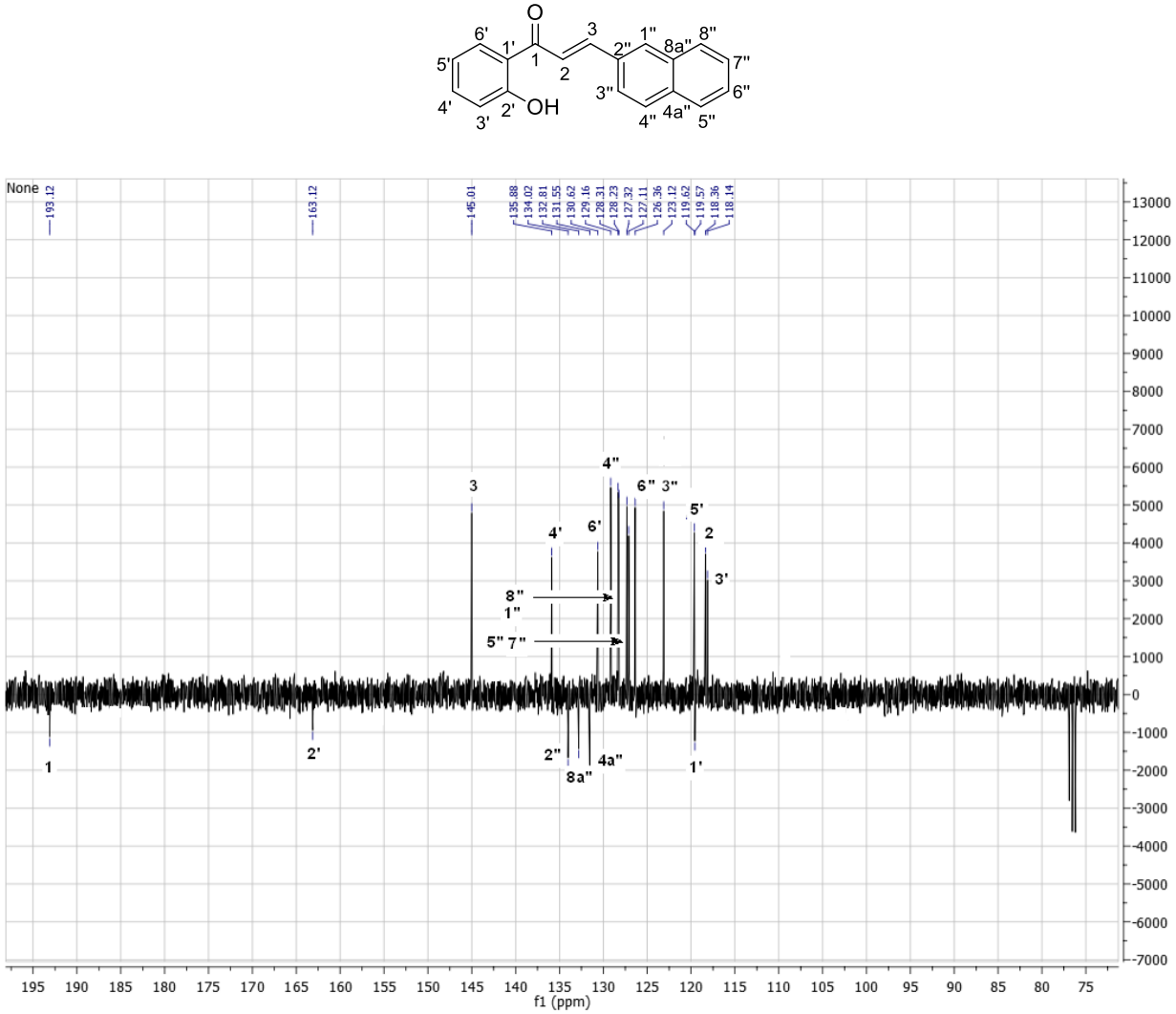

Figure S59. ^{13}C NMR (90 MHz) spectrum of **12b** in $CDCl_3$

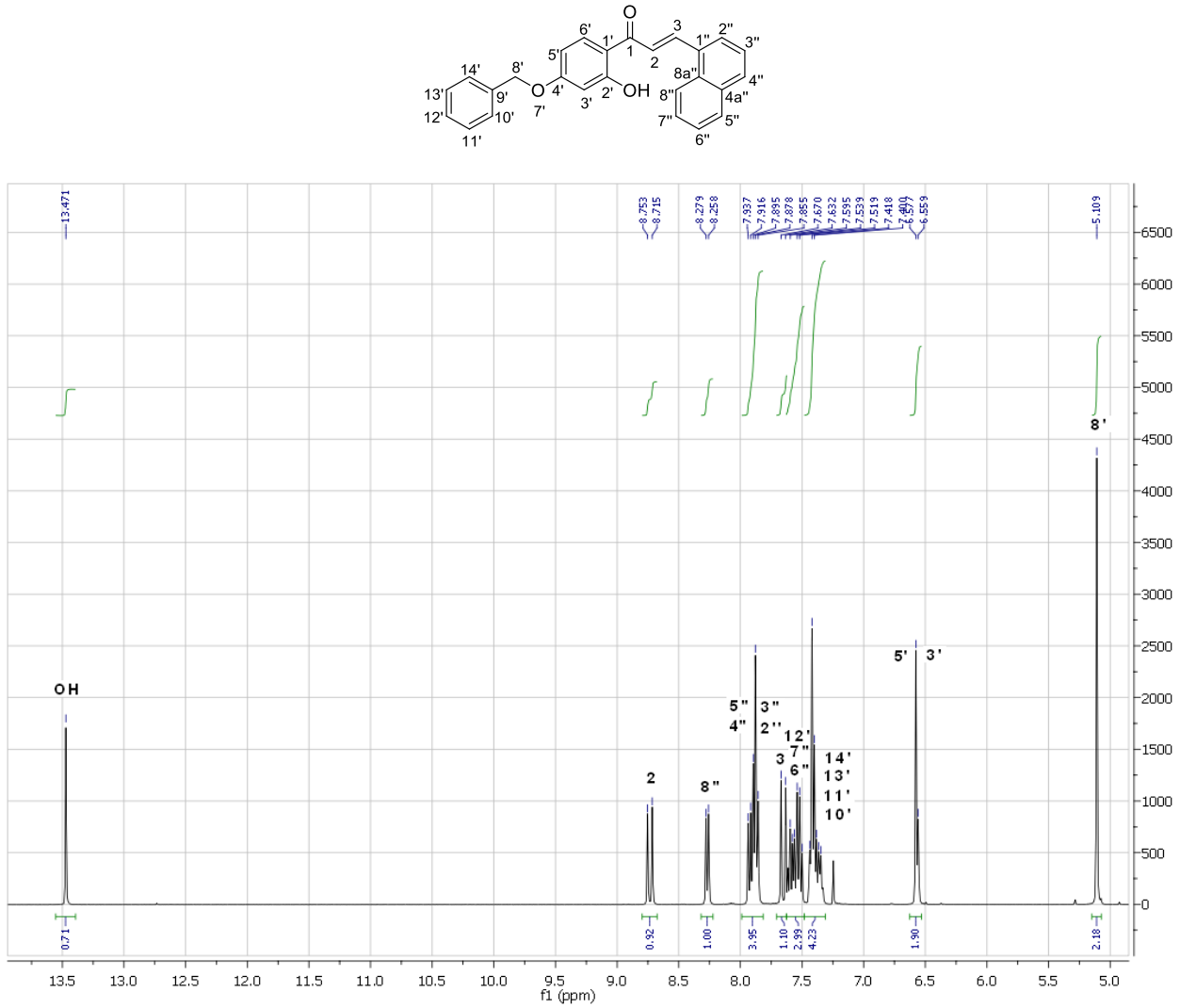

Figure S60. ^{1}H NMR (400 MHz) spectrum of **12c** in $CDCl_3$

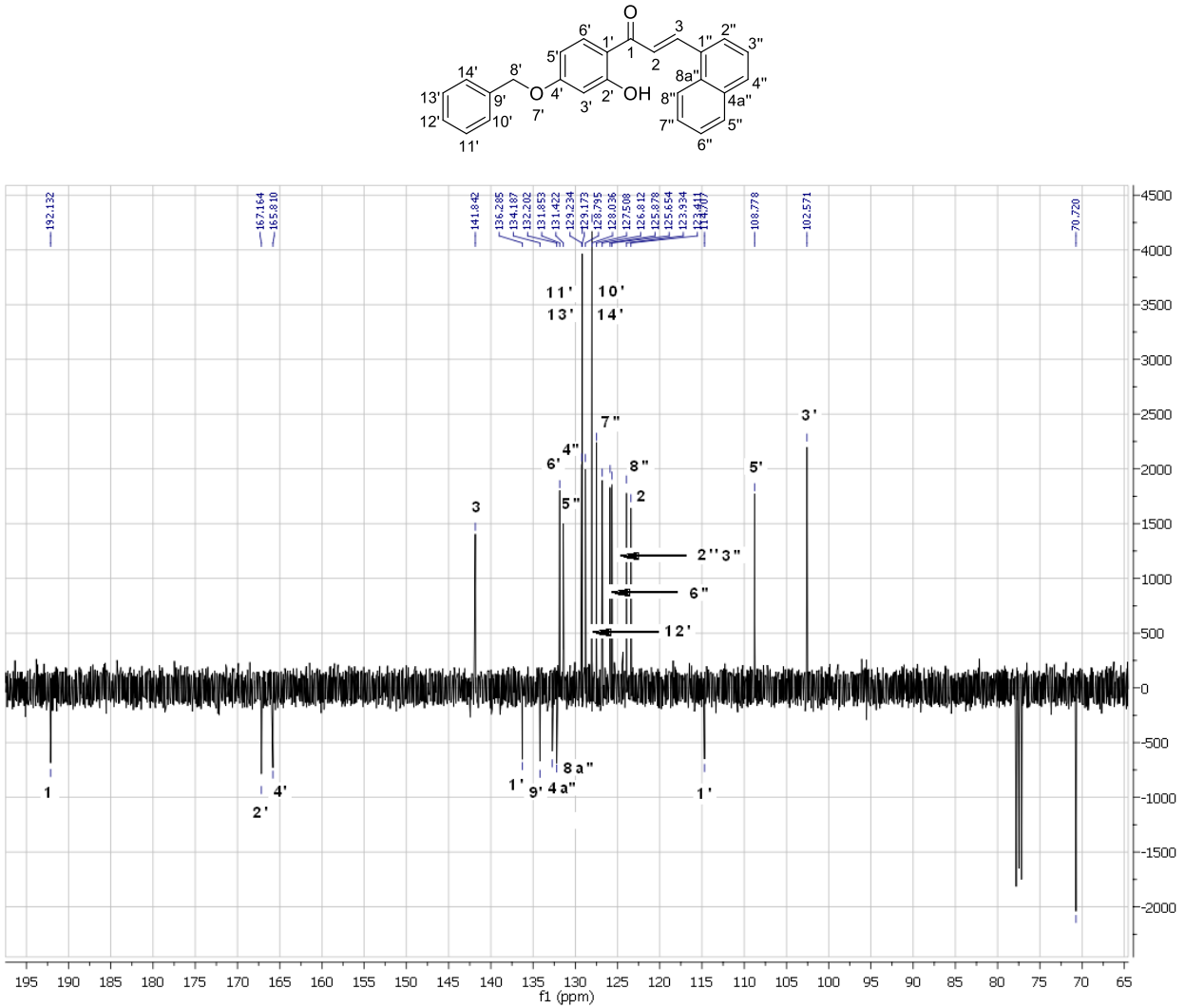

Figure S61. ^{13}C NMR (100 MHz) spectrum of **12c** in $CDCl_3$

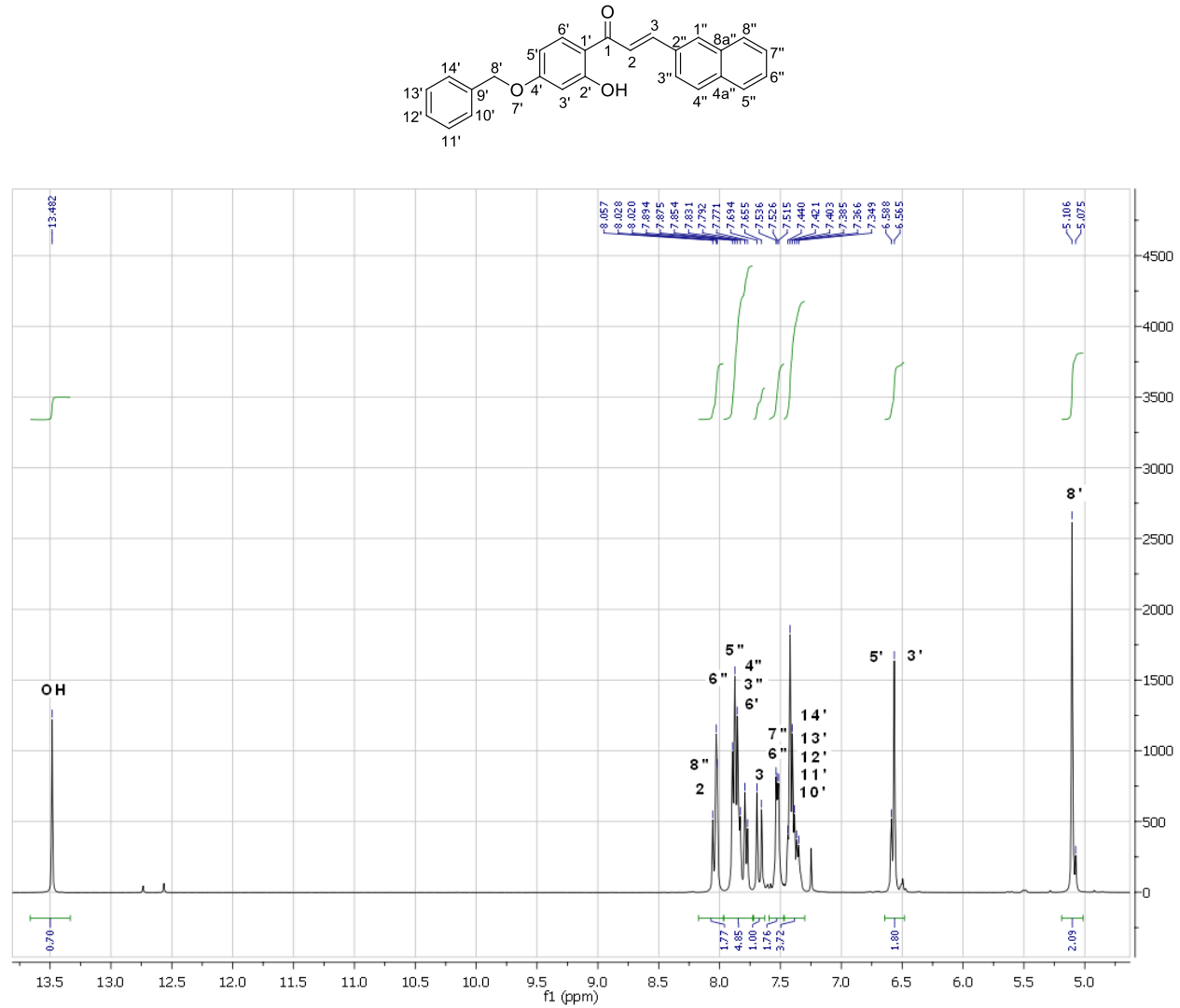

Figure S62. ^{1}H NMR (400 MHz) spectrum of **12d** in $CDCl_3$

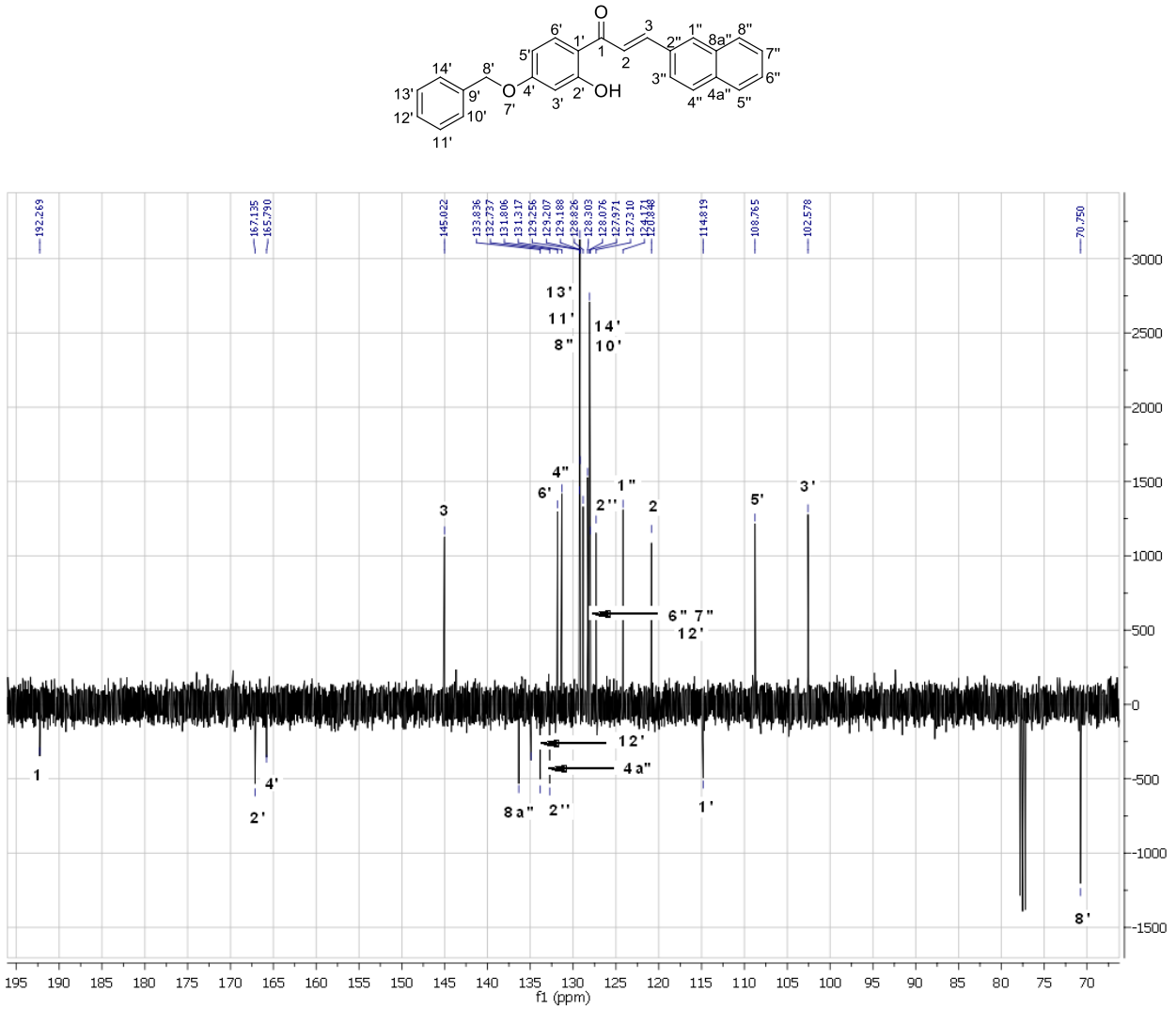

Figure S63. ^{13}C NMR (100 MHz) spectrum of **12d** in $CDCl_3$

3 Antiproliferative activity experiments

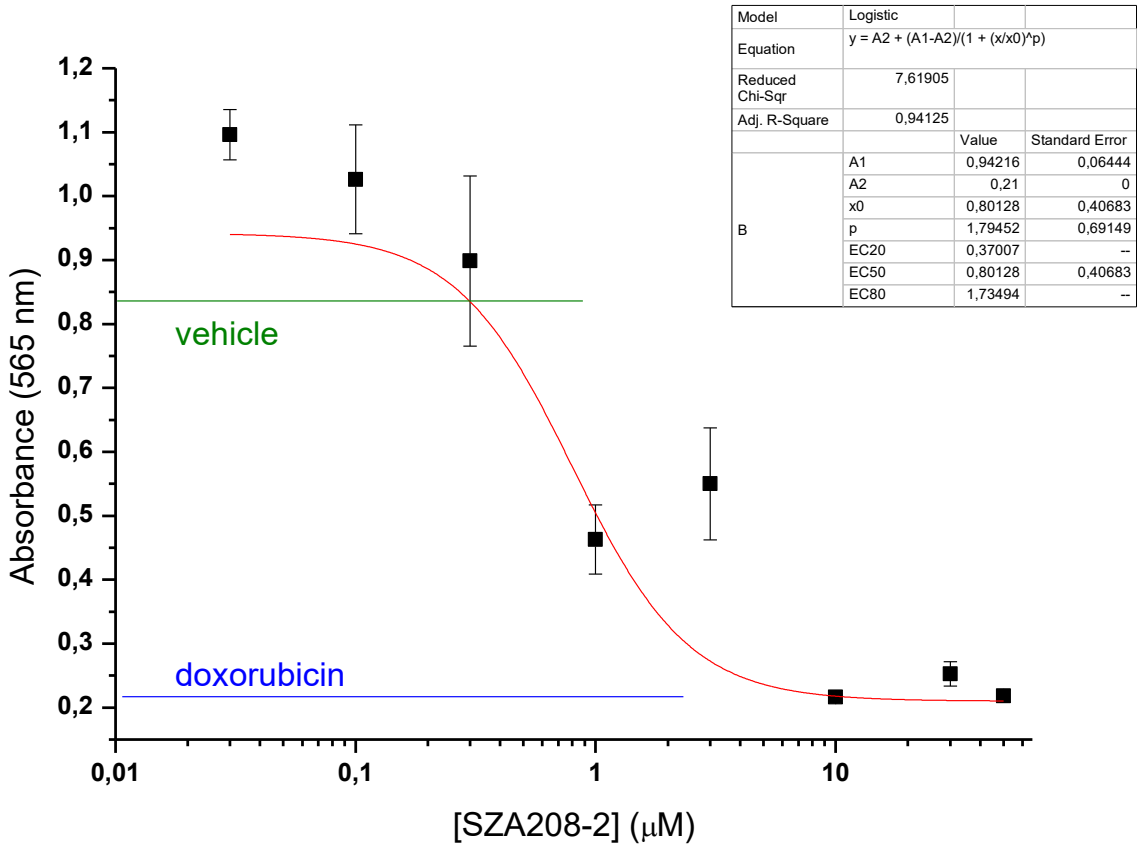

Figure S64. Concentration-dependent effect of **9a** on the viability of A2780 cells. Cells were treated daily for 3 days, subjected for MTT assay and IC_{50} value was determined as described in the Experimental section. Green line indicates the value of negative control treated with equal amount of vehicle solvent (DMSO) and blue line represents the effect of 1 μg/ml doxorubicin used as positive control. Data are presented as Mean±SEM, N=4 at each data point.

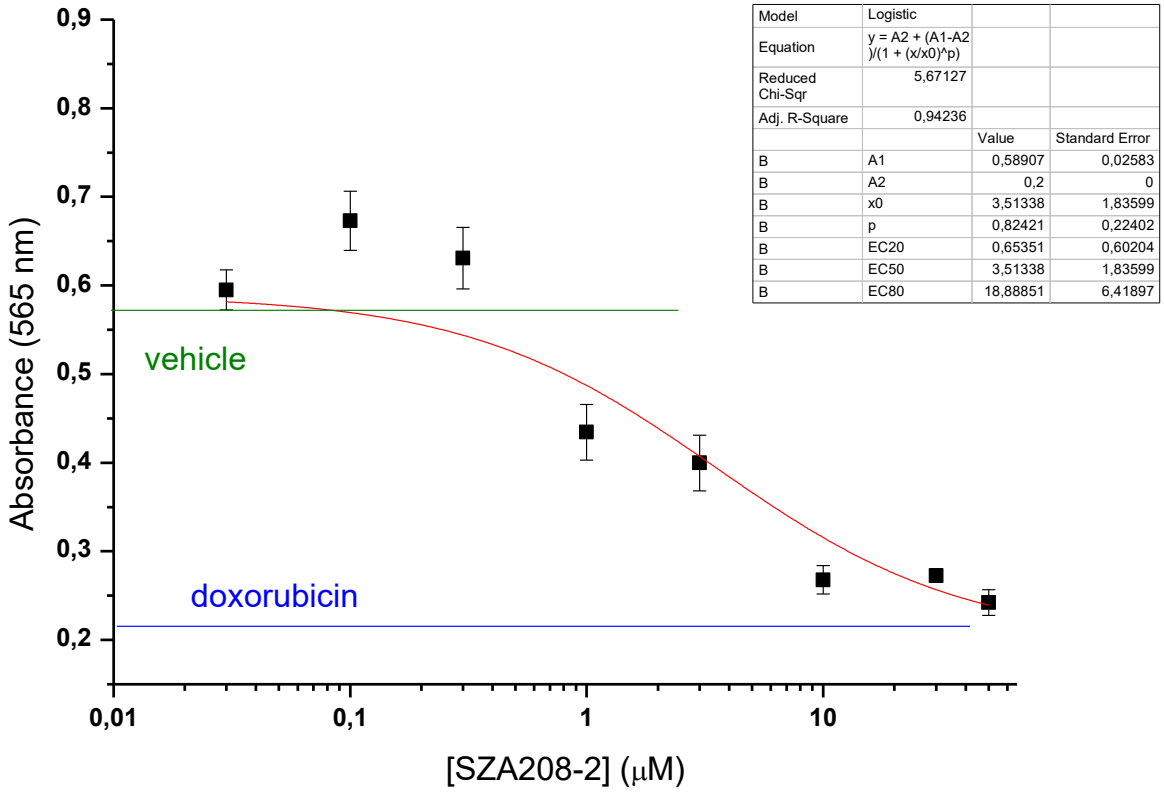

Figure S65. Concentration-dependent effect of **9a** on the viability of WM35 cells. Cells were treated daily for 3 days, subjected for MTT assay and IC_{50} value was determined as described in the Experimental section. Green line indicates the value of negative control treated with equal amount of vehicle solvent (DMSO) and blue line represents the effect of 1 μg/ml doxorubicin used as positive control. Data are presented as Mean±SEM, N=4 at each data point.

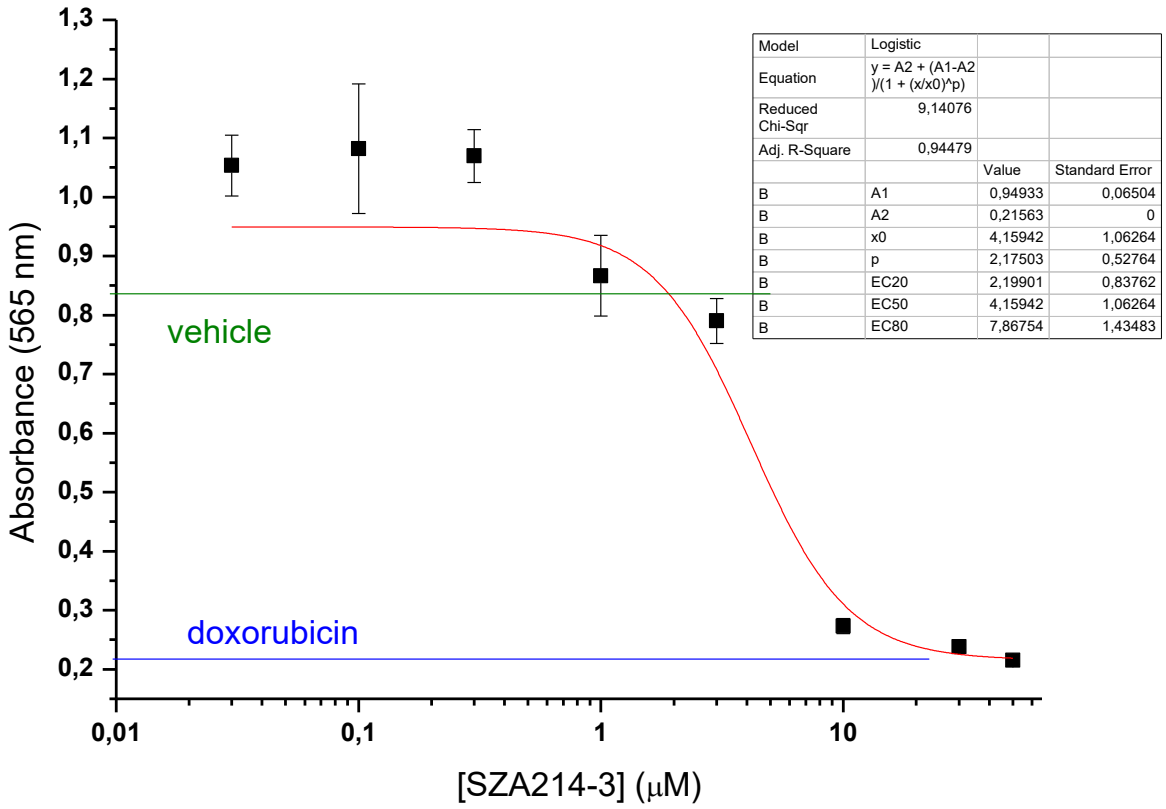

Figure S66. Concentration-dependent effect of **9b** on the viability of A2780 cells. Cells were treated daily for 3 days, subjected for MTT assay and IC_{50} value was determined as described in the Experimental section. Green line indicates the value of negative control treated with equal amount of vehicle solvent (DMSO) and blue line represents the effect of 1 μg/ml doxorubicin used as positive control. Data are presented as Mean±SEM, N=4 at each data point.

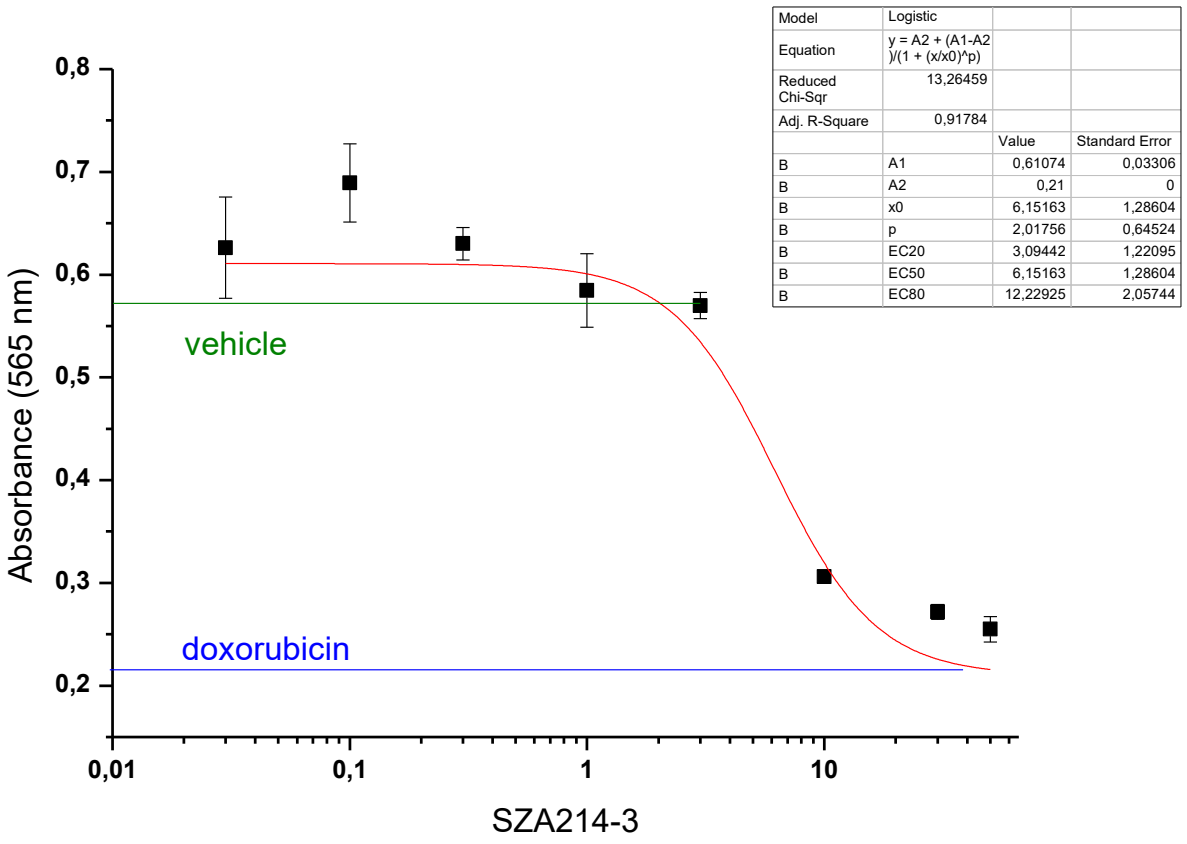

Figure S67. Concentration-dependent effect of **9b** on the viability of WM35 cells. Cells were treated daily for 3 days, subjected for MTT assay and IC50 value was determined as described in the "Experimental" section. Green line indicates the value of negative control treated with equal amount of vehicle solvent (DMSO) and blue line represents the effect of 1 µg/ml doxorubicin used as positive control. Data are presented as Mean±SEM, N=4 at each data point.

4 Chiral HPLC-ECD Spectra

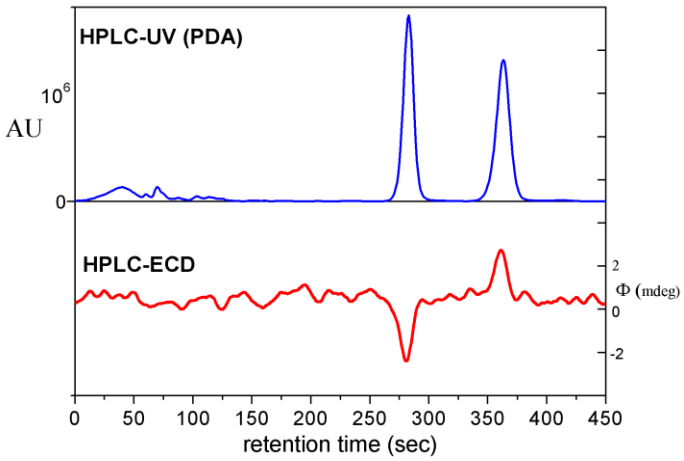

Figure S68. HPLC-UV and –ECD traces of **9c** on Chiralpak IA column with hexane/2-propanol 80:20 eluent monitored at 250 nm.

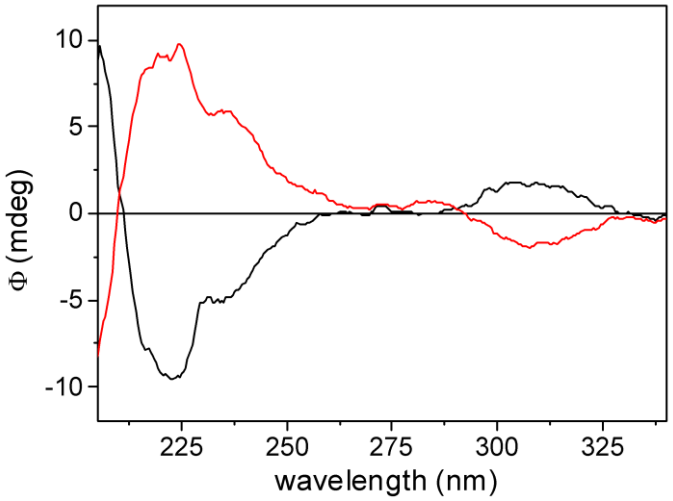

Figure S69. HPLC-ECD spectra of the first- [(6*S*,6a*R*,11a*R*), black] and second-eluting [(6*R*,6a*S*,11a*S*), red] enantiomers of **9c**.

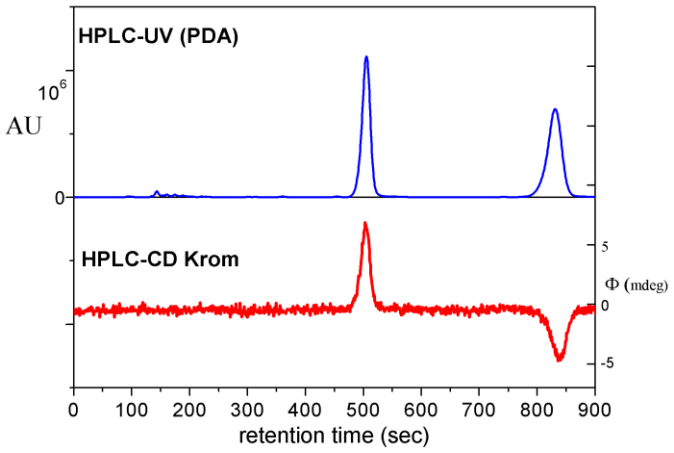

Figure S70. HPLC-UV and –ECD traces of **9d** on Chiralpak IA column with hexane/2-propanol 80:20 eluent monitored at 310 nm.

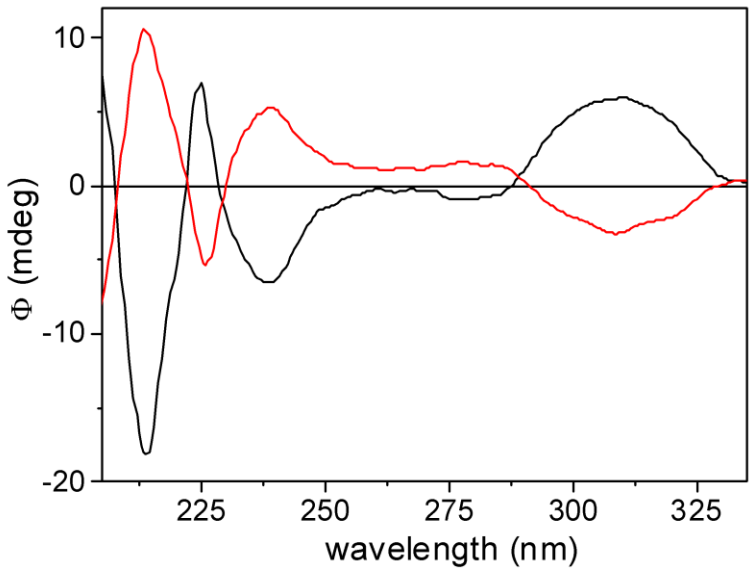

Figure S71. HPLC-ECD spectra of the first- [(6*S*,6a*R*,11a*R*), black] and second-eluting [(6*R*,6a*S*,11a*S*), red] enantiomers of **9d**.

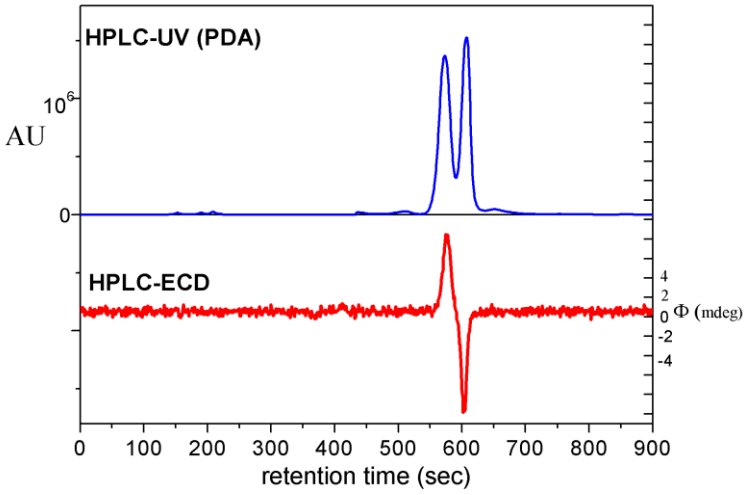

Figure S72. HPLC-UV and –ECD traces of **10a** on Chiralpak IA column with hexane/2-propanol 95:5 eluent monitored at 270 nm.

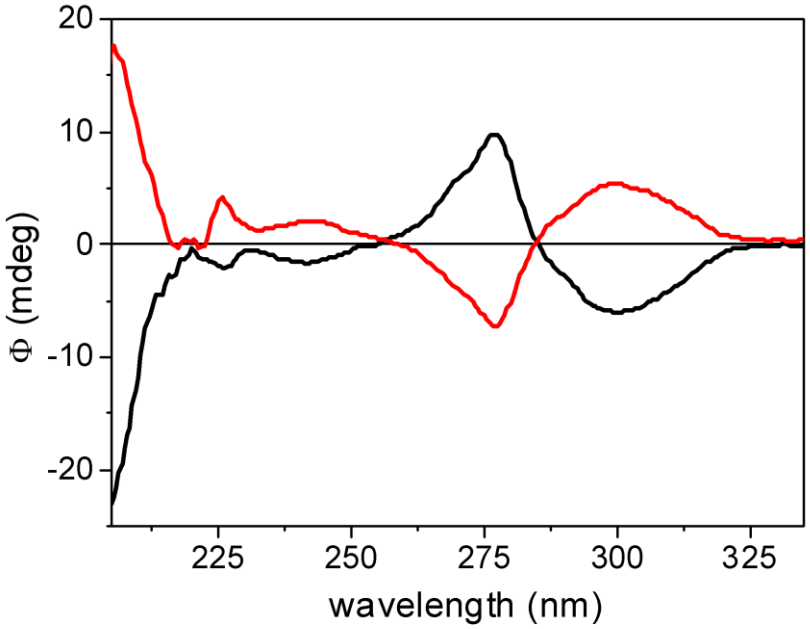

Figure S73. HPLC-ECD spectra of the first- [(6*S*,12*S*), black] and second-eluting [(6*R*,12*R*), red] enantiomers of **10a**.

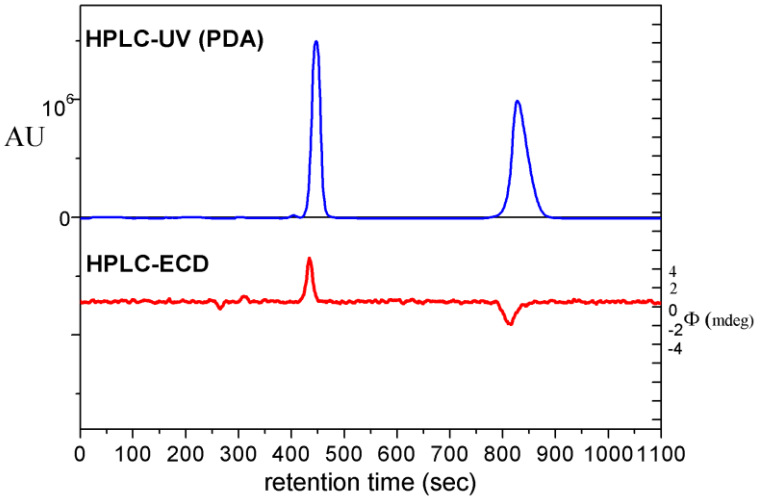

Figure S74. HPLC-UV and –ECD traces of **10b** on Chiralpak IA column with hexane/2-propanol 80:20 eluent monitored at 270 nm.

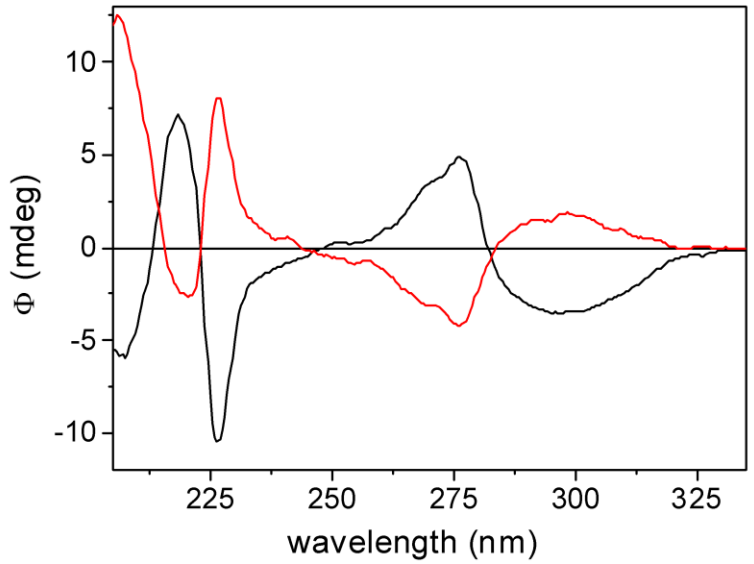

Figure S75. HPLC-ECD spectra of the first- [(6*S*,12*S*), black] and second-eluting [(6*R*,12*R*), red] enantiomers of **10b**.

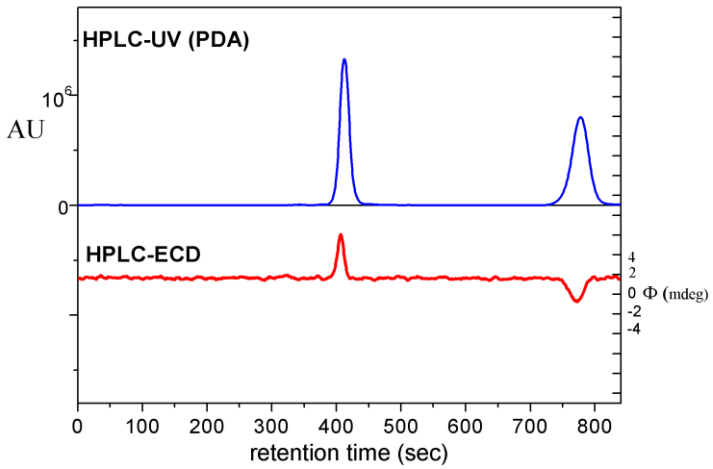

Figure S76. HPLC-UV and –ECD traces of **10c** on Chiralpak IA column with hexane/2-propanol 80:20 eluent monitored at 310 nm.

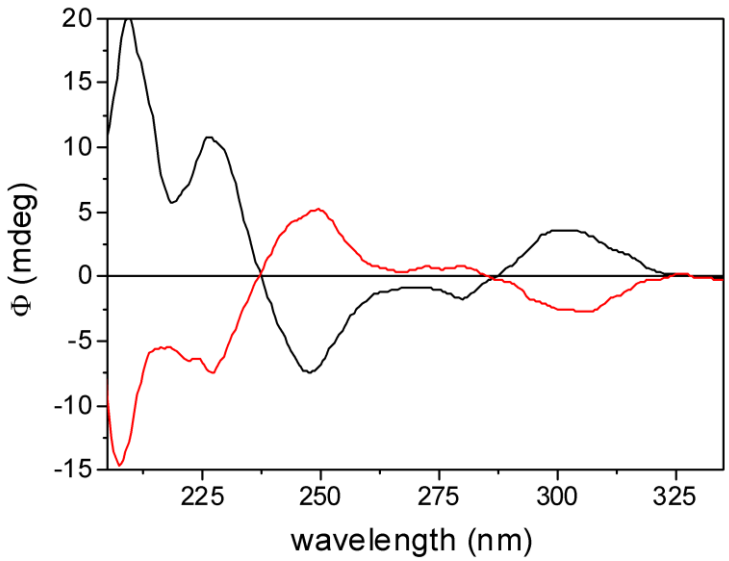

Figure S77. HPLC-ECD spectra of the first- [(6*R*,12*R*), black] and second-eluting [(6*S*,12*S*), red] enantiomers of **10c**.

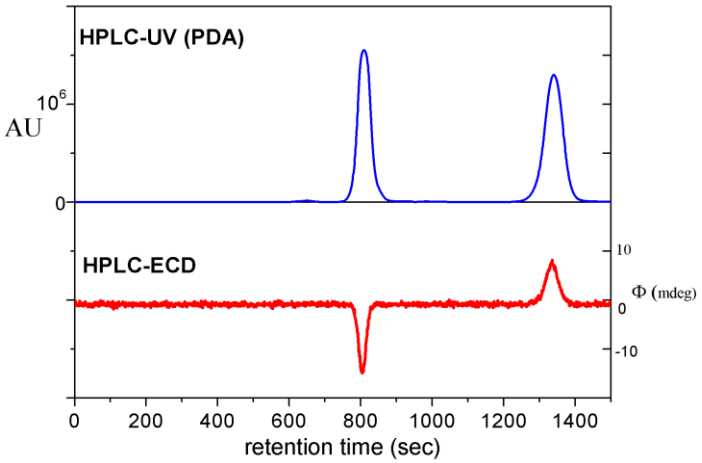

Figure S78. HPLC-UV and –ECD traces of **10d** on Chiralpak IA column with hexane/2-propanol 80:20 eluent monitored at 250 nm.

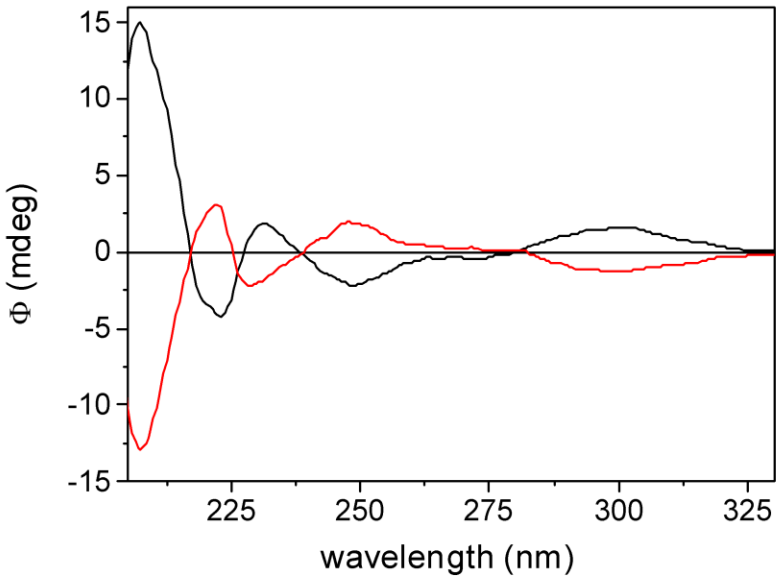

Figure S79. HPLC-ECD spectra of the first- [(6*R*,12*R*), black] and second-eluting [(6*S*,12*S*), red] enantiomers of **10d**.

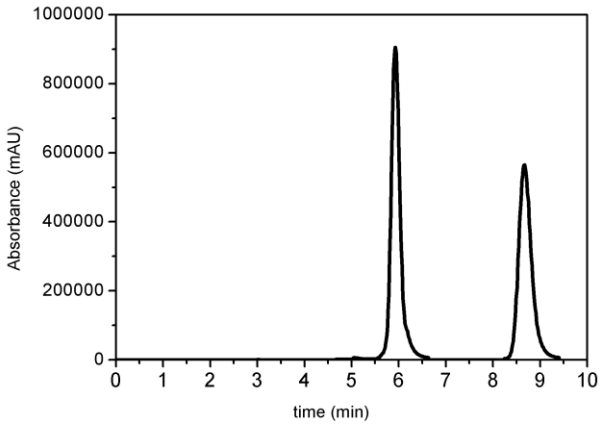

Figure S80. HPLC-UV trace of **13a** on Chiralpak IC column with hexane/2-propanol 75:25 eluent.

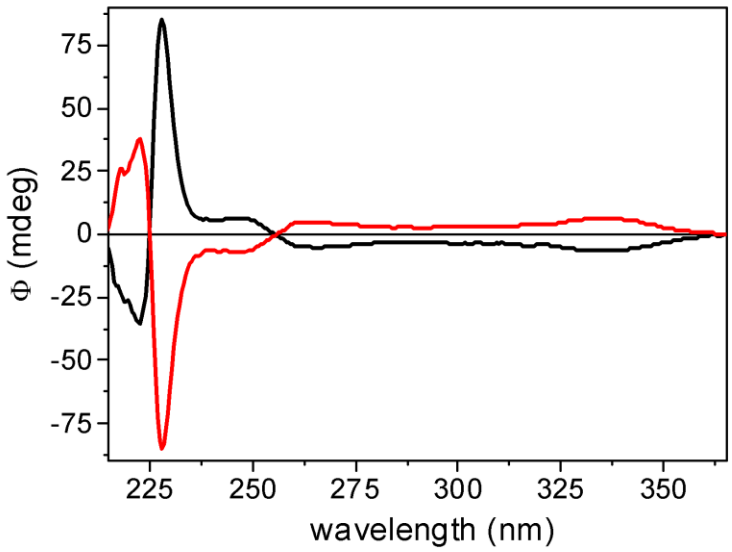

Figure S81. HPLC-ECD spectra of the first- [(2*S*), black] and second-eluting [(2*R*), red] enantiomers of **13a**.

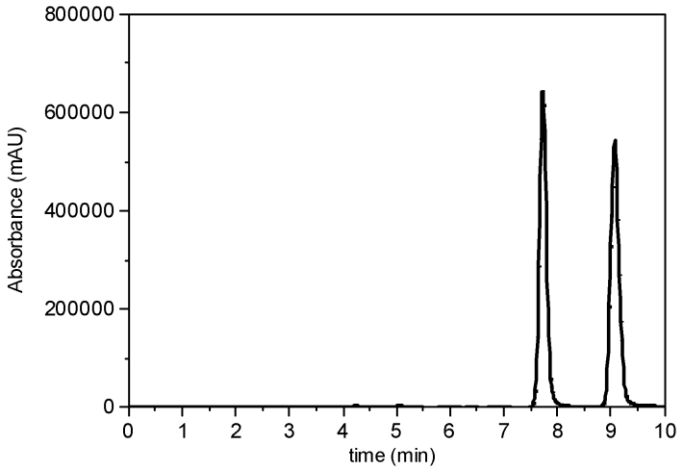

Figure S82. HPLC-UV trace of **13b** on Chiralpak IC column with hexane/2-propanol 75:25 eluent.

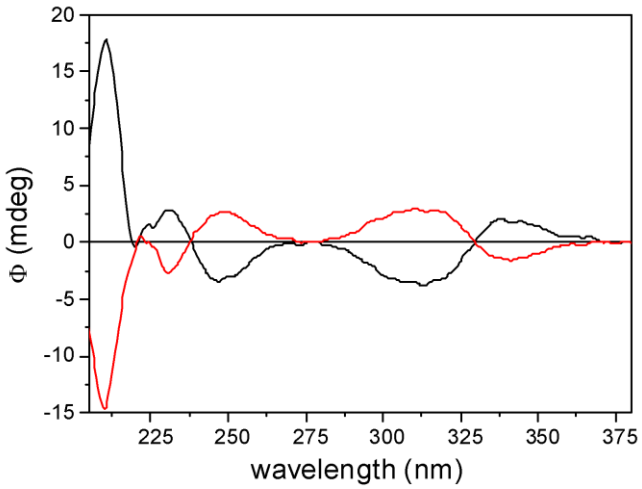

Figure S83. HPLC-ECD spectra of the first- [(2*S*), black] and second-eluting [(2*R*), red] enantiomers of **13b**.

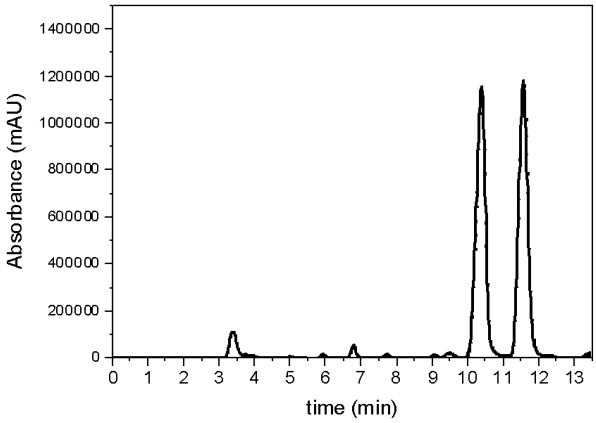

Figure S84. HPLC-UV trace of **13c** on Chiralpak IC column with hexane/2-propanol 75:25 eluent.

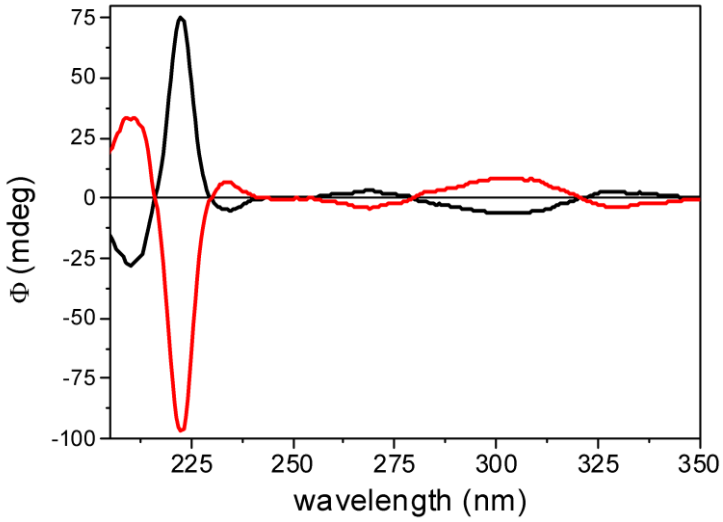

Figure S85. HPLC-ECD spectra of the first- [(2*S*), black] and second-eluting [(2*R*), red] enantiomers of **13c**.

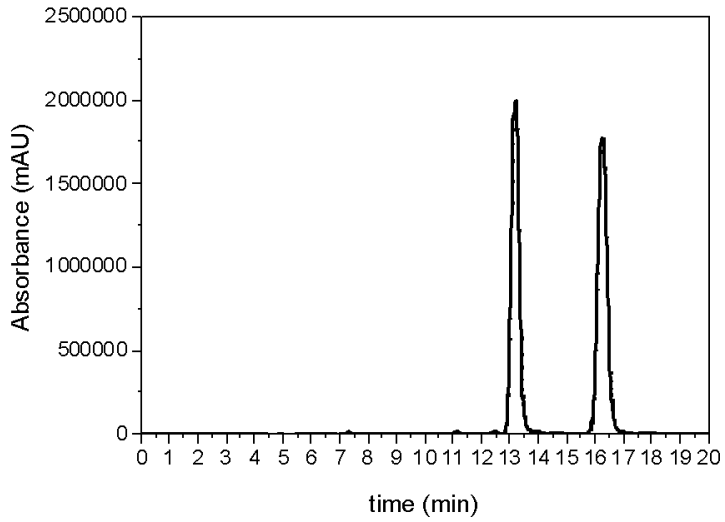

Figure S86. HPLC-UV trace of **13d** on Chiralpak IC column with hexane/2-propanol 75:25 eluent.

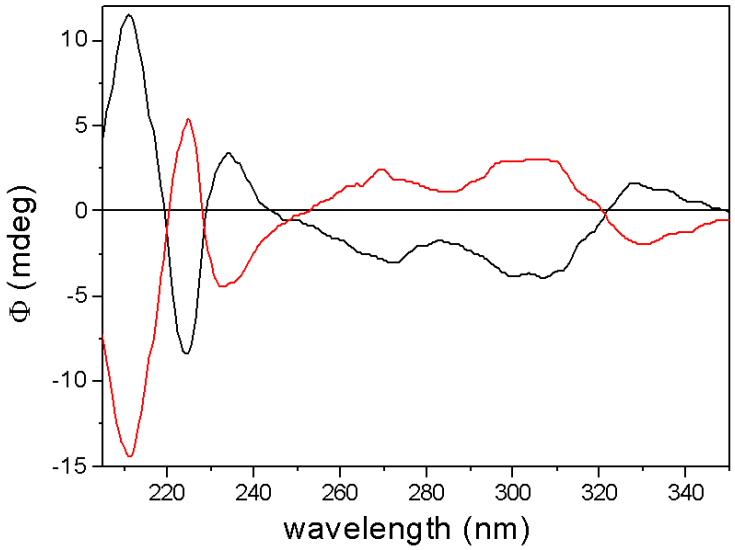

Figure S87. HPLC-ECD spectra of the first- [(2*S*), black] and second-eluting [(2*R*), red] enantiomers of **13d**.

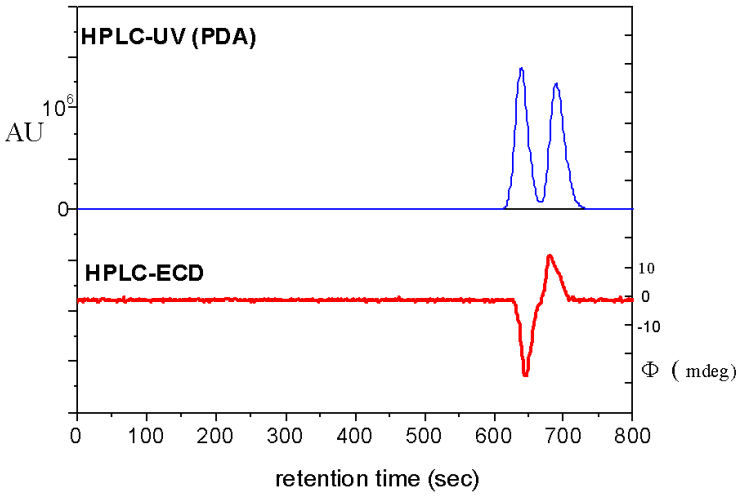

Figure S88. HPLC-UV trace of **7a** on Chiralcel OD column with hexane/2-propanol 95:5 eluent monitored at 260 nm.

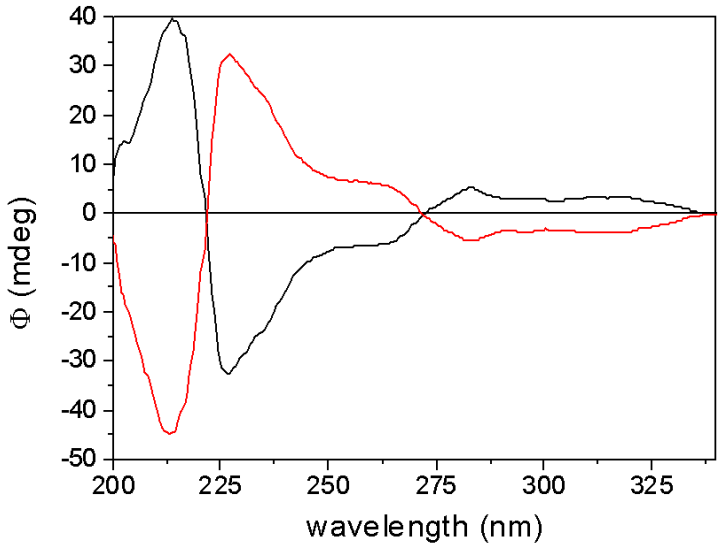

Figure S89. HPLC-ECD spectra of the first- [(2*R*), black] and second-eluting [(2*S*), red] enantiomers of **7a**.

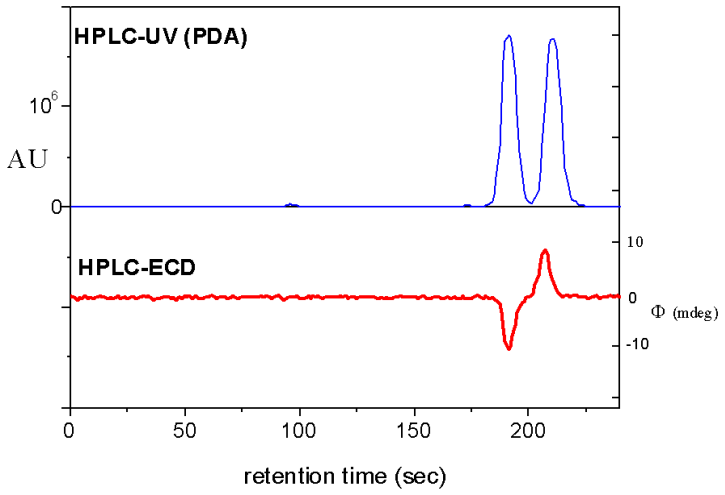

Figure S90. HPLC-UV trace of **7b** on Chiralpak IA column with hexane/2-propanol 95:5 eluent monitored at 280 nm.

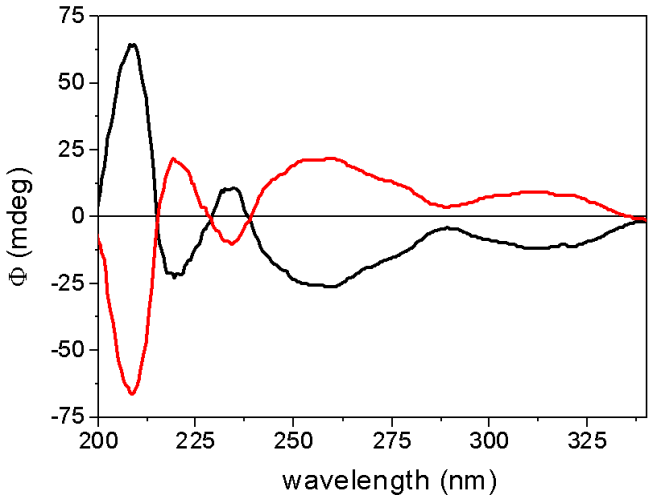

Figure S91. HPLC-ECD spectra of the first- [(2*S*), black] and second-eluting [(2*R*), red] enantiomers of **7b**.

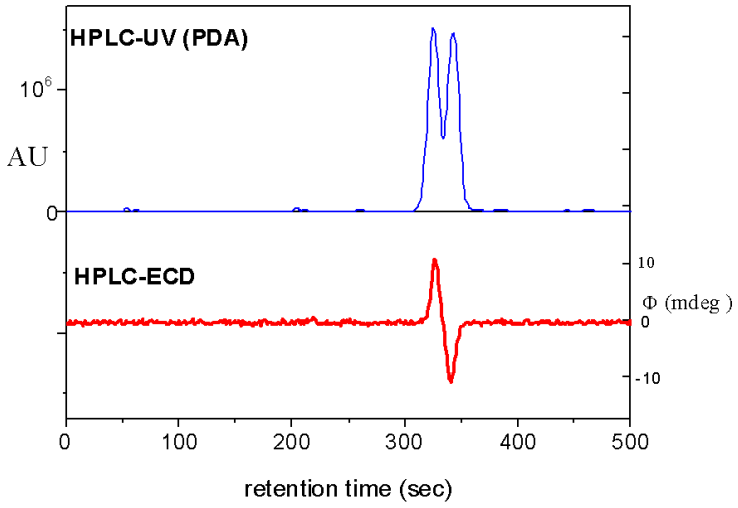

Figure S92. HPLC-UV trace of **7c** on Chirlpak IA column with hexane/2-propanol 95:5 eluent monitored at 270 nm.

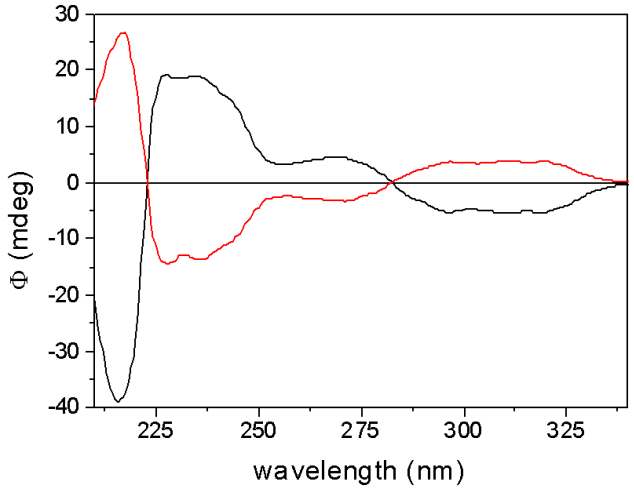

Figure S93. HPLC-ECD spectra of the first- [(2*S*), black] and second-eluting [(2*R*), red] enantiomers of **7c**.

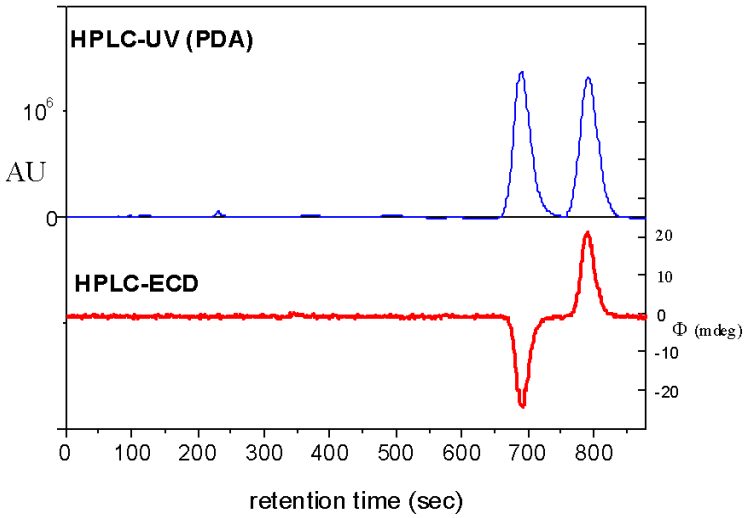

Figure S94. HPLC-UV trace of **7d** on Chiralcel OD column with hexane/2-propanol 95:5 eluent monitored at 225 nm.

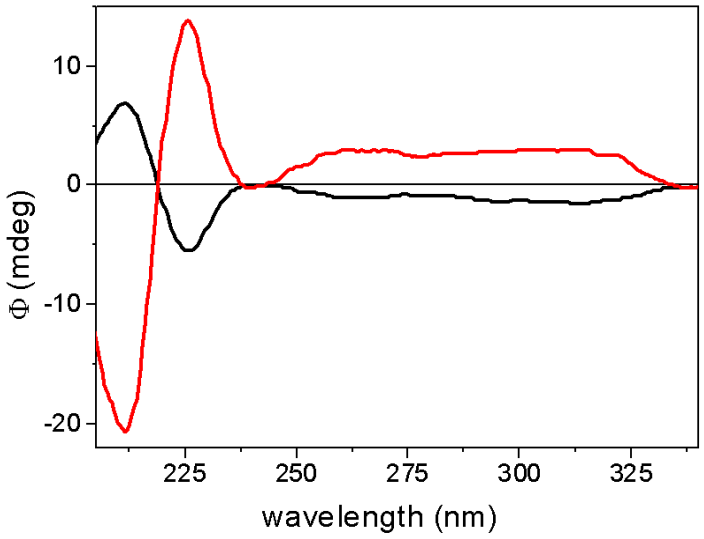

Figure S95. HPLC-ECD spectra of the first- [(2*S*), black] and second-eluting [(2*R*), red] enantiomers of **7d**.

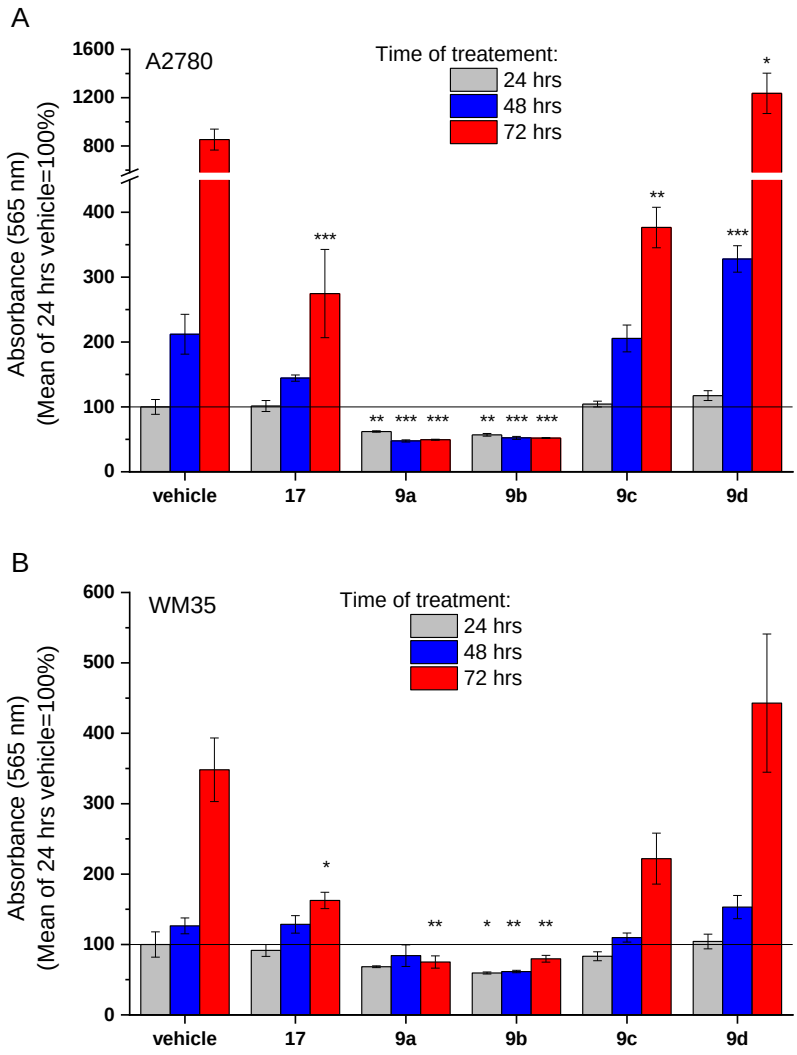

Figure S96. Effect of pectrocarpan derivatives on the viability and proliferation of tumorigenic cell lines.
Effect of pectrocarpans on the viable cell number of A2780 ovarian carcinoma (**A**), and WM35 melanoma (**B**). 50 μM solution of each compound was applied daily, for 3 days. Control cells were treated with equal amount of vehicle solvent (DMSO). Data are presented as Mean±SEM, N = 4 at each data point.*p<0.05; **p<0.01; ***p<0,001 compared to the vehicle treated control on the same day using ANOVA and Dunnett post-hoc test.

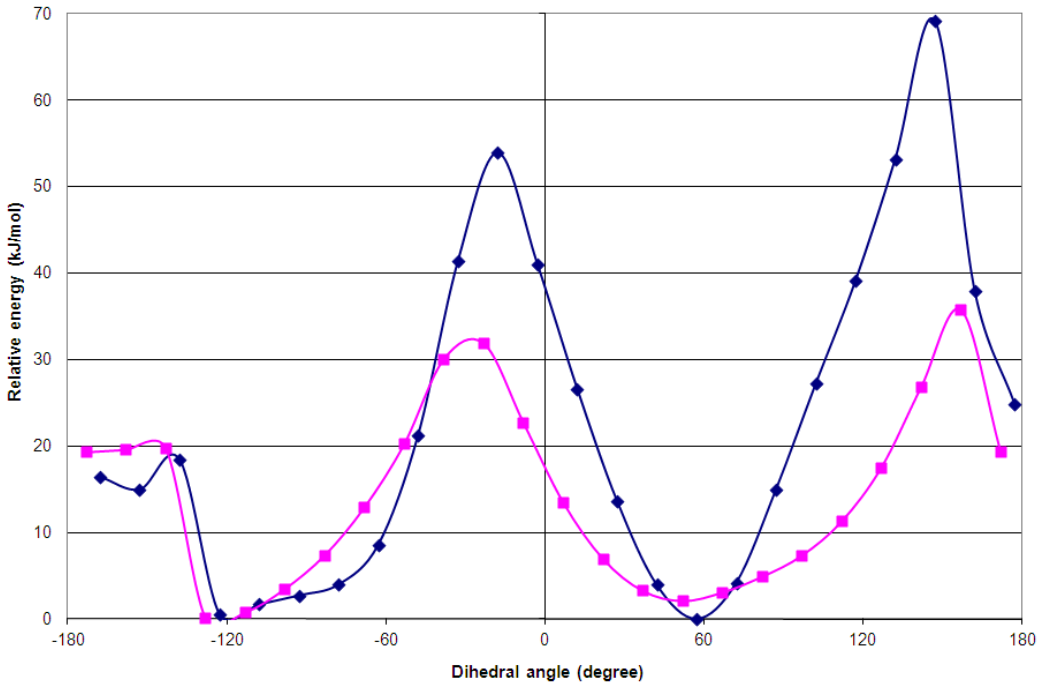

Figure S97. B3LYP/TZVP PCM/$CHCl_3$ torsional angle scans around the C-6–C-1' bond ($\omega_{O\text{-}5,C\text{-}6,C\text{-}1',C\text{-}8a'}$ torsional angle) of (6*R*,6a*S*,11a*S*)-**9a** (blue curve) and the C-6–C-2' bond ($\omega_{O\text{-}5,C\text{-}6,C\text{-}2',C\text{-}1'}$ torsional angle) of (6*R*,6a*S*,11a*S*)-**9b** (pink curve). Relative energy (kJ mol^{-1}) is plotted as a function of torsional angles.